Jordan Journal of Mechanical and Industrial Engineering (JJMIE)

JJMIE is a high-quality scientific journal devoted to fields of Mechanical and Industrial Engineering. It is published by The Jordanian Ministry of Higher Education and Scientific Research in corporation with the Hashemite University.

SUBMISSION ADDRESS:

Prof. **Mousa S. Mohsen**, Editor-in-Chief
Jordan Journal of Mechanical & Industrial Engineering,
Hashemite University,
PO Box 330127, Zarqa, 13133 , Jordan

E-mail: jjmie@hu.edu.jo

Hashemite Kingdom of Jordan

Hashemite University

Jordan Journal of Mechanical and Industrial Engineering

JJMIE

An International Peer-Reviewed Scientific Journal

http://jjmie.hu.edu.jo/

ISSN 1995-6665

Jordan Journal of Mechanical and Industrial Engineering (JJMIE)

JJMIE is a high-quality scientific journal devoted to fields of Mechanical and Industrial Engineering. It is published by The Jordanian Ministry of Higher Education and Scientific Research in corporation with the Hashemite University.

Intruduction: The Editorial Board is very committed to build the Journal as one of the leading international journals in mechanical and industrial engineering sciences in the next few years. With the support of the Ministry of Higher Education and Scientific Research and Jordanian Universities, it is expected that a heavy resource to be channeled into the Journal to establish its international reputation. The Journal's reputation will be enhanced from arrangements with several organizers of international conferences in publishing selected best papers of the conference proceedings.

Aims and Scope: Jordan Journal of Mechanical and Industrial Engineering (JJMIE) is a refereed international journal to be of interest and use to all those concerned with research in various fields of, or closely related to, mechanical and industrial engineering disciplines. Jordan Journal of Mechanical and Industrial Engineering aims to provide a highly readable and valuable addition to the literature which will serve as an indispensable reference tool for years to come. The coverage of the journal includes all new theoretical and experimental findings in the fields of mechanical and industrial engineering or any closely related fields. The journal also encourages the submission of critical review articles covering advances in recent research of such fields as well as technical notes.

Guide for Authors

Manuscript Submission

High-quality submissions to this new journal are welcome now and manuscripts may be either submitted online or mail.

Online: For online submission upload one copy of the full paper including graphics and all figures at the online submission site, accessed via E-mail: jjmie@hu.edu.jo. The manuscript must be written in MS Word Format. All correspondence, including notification of the Editor's decision and requests for revision, takes place by e-mail and via the Author's homepage, removing the need for a hard-copy paper trail.

By Mail: Manuscripts (1 original and 3 copies) accompanied by a covering letter may be sent to the Editor-in-Chief. However, a copy of the original manuscript, including original figures, and the electronic files should be sent to the Editor-in-Chief. Authors should also submit electronic files on disk (one disk for text material and a separate disk for graphics), retaining a backup copy for reference and safety.

Note that contributions may be either submitted online or sent by mail. Please do NOT submit via both routes. This will cause confusion and may lead to delay in article publication. Online submission is preferred.

Submission address and contact:

Prof. **Mousa S. Mohsen**, Editor-in-Chief
Jordan Journal of Mechanical & Industrial Engineering,
Hashemite University,
PO Box 330127, Zarqa, 13133 , Jordan
E-mail: jjmie@hu.edu.jo

Types of contributions: Original research papers

Corresponding author: Clearly indicate who is responsible for correspondence at all stages of refereeing and publication, including post-publication. Ensure that telephone and fax numbers (with country and area code) are provided in addition to the e-mail address and the complete postal address. Full postal addresses must be given for all co-authors.

Original material: Submission of an article implies that the work described has not been published previously (except in the form of an abstract or as part of a published lecture or academic thesis), that it is not under consideration for publication elsewhere, that its publication is approved by all authors and that, if accepted, it will not be published elsewhere in the same form, in English or in any other language, without the written consent of the Publisher. Authors found to be deliberately contravening the submission guidelines on originality and exclusivity shall not be considered for future publication in this journal.

Supplying Final Accepted Text on Disk: If online submission is not possible: Once the paper has been accepted by the editor, an electronic version of the text should be submitted together with the final hardcopy of the manuscript. The electronic version must match the hardcopy exactly. We accept MS Word format only. Always keep a backup copy of the electronic file for reference and safety. Label the disk with your name. Electronic files can be stored on CD.

Notification: Authors will be notified of the acceptance of their paper by the editor. The Publisher will also send a notification of receipt of the paper in production.

Copyright: All authors must sign the Transfer of Copyright agreement before the article can be published. This transfer agreement enables Jordan Journal of Mechanical and Industrial Engineering to protect the copyrighted material for the authors, but does not relinquish the authors' proprietary rights. The copyright transfer covers the exclusive rights to reproduce and distribute the article, including reprints, photographic reproductions, microfilm or any other reproductions of similar nature and translations.

PDF Proofs: One set of page proofs in PDF format will be sent by e-mail to the corresponding author, to be checked for typesetting/editing. The corrections should be returned within 48 hours. No changes in, or additions to, the accepted (and subsequently edited) manuscript will be allowed at this stage. Proofreading is solely the author's responsibility. Any queries should be answered in full. Please correct factual errors only, or errors introduced by typesetting. Please note that once your paper has been proofed we publish the identical paper online as in print.

Author Benefits

Page charge: Publication in this journal is free of charge.

Free off-prints: Three journal issues of which the article appears in along with twenty-five off-prints will be supplied free of charge to the corresponding author. Corresponding authors will be given the choice to buy extra off-prints before printing of the article.

Manuscript Preparation:

General: Editors reserve the right to adjust style to certain standards of uniformity. Original manuscripts are discarded after publication unless the Publisher is asked to return original material after use. If online submission is not possible, an electronic copy of the manuscript on disk should accompany the final accepted hardcopy version. Please use MS Word for the text of your manuscript.

Structure: Follow this order when typing manuscripts: Title, Authors, Affiliations, Abstract, Keywords, Introduction, Main text, Conclusions, Acknowledgements, Appendix, References, Figure Captions, Figures and then Tables. For submission in hardcopy, do not import figures into the text - see Illustrations. For online submission, please supply figures imported into the text AND also separately as original graphics files. Collate acknowledgements in a separate section at the end of the article and do not include them on the title page, as a footnote to the title or otherwise.

Text Layout: Use double spacing and wide (3 cm) margins. Ensure that each new paragraph is clearly indicated. Present tables and figure legends on separate pages at the end of the manuscript. If possible, consult a recent issue of the journal to become familiar with layout and conventions. All footnotes (except for table and corresponding author footnotes) should be identified with superscript Arabic numbers. To conserve space, authors are requested to mark the less important parts of the paper (such as records of experimental results) for printing in smaller type. For long papers (more that 4000 words) sections which could be deleted without destroying either the sense or the continuity of the paper should be indicated as a guide for the editor. Nomenclature should conform to that most frequently used in the scientific field concerned. Number all pages consecutively; use 12 or 10 pt font size and standard fonts. If submitting in hardcopy, print the entire manuscript on one side of the paper only.

Corresponding author: Clearly indicate who is responsible for correspondence at all stages of refereeing and publication, including post-publication. The corresponding author should be identified with an asterisk and footnote. Ensure that telephone and fax numbers (with country and area code) are provided in addition to the e-mail address and the complete postal address. Full postal addresses must be given for all co-authors. Please consult a recent journal paper for style if possible.

Abstract: A self-contained abstract outlining in a single paragraph the aims, scope and conclusions of the paper must be supplied.

Keywords: Immediately after the abstract, provide a maximum of six keywords (avoid, for example, 'and', 'of'). Be sparing with abbreviations: only abbreviations firmly established in the field may be eligible.

Symbols: All Greek letters and unusual symbols should be identified by name in the margin, the first time they are used.

Units: Follow internationally accepted rules and conventions: use the international system of units (SI). If other quantities are mentioned, give their equivalent in SI.

Maths: Number consecutively any equations that have to be displayed separately from the text (if referred to explicitly in the text).

References: All publications cited in the text should be presented in a list of references following the text of the manuscript.

Text: Indicate references by number(s) in square brackets in line with the text. The actual authors can be referred to, but the reference number(s) must always be given.

List: Number the references (numbers in square brackets) in the list in the order in which they appear in the text.

Examples:

Reference to a journal publication:

[1] M.S. Mohsen, B.A. Akash, "Evaluation of domestic solar water heating system in Jordan using analytic hierarchy process". Energy Conversion & Management, Vol. 38, No. 9, 1997, 1815-1822.

Reference to a book:

[2] Strunk Jr W, White EB. The elements of style. 3rd ed. New York: Macmillan; 1979.

Reference to a conference proceeding:

[3] B. Akash, S. Odeh, S. Nijmeh, "Modeling of solar-assisted double-tube evaporator heat pump system under local climate conditions". 5th Jordanian International Mechanical Engineering Conference, Amman, Jordan, 2004.

Reference to a chapter in an edited book:

[4] Mettam GR, Adams LB. How to prepare an electronic version of your article. In: Jones BS, Smith RZ, editors. Introduction to the electronic age, New York: E-Publishing Inc; 1999, p. 281-304

Free Online Color: If, together with your accepted article, you submit usable color and black/white figures then the journal will ensure that these figures will appear in color on the journal website electronic version.

Tables: Tables should be numbered consecutively and given suitable captions and each table should begin on a new page. No vertical rules should be used. Tables should not unnecessarily duplicate results presented elsewhere in the manuscript (for example, in graphs). Footnotes to tables should be typed below the table and should be referred to by superscript lowercase letters.

EDITORIAL PREFACE

It is my overwhelming pleasure to inform you of the success the first two issues of our journal JJMIE has made at all levels. For instance, tens of supporting and encouraging comments were received during the last couple of months. Moreover, quite a big number of professionally distinguished contributions have down poured from elite local and international scholars in the fields of Mechanical and Industrial Engineering. Needless to say, this echoing success is due to the cooperative efforts of the contributors, the reviewers, the editorial board, the technical aids and most importantly the limitless support of the Ministry of Higher Education and Scientific Research and the Hashemite University officials.

Both the Ministry and Hashemite University are committed to build the Journal as one of the leading international journals in mechanical and industrial engineering sciences in the next few years. To build JJMIE international reputation; ISI listing and a good impact number, you are all invited to participate in this effort, all scientists in the fields of mechanical and industrial engineering are invited to participate as authors and/or reviewers. Contributions from both academicians and practitioners are welcomed. Your effort in dissemination of JJMIE will help achieving international reputation.

Hoping that you will find a noticeable technical as well as contextual improvement in this issue of JJMIE, the editorial board and I promise you to spare no effort in developing our Journal and making it a top quality quarterly that local and out-of-kingdom mechanical and industrial engineering writers and reviewers compete to occupy a space on its pages.

Your comments, suggestions, and contributions are always solicited and highly appreciated.

Editor-in-Chief
Prof. Mousa S. Mohsen
Hashemite University
Zarqa, Jordan

JJMIE

Volume 2, Number 1, Mar. 2008
ISSN 1995-6665
Pages 1 - 14

Jordan Journal of Mechanical and Industrial Engineering

Hydrogen and Fuel Cell Technologies for Sustainable Future

Ibrahim Dincer *

Faculty of Engineering & Applied Science, University of Ontario Institute of Technology, North Oshawa, Canada

Abstract

This paper discusses some crucial energetic, environmental and sustainability issues and the role of hydrogen and fuel cell technologies as one of the potential solutions to these issues. The commercialization plans in various industrialized countries (USA, Canada, Japan, etc.) for these technologies have started by identifying the most likely early markets for hydrogen as an energy carrier and fuel cells as power producing devices from micro- to macro-applications, and set realistic near-term and mid-term goals for selected market penetration. The plans outline the major barriers to achieving those goals and recommends activities to capitalize on the incentives and overcome the market barriers. The paper also presents possible future hydrogen energy-utilization patterns for better environment and sustainable development, and shows how the principles of thermodynamics via energy can be beneficially used to evaluate hydrogen and fuel cell systems and their role in sustainability. Throughout the paper, current and future perspectives regarding thermodynamics and sustainable development are considered.

Keywords: Energy; exergy; fuel cell; hydrogen; life cycle assessment; environment; economics; sustainable development;

1. Introduction

Energy is a key element of the interactions between nature and society and is considered a key input for the environment and sustainable development. Environmental and sustainability issues span a continuously growing range of pollutants, hazards, and eco-system degradation factors that affect areas ranging from local through regional to global. Some of these concerns arise from observable, chronic effects on, for instance, human health, while others stem from actual or perceived environmental risks such as possible accidental releases of hazardous materials. Many environmental issues are caused by or related to the production, transformation, and use of energy, for example, acid rain, stratospheric ozone depletion, and global climate change. Recently, a variety of potential solutions to the current environmental problems associated with the harmful pollutant emissions has evolved. Hydrogen energy systems appear to be the one of the most effective solutions and can play a significant role in providing better environment and sustainability [1].

In the literature, there have been limited studies on sustainability aspects of hydrogen energy systems (including fuel cell systems) undertaken by several researchers [2-10]. Of these Afgan and Carvalho [6] give an overview of the potential on multi-criteria assessment of hydrogen systems. With respective selection of the criteria comprising performance, environment, market, and social indicators the assessment procedure is adapted for the assessment of the selected options of the hydrogen energy systems and their comparison with new and renewable energy systems. Hopwood et al. [8] pointed on that sustainable development, although a widely used phrase and idea, has many different meanings and therefore provokes many different responses. In broad terms, the concept of sustainable development is an attempt to combine growing concerns about a range of environmental issues with socio-economic issues. The sustainable development implies smooth transition to more effective technologies from a point view of an environmental impact and energy efficiency. According to Midilli et al. [9-10], increasing concerns about urban air pollution, energy security, and climate change will expedite the transition to "hydrogen economy." Kwak et al. [7] indicate that new hydrogen powered fuel cell technologies in both its high and low-temperature derivatives are more effective and cleaner than conventional energy technologies, and can be considered one of the pillars of a future sustainable energy system. Barreto et al. [4] examine future perspectives for fuel cells and develop a long-term hydrogen-based scenario of the global energy system. Their scenario illustrates in Figure 1 the key role of hydrogen in a long-term transition towards a clean and sustainable energy future. Hart [2] states that hydrogen from renewable, coupled with fuel cell

* Corresponding author. e-mail: Ibrahim.Dincer@uoit.ca

generation on demand, provides an elegant and complementary solution to this problem. Therefore, it is suggested that not only are fuel cells a future economically competitive option for sustainable energy conversion, they are also a complementary option in the sustainable energy system of the future.

The main goal of this paper is to discuss the role of hydrogen and fuel cell systems for sustainable future, and present a case study on the life cycle assessment of fuel cell vehicles from energy, environment, and sustainability points of views. The role of exergy in performance assessment and sustainability achievement is also discussed..

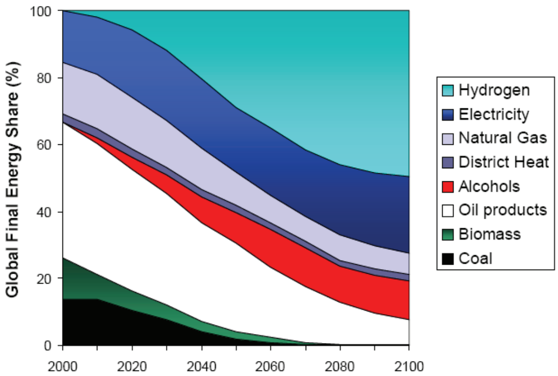

Figure 1. Evolution of global market shares of different final-energy carriers for the period 1990-2100 based on the scenario by Barreto et al. [4]. The alcohols category includes methanol and ethanol.

2. Sustainable Development

Sustainable development requires a sustainable supply of clean and affordable energy resources that do not cause negative societal impacts [5,11-16]. Supplies of such energy resources as fossil fuels and uranium are finite. Energy sources such as sunlight, wind, and falling water are generally considered renewable and therefore sustainable over the relatively long term. Wastes and biomass fuels are also usually viewed as sustainable energy sources. Wastes are convertible to useful energy forms through such technologies as waste-to-energy incineration facilities.

Environmental impact is associated with energy-resource utilization. Ideally, a society seeking sustainable development utilizes only energy resources that release no or minimal emissions to the environment and thus cause no or little environmental impact. However, since all energy resources may somehow lead to some environmental impact, increased efficiency can somewhat alleviate the concerns regarding environmental emissions and their negative impacts. For the same services or products, less resource utilization and pollution is normally associated with increased efficiency.

Sustainability often leads local and national authorities to incorporate environmental considerations into energy planning. The need to satisfy basic human needs and aspirations, combined with increasing world population, will make the need for successful implementation of sustainable development increasingly apparent. Various hydrogen energy-related criteria that are essential to achieving sustainable development in a society follow:

- information about and public awareness of the benefits of sustainability investments,
- environmental and sustainability education and training,
- appropriate energy and exergy strategies for better efficiency,
- promoting environmentally benign technologies,
- clean hydrogen production technologies,
- development of sustainable hydrogen economy infrastructure,
- commercially viable and reliable hydrogen energy systems, including fuel cells,
- availability and utilization of renewable energy resources,
- use of cleaner technologies for production, transportation, distribution, storage and use,
- a reasonable supply of financing and incentives,
- academia-industry-government partnership programs,
- policy development for sustainable energy programs,
- appropriate monitoring and evaluation tools, and
- road maps for future implementation.

Environmental concerns are significantly linked to sustainable development. Activities that continually degrade the environment are not sustainable. For example, the cumulative impact on the environment of such activities often leads over time to a variety of health, ecological and other problems.

Clearly, a strong relation exists between efficiency and environmental impact since, for the same services or products, less resource utilization and pollution is normally associated with increased efficiency. Note that improved energy efficiency leads to reduced energy losses. Most efficiency improvements produce direct environmental benefits in two ways: (I) Operating energy input requirements are reduced per unit output, and pollutants generated are correspondingly reduced. (ii) Consideration of the entire life cycle for energy resources and technologies suggests that improved efficiency reduces environmental impact during most stages of the life cycle. That is why assessing the future hydrogen technologies such as fuel cells over their entire life cycle is essential to obtain correct information on energy consumption and emissions during various life cycle stages, to determine competitive advantages over conventional technologies, and to develop future scenarios for better sustainability.

In recent years, the increased acknowledgment of humankind's interdependence with the environment has been embraced in the concept of sustainable development. With energy constituting a necessity for maintaining and improving standards of living throughout the world, the widespread use of fossil fuels may have affected the planet in ways far more significant than first thought. In addition to the manageable impacts of mining and drilling for fossil fuels and discharging wastes from processing and refining operations, the "greenhouse" gases created by burning these fuels is regarded as a major contributor to a global warming threat. Global warming and large-scale climate change have implications for food chain disruption, flooding and severe weather events, e.g., hurricanes.

It is obvious that utilization of hydrogen and fuel cell technologies can help reduce environmental damage and achieve sustainability. Such technologies essentially do not consume fuel, contribute to global warming, or generate substantial waste as long as hydrogen is produced through clean and renewable energy resources. In this respect, hydrogen and fuel cell technologies can provide more efficient, effective, environmentally benign and sustainable alternatives to conventional energy technologies, particularly fossil-fuel driven ones.

Hydrogen and fuel cell technologies have a crucial role to play in meeting future energy needs in both rural and urban areas. The development and utilization of such technologies should be given a high priority, especially in the light of increased awareness of the adverse environmental impacts and political consequences of fossil-based generation. The need for sustainable energy development is increasing rapidly in the world. In fact, widespread use of these technologies is important for achieving sustainability in the energy sectors in both developing and industrialized countries. These technologies are a key component of sustainable development for four main reasons:

- They have numerous advantages, such as energy efficient and compatible with renewable energy sources and carriers for future energy security, economic growth and sustainable development.
- They generally cause much less environmental impact than other conventional energy sources and technologies. The variety of hydrogen and fuel cell technologies provides a flexible array of options for their use in various applications.
- Hydrogen cannot be depleted because the basic source is water. If used carefully in appropriate applications, it can provide a fully reliable and sustainable supply of energy almost indefinitely. In contrast, fossil fuel and uranium resources are diminished by extraction and consumption.
- These technologies favor system decentralization and local and individual solutions that are somewhat independent of the national network, thus enhancing the flexibility of the system and providing economic and environmental benefits to small isolated populations. In addition, the small scale of the equipment often reduces the time required from initial design to operation, providing greater adaptability in responding to unpredictable growth and/or changes in energy demand.

It is important to note that if we produce hydrogen through conventional technologies using fossil fuels, this will not make hydrogen inherently clean in that they may cause some burden on the environment in terms of pollutant emissions, solid wastes, resource extraction, or other environmental disruptions. Nevertheless, the overall use of these technologies almost certainly can provide a cleaner and more sustainable energy system than increased controls on conventional energy systems. This is in fact clearly shown in the case studies.

To overcome obstacles in initial implementation, programs should be designed to stimulate a hydrogen energy market so that options can be exploited by industries as soon as they become cost-effective. Financial incentives should be provided to reduce up-front investment commitments and infrastructure costs for production, transportation, distribution, storage, and use, and to encourage design innovation, as well as research and development activities along with commercialization practices.

3. Sustainable Development And Thermodynamic Principles

As mentioned earlier, energy is a key element of the interactions between nature and society and is considered a key input for economic development and sustainable development. Energy use is very much governed by thermodynamic principles and, therefore, an understanding of thermodynamic aspects of energy can help us understand pathways to sustainable development [15]. The impact of energy resource utilization on the environment and the achievement of increased resource-utilization efficiency are best addressed by considering exergy. The exergy of an energy form or a substance is a measure of its usefulness or quality or potential to cause change and provide the basis for an effective measure of the potential of a substance or energy form to affect the environment. It is important to mention that in practice a thorough understanding of exergy and the insights it can provide into the efficiency, environmental impact and sustainability of energy systems, are required for the engineer or scientist working in the area of energy systems and the environment. During the past decade, the need to understand the linkages between exergy and energy, and environmental impact has become increasingly significant [17-18]. In one of the recent works, Dincer and Rosen [19] considered exergy as the confluence of energy, environment, and sustainable development and illustrated this in a triangle in Figure 2a. The basis for this treatment is the interdisciplinary character of exergy and its relation to each of these disciplines.

When we look at the general energy efficiency (η) and exergy efficiency (ψ) definitions as follows:

$$\eta = \frac{Energy\ in\ product\ outputs}{Energy\ in\ inputs} = 1 - \frac{Energy\ loss}{Energy\ in\ inputs}$$

and

$$\psi = \frac{Exergy\ in\ product\ outputs}{Exergy\ in\ inputs} = 1 - \frac{Exergy\ loss + Exergy\ consumption}{Exergy\ in\ inputs}$$

It is obvious that reducing losses will increase the efficiency. The relation between exergy efficiency, sustainability, and environmental impact is illustrated in Figure 2b. There, sustainability is seen to increase and environmental impact to decrease as the exergy efficiency of a process increases. The two limiting efficiency cases in Figure 2b appear to be significant:

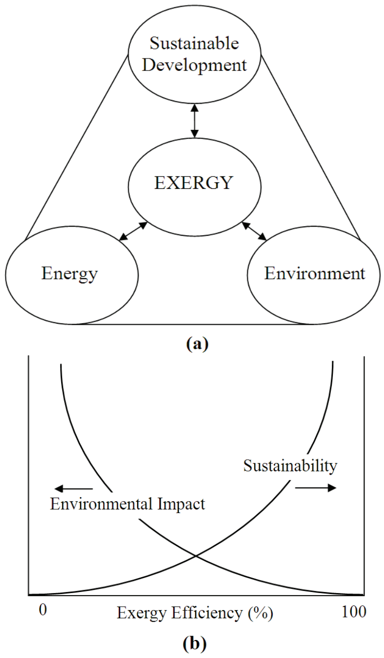

Figure 2. (a) The interdisciplinary triangle of exergy. (b) Qualitative illustration of the relation between the environmental impact and sustainability of a process, and its exergy efficiency.

- As exergy efficiency approaches 100%, the environmental impact associated with process operation approaches zero, since exergy is only converted from one form to another without loss (either through internal consumption or losses). In addition, sustainability approaches infinity because the process approaches reversibility.
- As exergy efficiency approaches 0%, sustainability approaches zero because exergy-containing resources are used but nothing is accomplished. In addition, environmental impact approaches infinity because, to provide a fixed service, an ever-increasing quantity of resources must be used and correspondingly increasing amounts of exergy-containing wastes are emitted.

Although this paper discusses the benefits of using thermodynamic principles, especially for exergy, to assess the sustainability and environmental impact of energy systems, this area of work, particularly for hydrogen and fuel cell systems is relatively new. Further research is of course needed to ascertain a better understanding of the potential role of exergy in such a comprehensive perspective. This includes the need for research to (i) better define the role of exergy in environmental impact and design, (ii) identify how exergy can be better used as an indicator of potential environmental impact, and (iii) develop holistic exergy-based methods that simultaneously account for technical, economic, environmental, sustainability and other factors.

Nevertheless, hydrogen appears to be one of the most promising energy carriers for the future. It is considered an energy-efficient, non-polluting fuel. When hydrogen is used in a fuel cell to generate electricity or is combusted with air, the only products are water and a small amount of NOx, depending on the source of hydrogen and its impurity. Hydrogen that is produced from renewable resources and used in fuel cells can provide sustainable energy to power fuel cell vehicles. The total system, including distribution, refueling and on-board storage of hydrogen may prove superior to batteries recharged with grid power. A hydrogen-powered fuel cell vehicle may offer a market entry for hydrogen and renewable resources in transportation. Attractive transitional applications of hydrogen include use in combustion engine vehicles and production from natural gas. In both case, the environmental and energy policy consequences are significantly less than continued use of oil-derived fuels in conventional combustion engine vehicles. Fuel cells, which employ hydrogen to produce electricity, particularly proton exchange membrane (PEM) fuel cells, can be used to power a wide variety of applications. This is especially true in transportation, where there are several options for providing hydrogen for the fuel cells.

Recently, there has been increased interest in hydrogen energy and fuel cell applications for both stationary and mobile power generation. This interest has been motivated by the fuel cells' high efficiency, even in small-scale installations, and their low waste emissions. Recent legislative initiatives in California, USA aimed at mandating the introduction of zero-emission vehicles, and the failings of other technologies (e.g., the limited range and long refueling times of battery-powered vehicles) have further promoted the investigation of fuel cells in mobile applications.

Thermodynamic principles can be used to assess, design, and improve energy and other systems, and to comprehend environmental impact and sustainability issues. For the broadest understanding, all thermodynamic principles must be used, not just those pertaining to energy. Thus, many researchers feel that an understanding and appreciation of exergy, as defined earlier (see Fig. 2a), is essential to discussions of sustainable development.

Beyond individual behavior, we should think collectively about how society meets its energy needs, including decisions about energy resource selection, efficiency and the role of hydrogen and fuel cell technologies.

An inexpensive and stable energy supply is a prerequisite for social and economic development, in households as well as at the national level. Indeed, energy is essential to human welfare and quality of life. However, energy production and consumption generate significant environmental problems (at global, regional, and local levels) that can have serious consequences and even put at risk the long-term sustainability of the planet's ecosystems. The relationship between energy consumption and production and sustainability is, therefore, complex as shown earlier by Dincer and Rosen [19].

We consider sustainable development here to involve four key factors in terms of environmental, economic, social and resource/energy sustainability under global sustainability, as shown in Figure 3. It is clearly seen that all these factors are interrelated.

4. Fuel Cells as Hydrogen Energy Systems

Fuel cell technology is clean, quiet, and flexible one and is already beginning to serve humanity in a variety of useful ways. Nevertheless, production volume is low and costs are too high. Public support is needed to help generate initial demand to break this cycle. The market for automotive power and stationary generation conversion equipment is the largest market for capital equipment in the world. Fuel cells and fuel cell powered vehicles will be an economic growth leader in the coming decades securing high quality employment for many thousands of people.

Figure 3. Four key factors of sustainable development under global sustainability.

Fuel cells are considerably efficient power producers and create electricity in one simple step, with no moving parts and (at least in the case of PEMFC) at a very low temperature. (Compare this to the combustion process employed by traditional power plants: A fuel is burned at high temperature to create heat, the heat energy is then converted to mechanical energy, and that mechanical energy is finally converted into electricity.) Since fuel cells do not combust fossil fuels, they are known as clean power producers, they emit none of the acid rain or smog producing pollutants that are the inevitable by-product of burning coal or oil or natural gas.

In principle, a fuel cell operates like a battery. Unlike a battery, it does not run down or require recharging, and produces energy in the form of electricity and heat as long as fuel is supplied. The fuel cell converts chemical energy directly into electricity without combustion by combining oxygen from the air with hydrogen gas. It produces electricity as long as fuel, in the form of hydrogen, is supplied. The only by-products are water and heat (Fig. 4). No pollutants are produced if pure hydrogen is used. However, very low levels of nitrogen oxides are emitted, but usually in the undetectable range. The carbon dioxide emissions, which come out from the electrochemical conversion, are relatively low because of high efficiency, and are in concentrated form, facilitating capture Hydrogen can be produced from water using renewable solar, wind, hydro or geothermal energy. Hydrogen also can be extracted from anything that contains hydrocarbons, including gasoline, natural gas, biomass, landfill gas, methanol, ethanol, methane, and coal-based gas.

The type of fuel cells is typically distinguished by the electrolyte that is utilized and can be classified into two main categories, based on their operating temperatures, such as low temperature fuel cells (e.g., 60-250°C) and high temperature fuel cells (e.g., 600-1000°C). Low temperature fuel cells have made significant progress in transportation applications due to their quick start times, compact volume and lower weight compared to high temperature fuel cells. The common types of low temperature fuel cells are proton exchange membrane fuel cells, phosphoric acid fuel cells, alkaline fuel cells, unitized regenerative fuel cells, direct methanol fuel cells. The high temperature fuel cells are more efficient than low temperature ones in generating electrical energy. In addition, they provide high temperature waste heat, which is a benefit in stationary cogeneration applications, but presents a problem for transportation applications. Two common ones are molten carbonate fuel cells and solid oxide electrolyte fuel cells [1].

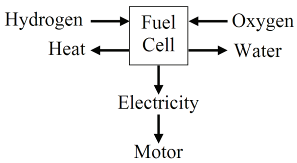

Figure 4. Operation of a fuel cell, converting hydrogen and oxygen (from the air) into electricity, water, and heat.

5. Technical Aspects of Hydrogen Energy

5.1. Hydrogen Production

Although hydrogen is the universe's most abundant element, it is present in the atmosphere only in concentrations of less than one part per million. Most of the Earth's hydrogen is bound up in chemical compounds. Hydrogen for large-scale use should therefore be extracted from a source such as water, coal, natural gas, or plant matter. It cannot simply be produced from a mine or a well. Since considerable energy is consumed in the extraction process, hydrogen should properly be considered an energy carrier rather than an energy source; the energy released when it is finally used is just the energy that was invested in its original manufacture (minus any losses). Recognizing this fact is of critical importance. Any analysis of how hydrogen is to be used must also consider how the hydrogen is to be produced. A variety of alternative hydrogen energy production technologies is available in practice, including [1,20]:

- **Steam reforming**: Steam reforming is a chemical process that makes hydrogen from a mixture of water and a hydrocarbon feedstock, usually a fossil fuel. The most common feedstock is natural gas, consisting primarily of methane. When steam and methane are combined at high pressure and temperature, a chemical reaction converts them into hydrogen and carbon dioxide. The energy content of the hydrogen produced is actually higher than that of the natural gas consumed, but considerable energy is required to operate the reformer, so the net conversion efficiency may typically be only about 65-70%. Hydrogen produced by this technique may cost as little as 65¢/kg.
- **Off-gas cleanup**: After steam reforming, the next most common source of hydrogen at present is the cleanup of industrial off-gases. Numerous industries give off high concentrations of hydrogen in their waste streams

petroleum refineries, blast furnaces, and some chemical plants, for example. Collecting and purifying these gases is often cost-effective, with costs typically ranging between 80 and 120 ¢/kg. Most off-gas hydrogen is used on-site by the industry that produces it, so although off-gas cleanup is an important feature of today's market, it seems unlikely that it could be expanded enough to meet the increased demand that would result from widespread use of hydrogen as a fuel.

- **Electrolysis**: Electrolysis means passing an electrical current through water to split individual water molecules into their constituent hydrogen and oxygen. Energy losses during this process are relatively modest: 65% energy efficiency is common, and state-of-the-art large electrolyzers can be 80 to 85% efficient. Electrolysis has captured considerable attention, even though it accounts for only a small fraction of current hydrogen production, because it is a clean process and water is abundant. At present, however, the technique is only used at relatively small plants, with a cost of 2.40-3.60 $/kg of hydrogen produced. This high cost is expected to limit electrolysis to niche markets in the near and mid term. In the long term, could electrolysis become more competitive? At present, natural gas reforming is more than three times more energy efficient than electrolysis if fossil-source electricity is used.
- **Photo process**: Photo processes use the energy and other special properties of light (usually sunlight) to produce hydrogen from either water or biomass. There are three broad categories of photo process. Photo biological techniques are based on the photosynthesis cycle used by plants and by some bacteria and algae. The efficiency of photo biological hydrogen production is only 1 to 5%, but researchers hope to increase it to 10% or more. Photochemical processes mimic natural photosynthesis using synthetic molecules. This technique is only about 0.1% efficient now, but it can be improved. Photo electrochemical techniques use layers of semiconductor material separated by water. When exposed to light, the semiconductor layers produce an electrical voltage that splits the water into hydrogen and oxygen. The best prototypes yet demonstrated in the laboratory are about 13% efficient, but the maximum theoretical efficiency is believed to be more than 35%. It has been estimated that efficiency in the field of 10 to 15% may be economical, but such estimates depend strongly on projections of equipment costs. Note that since all these photo processes use light as their primary energy source, their efficiencies should not be used directly in cost comparisons with processes that use hydrocarbon fuels or electricity. Photo processes are a major component of current hydrogen research programs.
- **Thermo chemical process**: This process uses heat to split water into hydrogen and oxygen. The conceptually simplest version of this technique is direct thermal conversion, i.e. heating water to extreme temperatures, perhaps 3400 K. Because of the high temperatures required, however, direct thermal conversion is yet impractical outside the laboratory. Chemical reactions can be employed to reduce the required temperature. Various alternatives have been studied, often involving complex multistep processes. Hybrid techniques that incorporate electrolysis into one or more of the reaction steps are under investigation. There has been little recent work available on thermo chemical techniques.
- **Radiolysis**: This process is the splitting of water molecules by collisions with high-energy particles produced in a nuclear reactor. Since the hydrogen and oxygen atoms thus produced quickly recombine to produce water again, radiolysis would probably be only about 1% efficient. Most experts agree that radiolysis is less promising than other techniques.
- **Solar hydrogen**: In this original and simplest form of hydrogen energy production, the solar hydrogen scenario envisions producing electricity from sunlight using photovoltaic cells, electrolyzing water to produce hydrogen, and substituting this hydrogen for the oil and other fossil fuels in general use today. The term is now often used more broadly to include electrolysis based on other renewable sources of electricity, such as wind. This idea has received considerable attention largely because of the environmental benefits of using hydrogen instead of fossil fuels. It also addresses two barriers to the ultimate achievement of large-scale use of solar energy: that solar electricity cannot be used directly for non-electric applications, such as combustion engines, and that electricity is difficult and expensive to store.
- **Partial oxidation of hydrocarbons:** Hydrogen may be formed from the no catalytic partial oxidation (i.e., gasification) of hydrocarbons such as residual oil. Any hydrocarbon feedstock that can be compressed or pumped may be used in this technology. However, the overall efficiency of the process is about 50% and pure oxygen is required. Two commercial technologies for this conversion are available: the Texaco gasification process and the Shell gasification process.

There are also some other hydrogen production technologies, such as:

- Thermal decomposition of hydrocarbon fuels
- Thermo catalytic CO_2-free production of hydrogen from hydrocarbon fuels
- Super adiabatic decomposition of hydrogen sulfide
- Auto thermal reforming (combining partial oxidation and steam reforming)
- Sorption Enhanced Reaction Process (SERP)
- Production of hydrogen from biomass-derived liquids
- Photo electrochemical hydrogen production
- Biological H_2 from fuel gases and from H_2O
- Two-phase photo biological algal H_2-production system
- H_2 Production from Glucose-6-Phosphate
- Most of the above listed methods are under heavy investigation for implementation and commercialization. The findings show that there is still much to do for achieving those.

5.2. Hydrogen Storage

5.2.1. Bulk Storage in Distribution System

It is expected that any large-scale hydrogen distribution system should address the problem of bulk storage, to provide a buffer between production facilities and fluctuations in demand. Low-cost and efficient bulk storage techniques are a major research goal. One can store hydrogen as either a gas or a liquid. The most widely studied options for storing gaseous hydrogen are underground caverns and depleted underground natural gas formations. Although hydrogen is more prone to leak than most other gases, leakage is shown not to be a problem for these techniques. For example, town gas mixture containing hydrogen) has been stored successfully in a cavern in France, and helium, which is even more leak-prone than hydrogen, has been stored in a depleted natural gas field near Amarillo, Texas. The energy consumed in pumping gas in and out of such storage facilities may be significant, however. Aboveground storage tanks at high pressure are another option.

A certain amount of gaseous storage can be achieved by allowing modest pressure changes in the distribution pipeline system. In the case of natural gas, this technique is used to help manage transient demand fluctuations, such as the morning and evening peaks in residential demand in urban areas. Though the same technique might be useful for hydrogen, its potential is limited, particularly if the hydrogen is to be produced from intermittent sources such as solar or wind.

Storage in liquid form uses tanks similar to those used for liquid hydrogen distribution. For example, Kennedy Space Center uses a 3217 m^3 sphere near the launch pad, and can transfer fuel from this tank to the space shuttle at up to 38 m^3 per minute. Storage at liquefier plants is in vacuum-insulated spherical tanks that usually hold about 1514 m^3 [20]. The energy required for liquefaction may not be a barrier if the hydrogen is to be transported as a liquid anyway, or if the end-use application requires its fuel to be in liquid form.

5.2.2. Hydrogen Storage in End Use

- The difficulty of onboard storage is the main barrier to fueling vehicles with hydrogen. Because it is a gas, hydrogen at room temperature and pressure takes up about 3,000 times more space than an energy-equivalent amount of gasoline. This obviously means that compression, liquefaction, or some other technique is essential for a practical vehicle. So far, storage requirements tend to limit range severely. During the past two decades, several techniques were examined to overcome this problem. The four main contenders are compressed gas, cryogenic liquid, metal hydride, and carbon adsorption. Of these, the first two appear most promising for the short-term. Metal hydrides are also relatively mature, but require further research to be competitive. Carbon adsorption is not yet a mature technique, but it appears very promising if the research goals may be met. Glass micro spheres and onboard partial oxidation reactors are currently under investigation, but as yet are "insufficiently characterized for evaluation at the systems level." It is likely that different techniques will turn out to be most appropriate for different applications, for example buses are less size-sensitive than cars [20].
- Compressed gaseous hydrogen storage is at room temperature in a high-strength pressure tank. Including the weight of the tank, compressed gas storage holds about 1 to 7% hydrogen by weight, depending on the type of tank used. Lighter, stronger tanks, capable of holding more hydrogen with less weight, are more expensive. Compressing the hydrogen gas at the filling station requires about 20% as much energy as is contained in the fuel.
- Cryogenic liquid storage is at 20K in a heavily insulated tank at ordinary atmospheric pressure. As a liquid, hydrogen contains almost three times more energy than an equal weight of gasoline, and takes up only about 2.7 times as much space for an equal energy content. Including the tank and insulation, this technique can hold as much as 16% hydrogen by weight. Furthermore, liquefaction at the filling station requires about 40% as much energy as is contained in the fuel. Another disadvantage is the so-called "dormancy problem": despite the insulation, some heat leaks into the tank, eventually boiling off the hydrogen. A "cryopressure" system stores liquid hydrogen in a pressure vessel like that used for compressed gaseous storage, allowing containment of the boiled-off gas. This helps with dormancy, but increases weight and size.
- Metal hydride systems store hydrogen in the interatom spaces of a granular metal. Various metals can be used. The hydrogen is released by heating. Metal hydride systems are reliable and compact, but can be heavy and expensive. Varieties now under development can store about 7% hydrogen by weight. Unlike the compressed gas and cryogenic liquid techniques, metal hydrides require little or no "overhead" energy when refueling. They do require energy to release the fuel, however. For low-temperature varieties, this energy may be available as waste heat from the fuel cell or engine. For high-temperature varieties, which tend to be the less expensive ones, as much as half of the vehicle's energy consumption may go to releasing the fuel from the metal.
- The carbon adsorption technique stores hydrogen under pressure on the surface of highly porous super activated graphite. Some varieties are cooled; others are operated at room temperature. Current systems store as much as 4% hydrogen by weight. It is hoped to increase this efficiency to about 8%, even for the room temperature variety. Carbon adsorption is very similar to compressed gas storage except that the pressure tank is filled with graphite; the graphite adds some weight but allows more hydrogen to be stored at the same pressure and tank size.
- Glass micro spheres are small, hollow, glass micro-balloons whose diameters vary from about 25 microns to 500 microns, and whose wall thicknesses are about 1 micron. They can be used in large beds to store hydrogen at high pressures. The micro spheres are filled with hydrogen gas at temperatures of 200 to 400°C. The high temperature makes the glass walls permeable, and the gas fills the spheres. Once the glass is cooled to room temperature, the hydrogen is trapped inside the spheres. The hydrogen can be released as needed by heating the spheres. The spheres may also be crushed to release hydrogen. This option precludes sphere recycling, but is desirable for applications where weight is important.

- Onboard partial oxidation reactor is a concept proposed to help bring about a transition from conventional automobiles to cars powered by hydrogen fuel cells. First, a shift would be made from the internal combustion engine to the fuel cell using a conventional hydrocarbon fuel such as gasoline or diesel coupled to an onboard partial oxidation process and a water gas shift reaction process. The partial oxidation process yields 30% hydrogen gas directly and 20% carbon monoxide. Then, the carbon monoxide is chemically reacted with steam to produce additional hydrogen and carbon dioxide gas, which is readily usable by a hydrogen fuel cell. This fossil-to-hydrogen fuel system would be used as a "bridge" until research yields a commercially ready advanced hydrogen storage system or a suitable hydrogen carrier.
- Other techniques are still in the early stages of development. One uses powdered iron and water. At high temperatures, these react to produce rust and hydrogen. Other methods are similar to the metal hydride option, but substitute certain liquid hydrocarbons (also known as "recyclable liquid carriers") or other chemicals for the metal.

5.3. Hydrogen Safety

Hydrogen is intrinsically no more dangerous than many other fuels. Its different characteristics require different safety equipment and procedures, but all fuels have some potential for accidents; if they did not burn, they would not be much use as a fuel. Hydrogen is used worldwide in the petroleum and chemical industries and elsewhere. It was also routinely used in the USA as a fuel (a component of "town gas") before natural gas became widely available. Town gas is still used in some countries. Moreover, hydrogen ranks between propane and methane (natural gas) in safety.

The physical properties of hydrogen make its safety characteristics rather different from those of other fuels. Its low density means that it tends to rise and disperse into the atmosphere in the event of a leak, rather than remaining in a "puddle" near the ground. This increases safety in well-ventilated applications. Its low density also means that a hydrogen explosion releases less energy in a given volume than an explosion of other fuels, and compared to gasoline or natural gas, hydrogen requires much higher concentrations in the air to produce an explosion rather than just a flame. Furthermore, hydrogen's low ignition temperature and flammability over a wide range of concentrations make leaks a significant fire hazard, especially in confined spaces such as a garage. Because it is clear and odorless, leaking hydrogen is more likely to go undetected than a leak of gasoline or most other fuels. Even the flame of burning hydrogen is invisible. Techniques of leak detection have been and continue to be a research priority. A simple approach is to add an odorant like that added to natural gas, or possibly a colorant, or both. Any addition may detract somewhat from the environmental cleanliness inherent to pure hydrogen, however, and additives would need to be chosen with care to avoid destroying other important features. For example, contaminants may reduce the efficiency and/or lifetime of a fuel cell.

As with most fuels, the fire and explosion hazards discussed above are the main safety concerns. In some situations, there may be other safety issues, such as, in applications that involve hydrogen storage under high pressure or at extreme low temperatures. These problems can be minimized with proper equipment design and operating procedures, however, and are generally agreed to be of less concern than hydrogen's flammability.

5.4. Economics of Hydrogen

Hydrogen is currently more expensive than other fuel options, so it is likely to play a major role in the economy only in the long term, if technology improvements succeed in bringing down costs. Higher prices for fossil fuels would not necessarily make hydrogen more cost-competitive in the short term. Since fossil fuels are currently the main source of heat, feedstock, and electricity for hydrogen production plants, rising prices for gas, oil, or coal would also drive up the price of hydrogen. Since hydrogen is produced in many different ways, from many different sources, most hydrogen-related international commerce is likely to be not of fuel but of technology: plant components, engineering services, construction expertise, and so on. These areas could potentially represent new export markets.

5.5. Environmental Aspects of Hydrogen Energy

The use of hydrogen as a fuel is inherently very clean. Hydrogen consumed by either combustion or a fuel cell produces only water as a product. The high temperatures involved in combustion may stimulate some NOx production from nitrogen and oxygen in the air, but this problem is familiar from other fuels and can be controlled. Unlike other fuels, hydrogen contains no other pollutant-producing elements, so it has no potential to produce SO_2, CO, CO_2, volatile organic chemicals, etc. The environmental consequences of hydrogen production should also be considered, however. As mentioned above, production from fossil fuel feed stocks by steam reforming leads to carbon dioxide emissions greater than production from feedstock by itself.. Steam reformers should also somehow dispose of feedstock impurities such as sulfur. Electrolysis is responsible for the emissions of whatever power plants are used to generate the needed electricity. Production of hydrogen from sustainable harvested biomass, solar energy, or other renewable sources might considerably reduce production emissions, but (as described above) such techniques are being fully developed for commercialization. For example, the U.S. Department of Energy (has examined the full-cycle environmental effects of various scenarios for hydrogen production and use. It concludes, "Substantial emissions can be generated when hydrogen is produced from certain energy sources," namely fossil fuels. Thus, the technique of hydrogen production remains crucial.

5.6. Standards and Regulations

Countries have different regulations for hydrogen energy and these regulations are still under development. Area of regulation may include but not limited to commercial truck, bus, passenger plane, pipeline, tunnel, portable fuel container, stationary fuel cell, safety training for operators, and fueling station.

It is obvious that some key, harmonized regulations, codes, and standards are necessary in this regard. Wurster [21] has given the published and draft standards for hydrogen and fuel cells. Some published standards are currently available as follows:

- ISO 13984 Liquid hydrogen – Land vehicle fuelling system interface
- ISO 14687 Hydrogen fuel – Product specification

5.7. Publications and Patents

Thomson ISI Web of Knowledge is one of the most reliable sources to find out detailed information about journals and papers. It includes papers indexed in Science Citation Index-Expanded and patents included in Derwent Innovations Index. According to a query carried out at September 27, 2007; number of publications and patents related to 'fuel cells' and 'hydrogen energy' for all years and the last eight years are shown in Table 1 and 2, respectively.

Table 1. Number of journal papers for various year ranges.

Query keyword	Year range	Number of journal papers
Hydrogen energy	1900-2007	52,576
Fuel cell	1900-2007	14,711
Hydrogen energy	2000-2007	28,258
Fuel cell	2000-2007	11,165

Table 2. Number of patents for various year ranges.

Query keyword	Year range	Number of patents
Hydrogen energy	1963-2007	10,576
Fuel cell	1963-2007	47,120
Hydrogen energy	2000-2007	5,228
Fuel cell	2000-2007	34,756

5.8. Influence of Government and Industry

Two parties may influence the implementation of energy conservation problem. These are hydrogen and fuel cell technologies at the industrial sector, namely the government and the top managers of the industrial organizations. The most important measures that a government can take to implement energy conservation include [22]:

- Pricing policy: In the short term, energy prices influence the way of use of existing equipment and in the long-term energy prices effect the choice of equipment.
- Regulation and legislation: The government can enact a Heat Management Law. For such a law, the companies using more than a certain amount of oil equivalent must submit an annual plan for energy conservation and must employ a manager to monitor its execution for such a plan.
- Publicity campaigns: Government can hold seminars, training workshops for the qualified workers including managers, engineers, and technicians of different companies.
- Financial and fiscal incentive schemes: The government can give awards for the outstanding and successful projects. Tax incentives, such as depreciation allowance might encourage investments in some new equipment.

The main concern of the industry switching to hydrogen economy may be given as follows:

- The top managers resist investing in new technology because they want to acquire large profits in the short term.
- Some managers think that investing largely in new technology might lead to higher selling prices of their products. Hence, their competitiveness in the market will decrease.
- Others may have lack of knowledge about this new technology or they do not know how to implement it systematically.

5.9. Scientific and Technical Challenges

The scientific and technical challenges for the hydrogen economy may be given as follows [23]:

- Lowering the cost of hydrogen production to a level comparable to the energy cost of petrol.
- Development of a CO_2-free route for the mass production of sustainable hydrogen at a competitive cost.
- Development of a safe and efficient national infrastructure for hydrogen delivery and distribution.
- Development of viable hydrogen storage systems for both vehicular and stationary applications.
- Dramatic reduction in costs and significant improvement in the durability of fuel cell systems.

The pathway for the transition from current energy economies to hydrogen economy has some scientific, technological, and economical drawbacks. The most significant milestones for the hydrogen pathway must be mainly based on the intensification of research and innovation programs. Figure 5 shows some research and development priority areas.

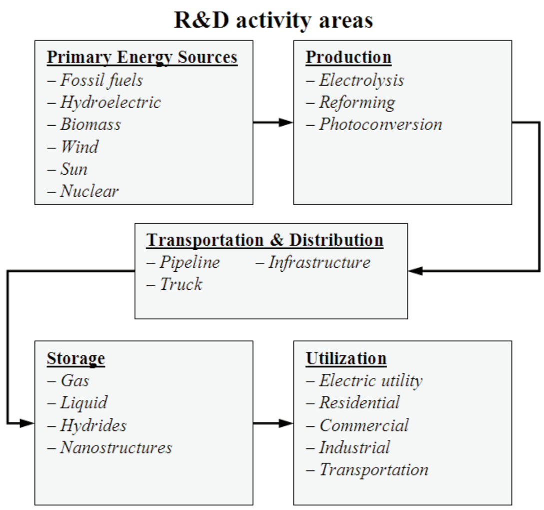

Figure 5. Major R&D activity areas for the pathway to hydrogen economy [31]

It should be noted that universities play an important role in providing the sustainable development of hydrogen and fuel cells through some partnership programs with the relevant industry and government organizations. The output of research conducted in universities is open to other researchers. Hence, being aware of the previous studies and getting benefit of them, new methodologies are developed for better design, analysis, and operation of these technologies. Some challenges to the universities in this issue may be summarized as follows:

- funding challenges,
- coordination of research efforts within and between academic/research institutions, and
- Collaboration between researchers and governmental institutions.

5.10. Priorities that Jordan should consider:

Jordan has limited energy sources such as oil shale deposits, tar sands, a small hydropower potential, a few low geothermal sources, and biogas [24]. It is mainly dependent on imported oil from neighboring countries to cover main portion of its energy demand. In year 2000, 94% of total energy requirement was supplied from imported oil [22]. The major sector of energy consumption is transportation, which is around 41%. Industrial sector, household, and others, which include service and agricultural sectors, follow it, respectively.

Since the oil reserves deplete in the world, alternative energy sources are required to provide the energy need of the world. In the case of Jordan, the transition to the new energy forms should be accelerated since this country is highly dependent on import oil. The priority should be given to the alternative energy sources that could be used in transportation sector since it has the biggest share among the different sectors. For this purpose, renewable energy such as befoul or hydrogen to be used in fuel cells may be considered. Since the main objective of this paper is to discuss hydrogen and fuel cell technologies, the latter one is discussed below.

For vehicle applications, fuel cells are not only preferable since they use hydrogen as fuel but also they have higher efficiency than internal combustion engines (ICEs), which is not restricted with Carnot efficiency; quieter than ICEs; and reduce environmental pollution. Among different types of fuel cells, Proton Exchange Membrane Fuel Cells (PEMFC), also known as Polymer Electrolyte Membrane Fuel Cells has proven to be the most attractive option. This type of fuel cell consists of a proton conducting membrane, such as Nafion, which is chemically highly resistant, mechanically strong, acidic, good proton conductor and water absorbent. Main advantages of this fuel cell may be given as: Fast startup capability since it works at low temperatures, compact since thin Membrane Electrode Assemblies (MEAs) can be made, and no corrosive fluid hazards because the only liquid present in the cell is water. The main disadvantage of this type of fuel cell is the need for expensive catalysts as promoters for the electrochemical reaction. Additionally, carbon monoxide cannot be used as a fuel since it poisons the cell. On the other hand, the main challenge for PEMFC is the water management, which may be summarized as follows: The proton conductivity of the electrolyte is directly proportional to the water content and high enough water content is necessary to avoid membrane dehydration. Contrarily, low enough water should be present in the electrolyte to avoid flooding the electrodes. Hence, a balance between the production of water by oxidation of the hydrogen and its evaporation has to be controlled.

PEMFCs may conquer the market of structured mobility (city buses, postal services, taxis, city cars etc.) where hydrogen can be supplied to the vehicles from central tanks at scheduled intervals. Nevertheless, they may not succeed in the much broader market sector of random mobility (private cars, trucks, tour busses, military vehicles etc.). Some claim that for that market the SOFC is more attractive. These fuel cells may operate between 600°C and 1000°C, respectively. The most common material used for electrolyte is ytrria-stabilized zirconium. The main advantages of this fuel cell are as follows: its fuel flexibility, which means fuel such as methane, propane, butane, JP-8, may be used as fuel, direct reforming at the anode catalyst, and no need for precious metal electro catalysts. The main disadvantage of this fuel cell may be given as the challenges for construction and durability due to its high temperature. Additionally, carbon deposition may be a problem.

In conclusion, the priority for Jordan should be considering fuel cells for transportation applications since it covers the biggest portion among the sectors. Among different fuel cell types, PEMFCs and SOFCs are the most promising ones for this sector.

6. Case Study

Here a life cycle assessment of a PEMFC vehicle, which includes not only operation of the vehicle on the road but also the manufacture and distribution of both the vehicle and the fuel during the vehicle's entire lifetime (Figure 6), is conducted and compared with the one for a conventional gasoline vehicle [25].

As illustrated in Figure 6, the fuel section of the life cycle begins with the primary energy source, e.g., crude oil or natural gas in underground reservoirs. This primary energy is then transported to a manufacturing site, in this case a reforming plant/oil refinery, where it is converted to the fuel suitable for a vehicle, e.g., gasoline or hydrogen. And this fuel has to be distributed from the central reforming plants/refinery by various means to the retail service station where it is deposited in the tanks of vehicles. This sequence constitutes the 'fuel cycle' part of the total automobile technology life cycle.

The vehicle part of life cycle starts with metal ores and other primary materials that eventually converted to components of the vehicle. These primary materials are transported to the vehicle manufacturer (includes manufacture of parts, metals, assembly, and other vehicle constituents). The vehicle itself is fabricated and assembled from these inputs and transported to distributors. Finally, vehicle and fuel cycles come together, which represent the purchaser (user) of both vehicle and fuel. At the end of its lifetime, the vehicle is scrapped or recycled.

The assessment of energy consumption, and greenhouse gases (GHGs) emissions associated with the production and distribution of hydrogen are based on the data published in the literature. Published data are also used to assess the energy consumption, and greenhouse gases (GHGs) emissions associated with producing, manufacturing, and assembling the materials and parts making up the PEMFC vehicle. The assessments of all the phases of each life cycle are then combined to make integrated comparisons with the conventional automobile technology i.e. ICE vehicle.

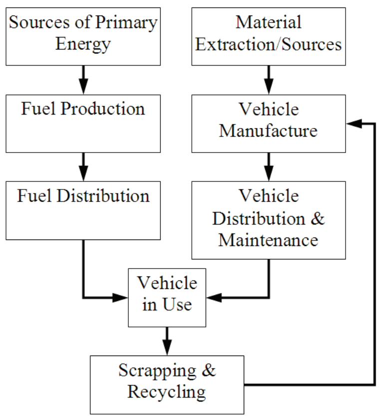

Figure 6. Illustration of life cycle of a vehicle.

6.1. Methodology

The above methodology is used to characterize the following fuel and vehicle cycles [25]:

- Fuels: (i) hydrogen from natural gas and (ii) gasoline from crude oil (for comparison).
- Vehicle Technologies: (i) PEMFC vehicle and (ii) spark ignition internal combustion engine vehicle (for comparison).

The present assessment is a preliminary assessment based on the published data available in the literature [26-27] and like any other assessment, has boundaries on its scope and makes simplifying assumptions. Some assumptions are:

- The boundaries of the physical system are such that secondary energy and environmental effects are not quantified. For example energy consumption and emissions during the operation of a steam reforming plant of natural gas are quantified, but the energy and emissions involved in making the steel, concrete or other elements embodied in the plant itself are not counted.
- Data used for assessment are from mid-size family passenger cars as US experience.
- Other production methods (e.g., electrolysis, nuclear, hydro, etc.) of hydrogen are not considered in the present assessment.

6.2. Results and Discussion

Here, the assessment from fuel cycles includes recovery of the raw material for each (e.g., natural gas for hydrogen or crude oil for gasoline) through conversion to the final fuel (e.g., hydrogen or gasoline) and delivery into the tank of the passenger car. The two characteristics of the fuel cycles are (i) total energy consumed originating from raw materials or other energy sources and (b) total greenhouse gases emitted from raw materials or other sources. The GHGs assessed in the present study are CO_2 and CH_4. N_2O is neglected since its greenhouse contribution for each of the fuel cycles accounts for less than 1% of the other GHGs [28-30].

Figures 7a, b show both the stages classified in both fuel and vehicle cycles. Figures 8a, b exhibit the comparison of energy consumption and GHGs emission during the fuel cycles of hydrogen and gasoline respectively. Here both energy consumption and GHGs emissions during fuel cycle of hydrogen are higher when compared to gasoline fuel cycle. Fuel production stage of hydrogen cycle is the major contributor to total energy consumption and GHGs emissions. The other significant contribution of energy consumption and GHGs emissions during hydrogen cycle comes from the fuel distribution stage which includes primary energy in generation of the electric power used for compressing hydrogen.

The comparison of energy consumption and GHGs emissions during vehicle cycle of PEMFC and internal combustion engine (ICE) vehicle are shown in Figures 9a, b respectively. The largest contributor to energy consumption and GHGs emissions for the ICE vehicle is the usage stage. The energy consumption of ICE vehicle is about three times higher than PEMFC vehicle. Moreover, GHGs emissions during the vehicle cycle of PEMFC vehicles is around 8% of the GHGs emissions of the ICE vehicle, which clearly indicates the environmental friendliness of PEMFC vehicles.

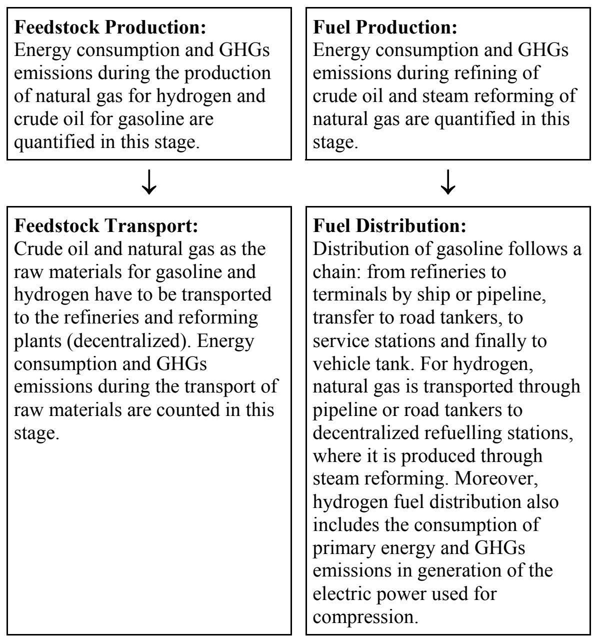

Figure 7a. Stages of fuel cycle.

Vehicle Material Production:
Energy use and GHGs emissions from vehicle materials production are counted in this stage. Typically vehicle incorporates nearly 890 kg of ferrous metals, 100 kg of different types of plastics, roughly 80 kg of aluminium, and about 200 kg of other materials (Weiss et al., 2000). And for PEM fuel cell powered automobile, some additional materials are needed for fuel cell components, e.g., polymer membrane, platinum as catalyst, graphite etc.

↓

Vehicle Assembly:
The energy required and GHGs emissions for transport of vehicles during assembly are quantified here. Because of the complex supply chain in the automobile industry and the associated difficulty in estimating vehicle assembly energy requirements, assembly energy is typically estimated as a linear function of vehicle mass (AE, 1996).

↓

Vehicle Distribution:
The energy needed and GHGs emissions during the transport of a vehicle from the assembly line to the dealership are counted in this stage.

↓

Vehicle Use:
It includes energy consumption (fuel) and GHGs emissions, maintenance and repair during the lifetime, which is assumed to be 300000 km, consistent with Sorensen (2004). In the present analysis, it is assumed that the fuel usage of PEM fuel cell and ICE vehicles are 0.65 MJ/km and 2.73 MJ/km, respectively.

↓

Vehicle Disposal:
After a vehicle's life, the automobile is shredded. The disposal energy is the sum of energy needed to move the bulk from the dismantler to a shredder and the shredding energy (AE, 1997).

Figure 7b. Stages of vehicle cycle.

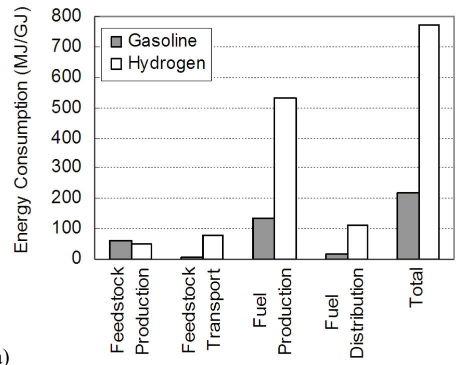

(a)

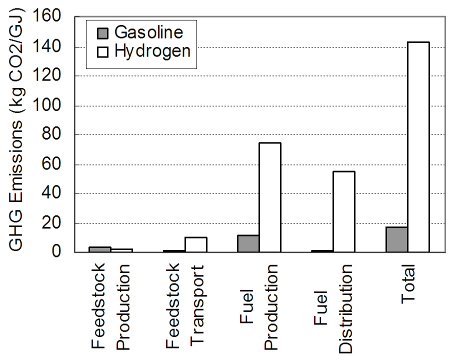

(b)

Figure 8. (a) Energy consumption and (b) greenhouse gases emissions during fuel cycles, using actual data from [32-34].

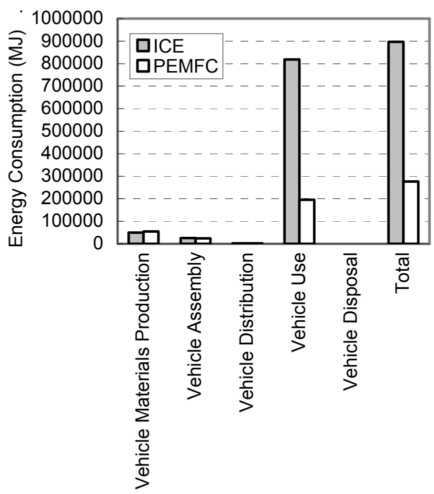

(a)

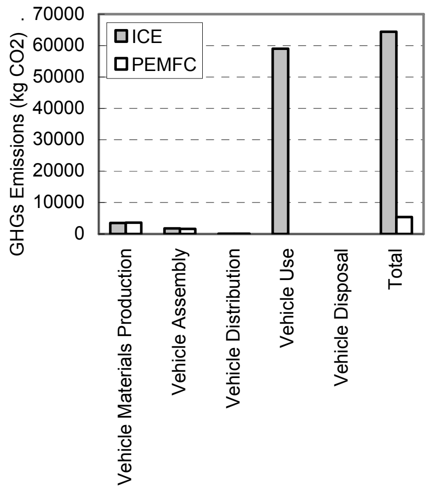

(b)

Figure 9. (a) Energy consumption and (b) GHGs emissions during vehicle cycles, using actual data from [32,35].

Figures 10a, b show the comparison of life cycle energy consumption and life cycle GHGs emissions of the two vehicles technologies considered in the present study. Although the fuel cycle energy consumption of PEMFC vehicle is about 3.5 times higher than ICE automobile, the overall life cycle energy consumption of PEM fuel cell vehicle is about 2.3 times less than that of ICE vehicle, which is due to high efficiency of PEMFC vehicle as compared to ICE vehicle during the vehicle use stage of the vehicle cycle. Similarly, the GHGs emissions of PEMFC automobile is 8.5 times higher than ICE vehicle during the fuel cycle, the overall life cycle GHGs emissions are about 2.6 times lower than ICE automobile, which is again due to no GHGs emissions as compared to ICE vehicle during the vehicle use stage of the vehicle cycle.

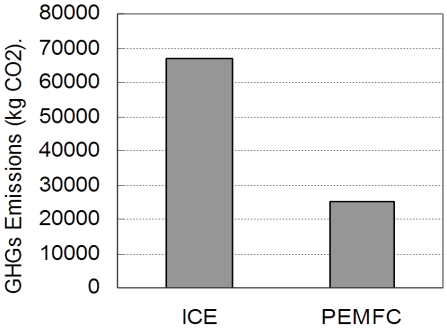

(a)

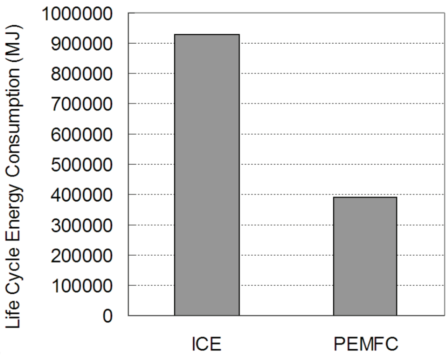

(b)

Figure 10. (a) Life cycle energy consumption and (b) GHGs emissions of vehicle technologies, using actual data from [32-35].

7. Conclusions

The benefits of hydrogen and fuel cell systems is highlighted of using the principles of thermodynamics (particularly exergy) and life cycle assessment to evaluate their key roles in sustainable development. The following concluding remarks, which will likely be useful to scientists, researchers and engineers as well as policy and decision makers, can be drawn from this study:

- Moving towards sustainable development requires that environmental problems be resolved. These problems cover a continuously growing range of air pollution, water pollution, solid wastes, pollutants, ecosystem degradation, and extend over ever-wider areas.
- Sustainable development requires a sustainable supply of energy resources that, in the long term, is sustainable available at reasonable cost and can be utilized for all required tasks without causing negative societal impacts. Energy resources such as solar, wind, hydro, and biomass are generally considered renewable and therefore sustainable over the relatively long term. The use of these sources in hydrogen production will be a key factor in sustainable development.
- Assessments of the sustainability of processes and systems, and efforts to improve sustainability, should be based in part upon thermodynamic principles, and especially the insights revealed through exergy analysis.
- For societies to attain or try to attain sustainable development, effort should be devoted to developing hydrogen and fuel cell technologies. Renewable energy utilization in hydrogen production can provide a potential solution to current environmental problems. Advanced hydrogen and fuel cell technologies can provide environmentally responsible alternatives to conventional energy systems, as well as more flexibility and decentralization.
- To realize the energy, exergy, economic and environmental benefits of hydrogen and fuel cell technologies, an integrated set of activities should be conducted including research and development, technology assessment, standards development and technology transfer. These can be aimed at improving efficiency, facilitating the substitution of these technologies and other environmentally benign energy currencies for more harmful ones, and improving the performance and implementation characteristics of these technologies.
- As illustrated in the case study, the results of a comprehensive life cycle assessment of PEMFC vehicles are presented based on the published data available in the literature. The two characteristics, which were assessed, are energy consumption and greenhouse gases (GHGs) emissions during the entire life cycle of an automobile. Moreover, conventional internal combustion engine (ICE) vehicle is also assessed based on the similar characteristics to compare with the PEMFC vehicle.

The results will likely be useful to scientists, researchers and engineers as well as policy and decision makers. The case study presented on the hydrogen and fuel cell systems highlights clearly the importance of the topic and show that these can help achieve better environment and sustainability.

Acknowledgement

The financial support of the Ontario Premier's Research Excellence Award and the Natural Sciences and Engineering Research Council of Canada is gratefully acknowledged.

References

[1] Dincer, I. "Technical, environmental and exergetic aspects of hydrogen energy systems". International Journal of Hydrogen Energy, Vol. 27, 2002, 265-285.

[2] Hart, D. "Sustainable energy conversion: fuel cells-the competitive options". Journal of Power Sources, Vol. 86, 2000, 23-27.

[3] Pehnt, M. "Assessing future energy and transport systems: the case of fuel cells. Part I: methodological aspects". International Journal of Life Cycle Assessment, Vol. 8, No.5, 2003, 283-289.

[4] Baretto, L., Makihira, A., and Riahi, K. "The hydrogen economy in the 21st century: a sustainable development scenario". International Journal of Hydrogen Energy, Vol. 28, 2003, 267-284.

[5] Afgan, N.H., Al-Gobaisi, D., Carvalho, M.G. and Cumoc, M. "Sustainable energy development". Renewable and Sustainable Energy Reviews, Vol.2, 1998, 235-286.

[6] Afgan, N.H. and Carvalho, M.G. "Sustainability assessment of hydrogen energy systems". International Journal of Hydrogen Energy, Vol. 29, 2004, 1327-1342.

[7] Kwak, H.-Y., Lee, H.-S., Jung, J.-Y., Jeon, J.-S. and Park, D.-R. "Exergetic and thermo economic analysis of a 200-kW

phosphoric acid fuel cell plant". Fuel, Vol.83, No. 14-15, 2004, 2087-2094

[8] Hopwood, B. Mellor, M. and O'Brien, G. "Sustainable development: mapping different approaches". Sustainable Development, Vol. 13, 2005, 38–52.

[9] Midilli, A., Ay, M., Dincer, I. and Rosen, M.A. "On hydrogen and hydrogen energy strategies-I- current status and needs". Renewable and Sustainable Energy Reviews Vol.9, No.3, 2005a, 291-307.

[10] Midilli, A., Ay, M., Dincer, I. and Rosen, M.A. (2005b). "On hydrogen and hydrogen energy strategies-II: future projections affecting global stability and unrest", Renewable and Sustainable Energy Reviews, Vol. 9, No.3, 2005, 309-323.

[11] McGowan, J.G. Large-scale solar/wind electrical production systems-predictions for the 21st century. In: Tester, J.W., Wood, D.O., and Ferran, N.A., editors. Energy and the Environment in the 21st Century . Massachusetts: MIT, 1990.

[12] Anon. Urban energy handbook. Paris: Organization for Economic Co-Operation and Development (OECD); 1995.

[13] Hui, S. C. M., "From renewable energy to sustainability: the challenge for Hong Kong". POLMET '97 Conference, , Hong Kong, 1997.

[14] Dincer, I., and Rosen, M.A., "A worldwide perspective on energy, environment and sustainable development". International Journal of Energy Research, Vol. 22, No. 15, , 1998, 1305-1321.

[15] Dincer, I. and Rosen, M.A., "Thermodynamic aspects of renewable and sustainable development". Renewable and Sustainable Energy Reviews, Vol. 9, No.2, 2005, 169-189.

[16] Hammond, G.P.," Towards sustainability: energy efficiency, thermodynamic analysis, and the 'two cultures". Energy Policy, Vol. 32, 2004, 1789-1798.

[17] Dincer, I., "Thermodynamics, exergy and environmental Impact". The ISTP-11, the Eleventh International Symposium on Transport Phenomena, Hsinchu, Taiwan, 1998.

[18] Dincer, I., and Rosen, M.A. The Intimate Connection between Exergy and the Environment.In: Bejan, A., and Mamut, E., editors. Thermodynamic Optimization of Complex Energy, the Netherlands: Kluwer Academic, , 1999, p. 221-230.

[19] Dincer, I. and Rosen, M. "Exergy as a drive for achieving sustainability:. International Journal of Green Energy, Vol.1, No.1,2004, 1-19.

[20] CNIE (2001). Hydrogen: Technology and Policy, Washington, D.C: The Committee for the National Institute for the Environment, Congressional Research Service. Report for Congress.

[21] Wurster, R. "Hydrogen regulations, codes and standards for road vehicles and their refueling infrastructure in Europe". CUTE – Bringing a Fuel Cell Bus Fleet on the Road in European Cities, , London,UK, 2004.

[22] Kablan, M.M., "Energy conservation projects implementation at Jordan's industrial sector: a total quality management approach". Energy, Vol.28,2003, 1533–1543.

[23] Edwards, P.P., Kuznetsov, V., David, W.I.F, Brandon, N. Hydrogen and fuel cells: towards a sustainable energy future. Mini Energy Project, Foresight;2006.

[24] Abdulla, F., Widyan, M., Al-Ghazawi, Z., Kiwan, S., Abu-Qdais, H., Hayajneh, M., Harb, A., Al-Nimr, M. "Status of Jordan renewable energy sector: Problems, needs and challenges. Beirut Regional Workshop on Energy Efficiency and Renewable Energy Technology". Beirut, Lebanon, 2004.

[25] Hussain, M.M., Dincer, I., and Li, X. (2004). "A preliminary life cycle assessment of PEM fuel cell vehicles", *Proceedings of the First Cappadocia Mechanical Engineering Symposium*, pp. 153-160, 14-16 July 2004, Nigde, Turkey.

[26] AE (Automotive Engineering). (1996). "Life cycle analysis: getting the total picture on vehicle engineering alternatives", March 1996, 49-52.

[27] AE (Automotive Engineering). (1997). "Progress in recycling specific materials from automobiles," August 1997, 51-53.

[28] Wang, M., and Huang, H.S. (1999). "A full fuel cycle analysis of energy and emissions impacts of transportation fuel produced from natural gas", Report ANL/EDSs-40, Prepared by Argonne National Laboratory, The Center for Transportation Research, Energy Systems Division for US DOE.

[29] EIA (Energy Information Administration). (1997). US DOE, "Emissions of greenhouse gases in the United States 1996," DOE/EIA-0573(96).

[30] EIA (Energy Information Administration). (2005). Official energy statistics from the U.S. Government. Via http://tonto.eia.doe.gov/steo_query/app/pricepage.htm.

[31] Conte, M., Iacobazzi, A., Ronchetti, M., Vellone, R. "Hydrogen economy for a sustainable development: state-of-the-art and technological perspectives". Journal of Power Sources, Vol.100, 001, 171-187

[32] Weiss, M.A., Heywood, J.B., Drake, E.M., Schafer, A., and AuYeung, F.F. (2000). "On the road in 2020", MIT EL 00-003, Energy Laboratory, Massachusetts Institute of Technology, Cambridge, Massachusetts 02139-4307.

[33] IEA (International Energy Agency). (1999). "Automotive fuels for the future: the search for alternatives", IEA-AFIS, Paris.

[34] Spath P.L. and M.K. Mann. (2001) Life cycle assessment of hydrogen production via natural gas steam reforming. National Renewable Energy Laboratory, Report No NREL/TP-570-27637. U.S. Department of Energy Laboratory.

[35] Sorensen, B. "Total life-cycle assessment of PEM fuel cell car". Denmark :Energy and Environment Group, Roskilde University; 2004.

JJMIE

Volume 2, Number 1, Mar. 2008
ISSN 1995-6665
Pages 15 - 21

Jordan Journal of Mechanical and Industrial Engineering

Temperature Dependence of Dynamic Modulus and Damping in Continuous Fiber- Reinforced Al-(alloy) Matrix Composites at Elevated Temperatures

Ramadan J. Mustafa *

Faculty of Engineering, Mu'tah University, Karak, Jordan

Abstract

Mechanical damping (in the longitudinal vibration mode only) and temperature dependence of dynamic modulus in the longitudinal (II) and transverse ($\perp$) fiber direction were measured for several metal matrix composites. The piezoelectric ultrasonic oscillator technique was used to generate ultrasonic stress waves for longitudinal measurements at 80 and 150 kHz. Tests were conducted at room temperature and at elevated temperatures up to 450°C and strain amplitudes in the range of 10^{-7} to 10^{-2}. The Metal Matrix Composites (MMC's) studied include Al_{pure} and Al(6061) alloy metal matrix reinforced continuous alumina (Al_2O_3), tungsten (w), high strength carbon (H.S.C), boron(B), and silicon carbide (SiC) fibers. The w-Al composite material showed a strain amplitude dependent damping at room temperature, while the Al2O3, B and SiC fiber reinforced Al_{alloy} matrix composites exhibited essentially amplitude independent over a strain range of 10^{-7} to 10^{-4} and a slight nonlinear amplitude dependent damping at higher strain amplitudes. Increasing the area of fiber-matrix interface in H.S.C-Al matrix composites appeared to increase damping in such composites. The measured longitudinal vibration mode damping for H.S.C-Al_{pure} matrix composite at temperature in the range of 25 to 350 ºC has shown to exhibit strain amplitude dependent damping. The temperature dependence of dynamic modulus in the tested composites showed a linear, monotonic decrease in modulus with increasing temperature, except in the case of H.S.C fiber reinforced Al matrix composites which showed a non-monotonic decrease in modulus as temperature increased from room temperature to 450°C. It is suggested that this behavior is caused by residual stresses at the fiber-matrix interface. The flaws detected by ultrasonic flaw detection techniques in the tested composite plates did not significantly affect the modulus as the fibers carry the majority of load in the longitudinal fiber direction. Additionally, the weak fiber-matrix interfacial strength, matrix ductility, and the flaws, which are a potential source of sliding friction and energy absorbing mechanisms, did affect the damping in tested MMC's specimens under longitudinal fiber vibration.

Keywords: Continuous Fibre-Reinforced Al-(alloy) Composites, elevated temperatures, dynamic modulus, dynamic damping;

Nomenclature

d	crystal drive
g	crystal gauge
λ	wavelength of longitudinal wave in component
p	specimen piece
RL	resonant length
EC	Modulus of composite material
ρ_c	density of composite material
f	frequency
c.s.r	ceramic spacer rod
Vg	gauge crystal voltage
ε_{amp}	maximum strain amplitude
V_d	drive gauge crystal voltage
R_{pd}	Resonant period of component
L	length of specimen
E_d	dynamic Young's Modulus of component
$R_{c.s.r}$	Resonant period of component (ceramic spacer rod)
T	temperature of specimen component
C.T.E	coefficient of thermal expansivity
m (i)	mass of component i
σ_f	fracture strength of component
$\sigma_{tensile}$	tensile strength of component

1. Introduction

The knowledge of internal friction and dynamic modulus of materials is important in the field of science and engineering. This knowledge of temperature

* Corresponding author. e-mail: dnimir@yahoo.co.uk

dependence of dynamic modulus can be critical in studies of buckling, stress-strain relations, and fracture mechanics, while in materials science studies, the modulus is related to inter-atomic forces, creep, thermal stresses, etc. Although damping measurements have technological applications in noise and vibration reduction and are extremely useful in fundamental investigations of defects in materials, as material scientists, engineers and designers, seek to understand the structure-property relationships for advanced engineering materials better, the temperature dependence of dynamic modulus and damping at elevated temperature studies is of prime importance.

Furthermore, metal matrix composites are used nowadays in aerospace, automobile industries, and load-bearing structural components, such as fuselage structures in newly developed aircrafts, because of their high specific strength, specific modulus , higher temperature capabilities and better wear resistance, [1,2], than most polymer matrix composites. Aluminum and its alloys are used as matrix materials because of their relatively low densities and good corrosion resistance, [3]. Continuous fiber reinforcement silicon carbide (SiC), high strength carbon fibre (H.S.C), boron (B), alumina (Al_2O_3), and tungsten (w), are of low cost, high performance reinforcements for Aluminum matrix composites since it possesses high temperature stability and it is compatible with molten aluminum.

This paper discusses the results from an ongoing study of the dynamic longitudinal Young's modulus of several metal matrix composites as a function of temperature for relatively small specimens, using the piezoelectric ultrasonic technique, [8-12]. This is ideal for obtaining longitudinal modulus values since it is a dynamic technique, employing ultrasonic stress waves generated by piezoelectric transducers attached to small specimens, during which the specimen temperature is varied from room temperature to 450°C. This versatile technique for making simultaneous measurements of damping, strain amplitude as function of temperature will also be employed for the tested MMC's. The study will examine the strain amplitude dependence of damping, the temperature dependence of dynamic modulus at temperatures in the range of 25 to 450 °C. Through these studies, some insight into the effects of the structure of tested MMC's on damping and modulus properties should be gained that will be useful in future research and design of these high performance materials.

Fracture behavior characterization and prediction have been extensively studied with reference to metals. In the case of composite materials, in general, the fracture behavior (at room temperature) experimental data of destructive testing and prediction models have to some degree been available in the literature, [4-8]. However, a renewed interest in nondestructive testing techniques (such as ultrasonic testing) has been shown to be aimed at providing direct information useful for the assessment of mechanical behavior such as damping and dynamic modulus (at room and at elevated temperatures). Studies on the comparison of different experimental techniques for determination of elastic properties of fiber reinforced and unreinforced metal matrix materials, [9,10], have shown that there is a good agreement between modulus values obtained using four point bending test and ultrasonic technique. This capability of the ultrasonic technique can be used as a method of testing allowing for real time decision making on the development of the applications of composite materials, [8-15], in noise and vibration reduction, and dynamic properties in the material under control.

2. Experimental

2.1. Materials

The metal matrix composites utilized in this study were made of cylindrical specimens of 99.995% pure aluminum (Al_{pure}) and aluminum alloy (6061) (Al_{alloy}) matrix material reinforced with continuous alumina (Al_2O_3), tungsten (w), boron (B), silicon carbide (SiC), and high strength carbon (H.S.C) fibers were used. The MMC's were fabricated using a hot consolidation technique of laid up well-coated fiber-matrix tapes of Al_{pure} and Al_{alloy}) matrix coated with Al_2O_3, w, B, SiC, and H.S.C continuous fibers.

The coatings of fiber-matrix tapes were in the range of 100 μm thickness and were deposited on fibers to produce, on consolidation, MMC's with volume fraction of 25-70%. The cutting up of suitable lengths of the fiber tape were stacked unidirectional in a cylindrical graphite die and hot consolidation process were carried out at 520 º C, pressure of 6 MPa for Al_{pure} matrix coated fibers, and 540 º C at 6 MPa pressure for Al(6061) matrix coated fibers. A consolidation time of 60 minutes were required to produce specimens of 20-40 mm long. Details of the fabrication process can be found in [5].

The mechanical properties of the selected continuous fiber reinforcement and metal matrix materials are shown in Tables 1 and 2, [16-18]

Table 1: The mechanical properties of continuous fiber reinforcement manufacturer specifications and ref [16, 17].

Fiber type	C.T.E (α_f) ($K^{-1}x10^6$)	E (GPa)	σ_f (GPa)	Diameter (μm)	Specific gravity
HSC (Y/C)	-0.4-1.2	270	4.2	7-30	1.9
α-Al_2O_3	7	380	1.5	15-25	3.9
SiC (Y/C)	4.5	190-200	2.5	12	2.6
Boron(B)	8	400	3.5	150	2.6
Tungsten(W)	5	400	2.5	10-150	19.2

Table 2: The mechanical properties of matrix material ref [18]

Material	E (GPa)	$\sigma_{tensile}$ (MPa)	σ_{yield} (MPa)	Strain to failure	Poisson ratio (ν)
99.995 % Al_{pure}	69	90	34	50-70	0.33
Al_{alloy} (6061)	72	310	275	12	0.33

2.2. Testing Procedure

The required lengths of the specimen were estimated using an initial estimate of modulus. Figure 1 shows the basic features of experimental arrangement, namely two piezoelectric quarts crystals as the drive (d) and gauge (g). These crystals are cemented together using a loctite adhesive. Under suitable electrical excitation, the crystals produce longitudinal, resonant ultrasonic stress waves (wavelength, λ) in the specimen piece (p) of resonant length attached to the gauge crystal. The resonant lengths R_L were estimated using the standard equation ref [18];

$$R_L = \frac{1}{2f}\sqrt{\frac{E_c}{\rho_c}} = \frac{\lambda}{2} \qquad (1)$$

Where E_c is the longitudinal modulus of composite specimen and ρ_c is the estimated density of the composite specimen type used for the tests, and f is the frequency, controlled by the length of the quarts crystals of up to 200 kHz. A typical length of specimens of 20-40 mm was chosen for all tests.

For room temperature tests, as in Fig.1, the specimen was adhered to the end of the gauge crystal using a loctite type of adhesive material.

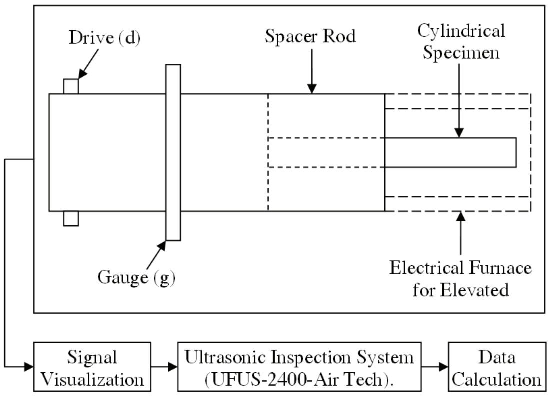

Fig. 1: Schematic diagram showing the four component system used for measurements at elevated temperatures (or at room temperature by removing the electrical furnace).

For elevated temperature testing, a ceramic (such as quartz) spacer rod (c.s.r) had to be cut and glued between the crystals and the specimen, and at high temperature testing the piezoelectric probes were also shielded and cooled by air.

After the specimen (p) had stabilized at the desired temperature (30-35 minutes), the crystal drive was tuned and the period recorded. The period of the specimen was then compared to the period of the crystals alone; in order to determine the validity of such tests, a ratio of only 0.95-1.05 between the two periods is desired. Furthermore, the spacer rod (c.s.r) serves the purpose of keeping the quartz crystals at room temperature, while the specimen is at high or elevated temperature. The ceramic spacer rod must be tuned to resonate for the frequency of the quarts crystals being used and for the particular temperature of the tests and the adhered joint between the specimen and the c.s.r. is made with sauereisen cement.

The electrical system is driven by a closed loop oscillator at a pre-selected gauge crystal voltage (V_g) and constant maximum strain amplitude (ε_{amp}) in the specimen.

The available frequencies with the technique is in the range of 20 to 200 KHz. In typical tests, the values of the drive and gauge crystal voltage V_d, and V_g, respectively, and the resonant period R_{pd} of the four component system were measured. These data with the individual masses m (i), where i = d, g, c.s.r, or p, and the values of the resonant period of the driver and gauge crystal, or driver, gauge, spacer rod, were also measured before the specimen was attached, using the closed loop crystal driven and a frequency counter, and the length of the specimen (L), permitted the calculation of the dynamic Young's modulus (E_d) of the tested composite specimen using the standard equations 2 and 3, ref[11,12,16,18].

$$R_{pd}(p) = \frac{(\sqrt{m_p})R_{pd}(d_g R_{c.s.r})R_{pd}(d_g R_{c.s.r}p)}{C} \qquad (2)$$

Where C is given by:

$$C = \sqrt{R_{pd}^2(d_g R_{c.s.r})m(d_g R_{c.s.r}P) - R_{pd}^2(d_g R_{c.s.r}P)m(d_g R_{c.s.r})}$$

$$E_d = 4\rho L^2 \Big/ R_{pd}^2(P) \qquad (3)$$

Corrections were made for changes in density (ρ) and length of the composite specimen at elevated temperature by including the coefficient of thermal expansion in the equations, in this study, the range of strain amplitudes (ε_a) investigated using this technique falls between 10^{-7} and 10^{-2}. The vibrational frequency controlled by the length of the quartz crystal was 80 KHz.

3. Results and Discussion

The average values of modulus for the tested composite materials at room and elevated temperatures are shown in Table 3 for both longitudinal (II) and transverse ($\perp$) fiber orientation. Figures (2, 3, 4, 5 and 6) show the temperature dependence of modulus for the tested MMC materials. Linear regression was used to determine the equation of a line which would most closely approximate the temperature dependence of the modulus for each material.

Table 3: The average values of modulus at room and elevated temperature for the tested composite materials.

Type of composite material	Fibre orientation	Modulus at T_{room} (GPa)	Modulus at $T_{450°C}$ (GPa)
55 v/o Al_{pure}-Al_2O_3	II	235.3	148.7
	$\perp$	140	56.4
55 v/o Al_{alloy}-Al_2O_3	II	210.5	122
	$\perp$	123	39.4
55 v/o Al_{pure}-B	II	216	92
	$\perp$	134	55
55 v/o Al_{alloy}-B	II	186.6	78
	$\perp$	115	47.4
55 v/o Al_{pure}-W	II	169	68.9
	$\perp$	123	50
55 v/o Al_{alloy}-W	II	151	62
	$\perp$	111	45
55 v/o Al_{pure}-SiC	II	132	99.5
	$\perp$	96.5	73.7
55 v/o Al_{alloy}-SiC	II	119	79
	$\perp$	108	89.5
55 v/o Al_{pure}-H.S.C	II	178	147
	$\perp$	102	98.8
55 v/o Al_{alloy}-H.S.C	II	152	136
	$\perp$	115	119

The resulting equations are listed in Table 4 along with the coefficient of determination (R^2). The temperature dependence of the modulus ranged from -0.0428 to -13.66 GPa /ºC (which represent the lowest and highest slope values obtained from E vs. T graphs, Fig's.2-5) for Al_{pure} and Al_{alloy} metal matrix reinforced Al_2O_3, B, W and SiC fibre composite materials, Table 4. In contrast, however, the H.S.C-Al composite materials showed a nonlinear temperature dependence of modulus behavior and polynomial regression was used. The boron fiber reinforced Al and Al_{alloy} specimens showed the greatest loss of modulus with respect to temperature.

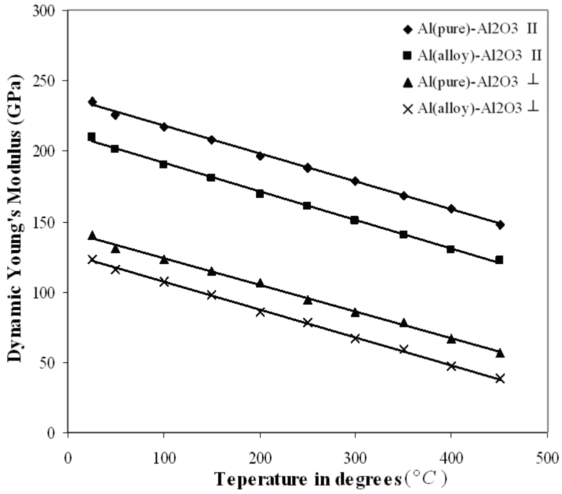

Figure 2: Temperature dependence of longitudinal (II) and transverse ($\perp$) dynamic modulus for Al_2O_3-Al_{pure} and Al_{alloy} matrix composites.

Table 4 also includes the values of the parameter $-\left(10^4/E(T_{test})\right)\left(dE/dT\right)$, at 25 ºC, which represents the normalized fall-off in modulus at temperature increases. The values for SiC (II and $\perp$), and Al_2O_3 (II) fiber reinforced Al and Al_{alloy} are in the range of 5×10^{-5} to $10\times10^{-4}\,°C^{-1}$ and this agrees with the range of values noted by, [13], for many metals at room temperature. For these two particular fiber oriented composite material, it seems that the decrease in modulus with increasing test temperature can be attributed mostly to the matrix material.

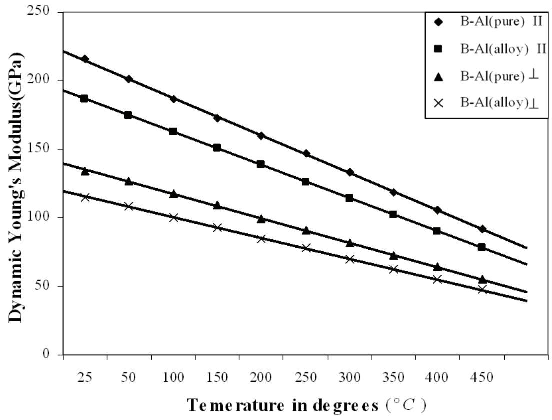

Figure 3: Temperature dependence of longitudinal (II) and transverse ($\perp$) dynamic modulus for B-Al_{pure} and Al_{alloy} matrix composites.

It has been suggested by, [3, 5, 13, and 26], that the presence of a strong fiber-matrix interfacial strength which exists in SiC and Al_2O_3 fiber reinforced Al_{alloy} matrix composite materials, (which occurs due to fiber-matrix interfacial reaction), has a detrimental effect on composite mechanical properties. The correlation among the melting point (T_m), the modulus and interatomic forces in materials is another contributing factor for this type of behavior, making the fall-off in modulus for Al high, ($T_{test}/T_{melting}$ approaches 0.7), and the fall-off for SiC low, ($T_{test}/T_{melting}$ approximately 0.22).

Table 4. Modulus-Temperature Equations and parameter [–(1/E (0)) (dE/dT)].

Figure number	Type of composite material	Fiber orientation	Equation, E in (GPa) ; T in (°C) **[E(T) = ….]**	(R^2)	$-\left(\frac{10^4}{E(T)}\right)\left(\frac{dE}{dT}\right)$ (K^{-1})
Fig. no. 2	55 v/o Al_{pure}-Al_2O_3	II	237.59 -0.198 T	0.998	8.52
		$\perp$	142.8 -0.19 T	0.997	13.76
	55 v/o Al_{alloy}-Al_2O_3	II	211.81 -0.204 T	0.997	9.87
		$\perp$	126.7 -0.1967 T	0.999	16.14
Fig. no. 3	55 v/o Al_{pure}-B	II	288.5 -13.66 T	0.999	53.7
		$\perp$	144.43 -8.89 T	0.999	72.81
	55 v/o Al_{alloy}-B	II	199.4 -12.13 T	0.999	70.82
		$\perp$	122.8 -7.541 T	0.999	72.14
Fig. no. 5	55 v/o Al_{pure}-W	II	170.99 -0.229 T	0.988	13.86
		$\perp$	124.6 -0.167 T	0.990	13.86
	55 v/o Al_{alloy}-W	II	152.43 -0.205 T	0.997	13.92
		$\perp$	108.2 -0.1604 T	0.816	15.39
Fig. no. 4	55 v/o Al_{pure}-SiC	II	134.62 -0.077 T	0.975	5.88
		$\perp$	97.13 -0.0509 T	0.998	5.31
	55 v/o Al_{alloy}-SiC	II	120.1 -0.0924 T	0.995	7.84
		$\perp$	108.61 -0.0428 T	0.992	3.98
Fig. no. 6	55 v/o Al_{pure}-H.S.C	II	$208.2 -(3\times10^{-7})T^4 -(7\times10^{-6})T^3 +0.013\,T^2 -1.57\,T$	0.933	52.48
		$\perp$	$85.98 -(8\times10^{-7})T^4 +0.0002\,T^3 +0.022\,T^2 -1.096\,T$	0.823	30.57
	55 v/o Al_{alloy}-H.S.C	II	$186.6 +(1\times10^{-6})T^4 -0.0003\,T^3 +0.044\,T^2 -2.28\,T$	0.928	39.68
		$\perp$	$126 -(6\times10^{-8})T^4 -(1\times10^{-5})T^3 +0.006\,T^2 -0.546\,T$	0.879	23.14

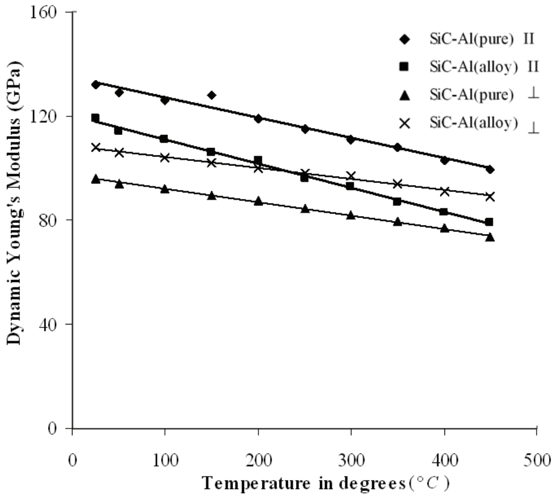

Figure 4: Temperature dependence of longitudinal (II) and transverse ($\perp$) dynamic modulus for SiC-Al_{pure} and Al_{alloy} matrix composites.

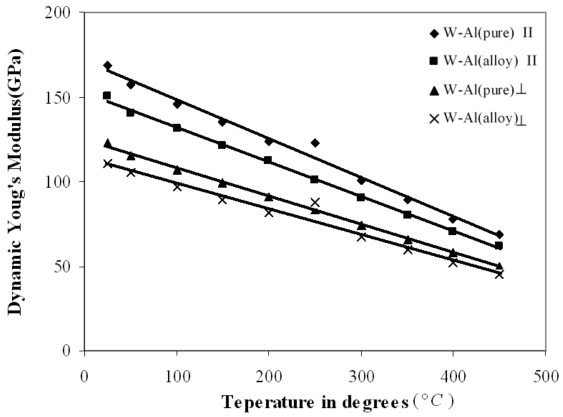

Figure 5: Temperature dependence of longitudinal (II) and transverse ($\perp$) dynamic modulus for W-Al_{pure} and Al_{alloy} matrix composites.

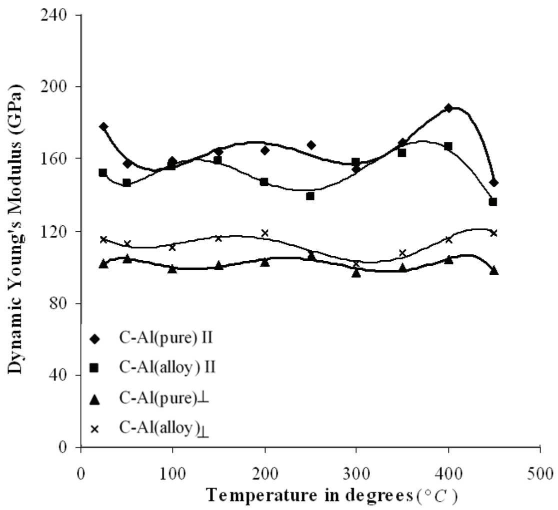

Figure 6: Temperature dependence of longitudinal (II) and transverse ($\perp$) dynamic modulus for H.S.C-Al_{pure} and Al_{alloy} matrix composites.

Figure 6 presents the modulus as a function of temperature for H.S.C fiber reinforced Al and Al_{alloy} matrix composites, where the presence of H.S.C reinforcement has led to a non-monotonic decrease in modulus in both II and $\perp$ fiber directions. A specimen from H.S.C-Al_{pure} and H.S.C-Al_{alloy} composite plates were tested with each specimen being tested over the temperature range of 25 to 450 ºC, and then retested over the range of 50 to 400 ºC. A second specimen was tested over a 25 to 450 ºC temperature range. For all tests, the modulus first decreased to a minimum of 154 GPa as the temperature increased, and then increased to a maximum of 188 GPa at 400 ºC for H.S.C-Al_{pure}, and for H.S.C-Al_{alloy} composite plate from a minimum of 136 GPa (at 250 ºC) to 167 GPa (at 400 ºC). From the obtained results, it is evident that there was a non-monotonic response of modulus with temperature, and a hysteresis effect with respect to thermal cycling has resulted in different responses as successive runs were carried on the same specimen.

The non-monotonic behavior has also been observed for Gr-Al composite system by, [14, 20], in which the modulus decreased with decreasing temperature over the range of 80 to -60 ºC. This behavior may be attributed to the strong dependence of the modulus of the fiber on residual stresses that exist at fiber-matrix interface as a result of the mismatch of coefficients of thermal expansivity (CTE) between fiber and matrix (carbon has negative CTE, -0.4 to -1.2). However, it is possible that successive thermal cycling may have alleviated the residual stresses, possibly through dislocation generation, [8], and reduced the amount of initial modulus loss.

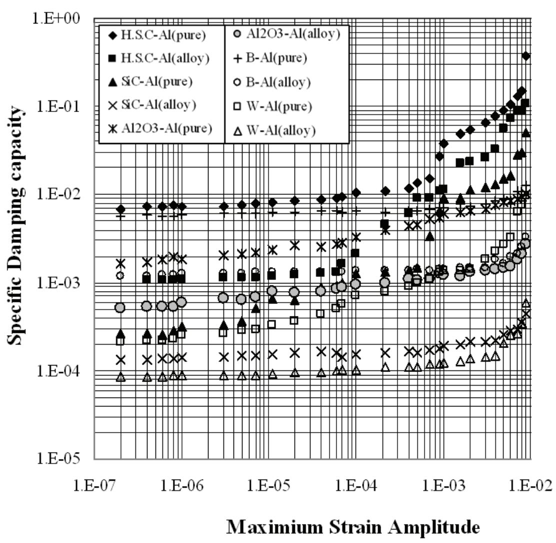

Figure 7: Strain dependence of mechanical damping at room temperature in the tested Al_{pure} and Al_{alloy} matrix composites with fiber volume fraction of 50%. (80 to 150 kHz longitudinal vibration mode).

The strain amplitude dependence of damping was investigated for all MMC tested specimens with results shown in Figures 7 and 8. The B- Al_{pure}, B- Al_{alloy}, SiC-Al_{alloy}, and Al2O3- Al_{alloy} composite specimens, as in Fig.7, exhibited a strain amplitude independent behavior over a strain range of 10^{-7} to 10^{-4} and a slight nonlinear amplitude dependent damping at higher strain amplitude of

10^{-2}. The damping data for fiber reinforced Al_{pure} matrix composite materials; show a small region of strain amplitude independent damping at low strains 10^{-7} - 10^{-6}, followed by a region of nonlinear, amplitude dependent damping at higher strains of 10^{-6} - 10^{-2} strain amplitude. In the composite systems with no strain amplitude dependence were observed, it is unlikely that interfacial friction (i.e. frictional sliding) is responsible in these types of composites, however, it is possible that interfacial microplasticity or matrix microcracking is responsible.

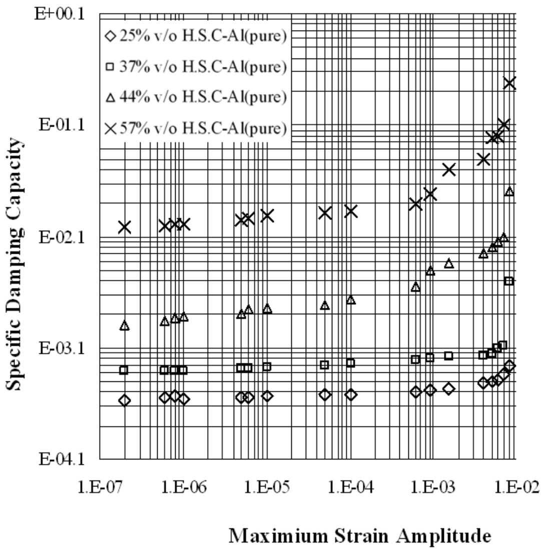

Figure 8: Strain dependence of mechanical damping at T_{room} in H.S.C-Al_{pure} matrix composites. (80 to 150 KHz longitudinal vibration mode).

It is apparent that in the case of ceramic fiber reinforced Al_{pure}, and in some cases Al_{alloy} metal matrix composites, the relatively large difference between CTE's for the fiber and matrix caused a rise in thermal stresses during the cooling process of the fabricated specimens, resulting in a high dislocation density near fiber-matrix region (i.e. frictional bonding has occurred). It can be suggested that fiber-matrix frictional sliding, (due to the presence of weak fiber-matrix interfacial bonding), has led to enhance damping at high frequency and low strain amplitudes 10^{-7} - 10^{-2}. These observations are in agreement with previous studies on SiC and C fiber reinforced Al metal matrix composite systems by [5] which indicated that the high impact and tensile strength in the longitudinal fiber direction reinforcement is mainly due to the presence of energy absorbing mechanisms, such as matrix ductility and fiber-matrix weak interfacial strength are responsible for the improved mechanical properties. Further investigation on the effect of matrix ductility and fiber-matrix interfacial region on damping were carried out, the trend here is to increase fiber volume fraction of H.S.C-Al_{pure} metal matrix composite ranging from 25% to 57% v/o, in order to increase the fiber-matrix interface area. It was clear from Fig. 8, that this (increasing the percentage of fiber v/o) has resulted in strain amplitude dependence, which clearly means that increasing fiber-matrix interfacial area in frictionally bonded composite materials, and increasing matrix ductility will enhance damping levels in such tailor made composites.

The obtained results for W-Al composite material, Figures (5 and 7), show that in spite of the large difference between matrix and fiber CTE's, a less severe modulus between fiber and matrix than in the ceramic fiber case may have led to the reduced interfacial sliding. Henceforth, it can be said that increasing fiber-matrix interface and matrix ductility in the studied MMC's did translate into increased damping. However, more detailed studies of interactions at the interface region are needed in order to further understand the damping behavior and effectively design composites with increased damping.

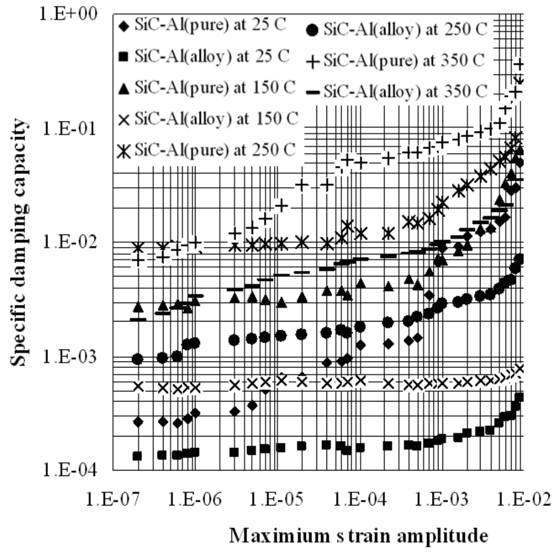

Figure 9: Strain dependence of mechanical damping at room and elevated temperature in SiC-Al_{pure} and Al_{alloy} matrix composites with fiber volume fraction of 30%. (80 to 150 KHz, longitudinal vibration mode).

The strain amplitude dependence of mechanical damping in the longitudinal vibration mode in the temperature range of 25 to 350 ºC, for H.S.C-Al_{pure} matrix composite, is shown in Fig.9. It is evident that increasing composite matrix ductility seems to further weaken the fiber-matrix interfacial region, resulting in higher specific damping values particularly at increasing strain amplitude. From these results it is also apparent that continuous ceramic fiber reinforced MMC's retain their mechanical properties and thermal stability even at elevated temperatures because any interaction between fiber and matrix constituents occurs very slowly in the solid state.

Little or no information were reported in the literature pertinent to temperature dependence of dynamic modulus and damping for continuous fiber reinforced metal matrix materials at elevated temperature. Previous studies, [20-25], on temperature dependence of dynamic modulus and damping were all carried out at room temperature and on either whisker or discontinuous fiber reinforced metal matrix composites. Therefore, making these results obtained in this paper, to be the first such reported information for continuous ceramic fiber reinforced MMC's at elevated temperatures.

4. Conclusions

The dynamic modulus in the longitudinal (II) and transverse ($\perp$) fiber direction, and mechanical damping in the longitudinal vibration mode only, were measured for the tested MMC's at room and elevated temperatures and conducted at up to 150 kHz. The temperature dependence of dynamic modulus in all tested MMC's showed a linear, monotonic decrease in modulus with increase in temperature, except in the case of H.S.C-Al_{pure} and Al_{alloy} matrix composites, the presence of H.S.C fibre reinforcement has led to a non-monotonic decrease in modulus.

The obtained results for fiber reinforced Al_{pure} matrix composites, showed a strain amplitude dependent damping at room temperature, while the B, SiC, and Al_2O_3, fiber reinforced Al_{alloy} matrix material exhibited essentially an amplitude independent damping at high strain amplitudes. At lower strain amplitudes, these composites became strain amplitude dependent on damping.

Increasing the volume fraction of high strength carbon fiber in Al_{pure} matrix in the range of 25 to 57%, has resulted in increasing the fiber-matrix interfacial areas, this seems to be effective in increasing the damping in such composites. The measured longitudinal vibration mode of damping for H.S.C-Al_{pure} matrix composite at temperature in the range of 25 to 350 ºC has shown to exhibit strain amplitude dependent damping.

References

[1] Ming Yang, V.D. Scott and R.L.Trumper, "The role of interface on the mechanical behaviour of carbon fibre reinforced aluminium alloy composites". Metal Matrix Composites 2nd Conference. The Royal Society, U.K, 1989.

[2] Evans A, March, C.S, Mortensen. Metal Matrix Composites in industry. An Introduction and Survey. Klumer Academic Publisher; 2003, 375-386.

[3] Arsenault, R.J. and Fisher, R.M. , " Microstructure of fibre and particulate SiC in 6061 Al composites. Scripta. Met. Vol.17, 1983,67-71.

[4] Hunt, W.H. Interfacial zones and mechanical properties in continuous fiber FP/Al-Li metal matrix composites. In: Dhingra and Fishman. Interfaces in metal matrix composites. (, Warrendale: Met. Soc.AIME; 1986, 3-25.

[5] Ramadan J. Mustafa and Yassin L. Nimir, "A New Process for Manufacturing Continuously Reinforced Aluminium Alloy MMC". Mu'tah Lil-Buhuth wad-Dirasat (Mu'tah Journal for Research and Studies), Natural and Applied Sciences Series, Vol.21, No. 2, 2006, 183-206.

[6] P.J. de Groot, P.M. Wijnen, and R.B.F. Janssen,"Real-Time Frequency Determination of Acoustic Emission for Different Fracture Mechanics Carbon/Epoxy Composites".Comp. Sci. and Tech.,Vol.55 , 1995, 405-412

[7] M. V. Lysak, Development of the theory of Acoustic Emission by Propagating Cracks in Terms of Fracture Mechanics. Eng. Fracture Mechanics, Vol.55, No.6,. 1996, 443-452.

[8] M. Radovic, E. Lara-Curzio, L.Riester in "Comparison of Different Experimental Techniques for Determination of Elastic Properties of Solids". Material Science and Eng., 368, 2004, 56-70.

[9] Granato, A. and Lucke, K.," Application of dislocation theory to internal friction phenomena at high frequencies". Journal of Applied Phyiscs, Vol.27, 1956b,789-805.

[10] Markham, M. F. Measurement of the elastic constants of fibre composites by ultrasonic. Composites, Part A; 1970.

[11] Robinson, W.H. and Edgar A.," The piezoelectric method of determining mechanical damping at frequencies of 30 to 200KHz". IEEE Trans. Sonics and Ultrasonic SU-Vol. 21,1974, 98-105.

[12] Lin, D. X., R. G. Ni and R. C. Adams.," Prediction and Measurement of the Vibrational Damping Parameters of Carbon and Glass Fibre Reinforced Plastic Plates". J. Composite Materials, Vol.18, No.2, 1984,132-152.

[13] Friedel, J. Dislocations. Vol.3, New York.: Pergammon Press, ;1964; pp. 454-457.

[14] Audoin B., Baste S., "Ultrasonic evaluation of stiffness tensor changes and associated anisotropic damage in a ceramic matrix composite". Journal of Applied Mechanics, Vol. 59, 1994, 445-448

[15] Ni, R. G. and R. C. Adams, " The Damping and Dynamic Moduli of Symmetric Laminated Composite Beams-Theoretical and Experimental Results". Journal Composite Materials, Vol.18, No.2, 1984, 104-121.

[16] Schoenberg, T. Boron and Silicon Carbide fibres.In: C.A Dostal. Composites, Vol. 1 , Ohio: ASM International, Metals Parks; 1987, 54-65.

[17] ASM Engineered Materials Handbook, Composites ,Vol.1, ASM International Metals, Metals Park, Ohio,1987.

[18] J.R. Davis (Ed), Metals Handbook, ASM International, Materials Park; Ohio, 1990.

[19] Harmouche, M., and Wolfenden, A., "Temperature and Composition Dependence of Young's Modulus for Ordered B2 polycrystalline CoAl and FeAl". Mat. Sci, Eng A, Vol.84, 1986, 35-41.

[20] Liu, J.M. "Temperature dependence and hysteresis of Young's modulus in a graphite/aluminum metal matrix composite". Appl. Phys. Lett. Vol.48, 1986, 469-471

[21] Castagnede B., Jenkings, J. T., Sachse W., Baste S. "Optimal determination of the elastic constants of composite materials from ultrasonic wave-speed measurements". Journal of Applied Physics, Vol. 67, 1990, 657-665

[22] H.W. Viehrig, K.Popp, and R. Rintamaa, Measurement of Dynamic Elastic-Plastic Fracture Toughness Parameters Using Various Methods, Int. J. Press. Ves. And Piping, Vol. 55 ,1993, 233-241.

[23] Sahay, S, Kline R., Mignogna, R.," Phase and group velocity considerations for dynamic modulus measurements in anisotropic media". Ultrasonic, Vol. 30., No. 6, 1992, 373-382.

[24] Hufenbach, W., Langkamp, A., Kroll, L., Bohm, R., "Experimental investigation and modeling of failure and damage behaviour of multi-layered carbon fibre reinforced". PEEK14th International Conference on Composite Materials Proceedings (ICCM 14), San Diego, USA, 2003.

[25] Hufenbach, W., Bohm, R., Kroll, L., Langkamp, A., "Theoretical and experimental investigation of anisotropic damage in textile reinforced composite structures". Mechanics of Composites, Vol. 40, No.6, 2004,.519-532.

[26] Ramadan. J. Mustafa and Yassin L. Nimir, "The Fracture Behaviour of Continuous SiC and Carbon Fibre Al-Matrix Composites under Mode II Loading Conditions". Mu'tah Lil-Buhuth wad-Dirasat (Mu'tah Journal for Research and Studies), Natural and Applied Sciences Series, Vol.18, No.1, 2003.

JJMIE

Volume 2, Number 1, Mar. 2008
ISSN 1995-6665
Pages 23 - 30

Jordan Journal of Mechanical and Industrial Engineering

Novel Thermal Resistance Network Analysis of Heat Sink with Embedded Heat Pipes

Jung-Chang Wang *

Taiwan Microloops Corporation, Taoyuan, Taiwan

Abstract

This article utilizes the experimental method to investigate the thermal performance of heat sinks with one and two pairs of embedded heat pipes. A heat sink with embedded heat pipes transfers the total heat capacity from the heat source to both the base plate and heat pipes, and then disperses heat into the surrounding air via the forced convection. The heat transference from base plate to fins can be conducted through the examined results of the heat sink with and without the function of heat pipes. The heat capacity from heat pipes to fins is equal to the total heat minus the heat from base plate to fins. Therefore, the heat carried by embedded heat pipes can be found using the thermal resistance analytical approach stated in this article. The results show that two and four heat pipes embedded in the base plate carry 36% and 48% of the total dissipated heat respectively; in addition, when the total heating power of the heat sink with two embedded heat pipes is 140W, the total thermal resistance reaches its minimum value of 0.27ºC/W, while for the heat sink with four embedded heat pipes, when the total heating power is between 40W and 240W, the total thermal resistance is 0.24ºC/W, meaning that the thermal performance is better than that of heat sink with two embedded heat pipes.

Keywords: Thermal Resistance; embedded heat pipes;

Nomenclature

h	heat transfer coefficient, W/m^2.K
H	length from base plate to condensation section of heat pipes, m
H_1	length from base plate to adiabatic line, m
H_2	length from adiabatic line to condensation section of heat pipes, m
k	thermal conductivity, W/ m.K
Q	total heat transfer rate, W
Q_b^i	heat transfer rate from base plate to fins, W
Q_j^i	heat transfer rate from j_{th} position heat pipes to fins, W
R	thermal resistance, K/W
R_t^i	total thermal resistance, K/W
R_c^i	thermal contact resistance, K/W
R_n^i	fin-base convective thermal resistance, K/W
R_{hj}^i	base to j_{th} position heat pipes thermal resistance, K/W
R_{pj}^i	j_{th} position heat pipes thermal resistance, K/W
R_{fj}^i	j_{th} position fin-pipe convective thermal resistance, K/W
T	temperature, K
T_b	one-dimensional temperature of adiabatic line, K
T_{cj}^i	mean temperature of condensation section of heat pipes, K
T_{ej}^i	mean temperature of evaporation section of heat pipes, K
T_u^i	mean upper surface temperature of base plate, K

Subscripts

a	ambient
b	base plate
d	lower central surface of base plate
f	fin
h	heat source
j	position of embedded heat pipes

Superscript

i	the sum of embedded heat pipes

* Corresponding author. e-mail: jc_wang@microloops.com

1. Introduction

Since 1971, when the Intel Corporation launched the first chip (with 10μm wires and 2300 transistors) , the number of transistors in a chip has increased to over ten million. This means that an equivalent surface area of chip produces far greater heat than previously, leading to an increase in critical heat flux speed. The maximum limited temperature that can be borne by silicon chip in electronic components is 120ºC, with a normal operating temperature of under 70ºC. The reliability of electronic components drops by 10% for each increase of 2ºC in normal operating temperature[1], and high temperature is a major reason for the malfunctioning or shortening of life of electronic components. Thus, it is necessary to quickly remove high heat generated by electronic components for a normal operating temperature of under 70ºC.

In the past, the method used for solving the high heat capacity of electronic components has been to install a heat sink with a fan directly on the heat source, removing the heat through forced convection. Webb[2] pointed out that it is necessary to increase the fin surface and fan speed of the direct heat removal heat sink in order to solve the ever-increasing high heat flux generated by CPUs. The total thermal resistance is used to evaluate the thermal performance of a heat sink. Duan and Muzychka[3] increased the heat dispersing surface area of the heat sink fins, reducing the total thermal resistance from 0.55 ^{o}C/W to 0.35 ^{o}C/W. Lin et al.[4] boosted the fan speed to obtain an optimum total thermal resistance value of 0.33 ^{o}C/W at a maximum speed of 4000rpm. However, increasing the surface area results in an increase in cost and boosting the fan speed results in noise, vibration and more power consumption, which increase the probability of failure to electronic components.

In a heat sink with embedded heat pipes, the use of heat pipes to rapidly transfer heat from the heat source to the fins, without increasing the surface area of the fins or increasing the speed of the fan, makes it possible to reduce the total thermal resistance to under 0.3ºC/W. Due to high thermal conductivity of the heat pipes, the thermal resistance is very low at about $10^{-1} \sim 10^{-3}$ ^{o}C/W[5-7]. Xie et al.[8] conducted an experiment combining a 4mm diameter heat pipe and a heat sink, achieving an optimum total thermal resistance of 0.29 ^{o}C/W. Legierski and Wiecek [9] pointed out that the thermal performance of the heat sink with embedded heat pipes is better than that of an ordinary heat sink, with an optimum total thermal resistance value of 0.25 ^{o}C/W. Gernert et al.[10] used a heat sink with embedded heat pipes composed of a 25.4mm diameter heat pipe and an aluminum heat sink; when the maximum heat flux was 285W/cm^2, the minimum total thermal resistance value was 0.225ºC/W. Wang et al.[11] examined two horizontal embedded heat pipes of diameter 6mm inserted into base plate and fins in order to take heat capacity from heat source. From the results, the ratio of total heat capacity of embedded heat pipes is 36%. Therefore, a heat sink with embedded heat pipes is one of the best solutions for thermal problems of high heat generation in electronic components.

The heat sink with one and two pairs of embedded heat pipes studied in this article is shown in Fig.1(a) and Fig.1(b), respectively. The dimensions of the heat sink are 75 x 70 x 43 mm^3. The ends of heat pipes are inserted into the base plate as the evaporation section, and the other ends are embedded into the fins as the condensation section. Because the heat pipes are embedded into the left and right sides of the base plate in a parallel manner, and the heat source is placed directly onto the center of the base plate; therefore, the heat pipes bear equal heat from the heat source. Previous research only measures the contact, base plate and total thermal resistances of a heat sink with embedded heat pipes, without addressing the proportion of the total heat carried away via the heat pipes. In light of this, this study utilized experimental methods incorporating superposition method to calculate the heat carried to the fins through the base plate and embedded heat pipes, in order to find the ratio of total heat transferred through the heat pipes. These individual thermal resistances of contact, base plate, base to heat pipes, heat pipes, fins and the total thermal resistance can be obtained through thermal resistance analysis.

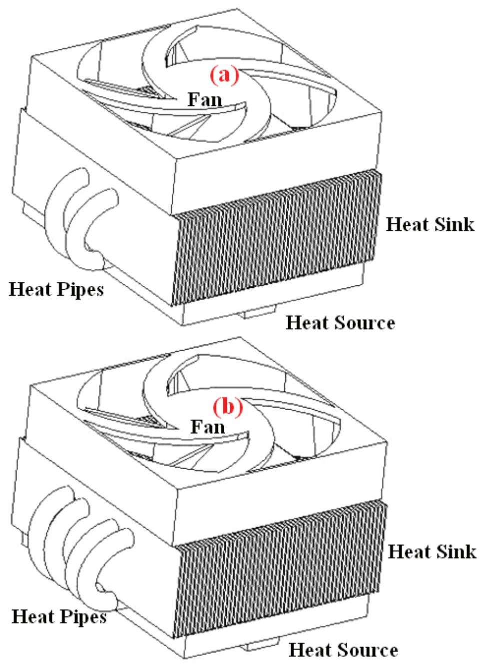

Figure 1: (a) Heat sink with one pair of embedded heat pipes, (b) Heat sink with two pairs of embedded heat pipes

2. Thermal Resistance Network

This paper use the superposition method for the heat sink with embedded heat pipes as shown in Fig. 2. The symbols i and j respectively denote the number and position of the embedded heat pipes. The total heating power Q is transferred from the heat source to the base plate and the heat pipes. The heating power Q_b^i is borne away by the base plate; the heat pipes are the adiabatic boundary conditions, and Q_b^i is transferred upward to the fins.

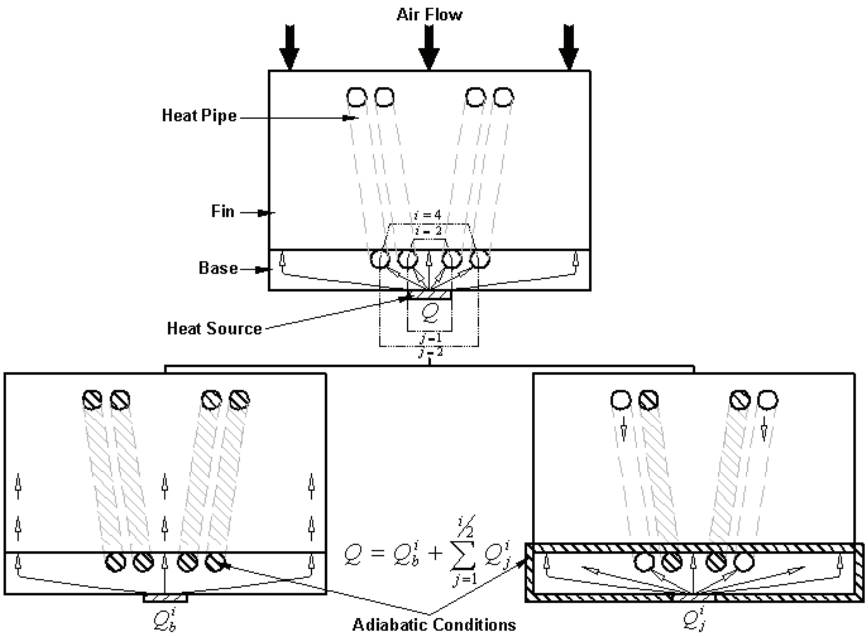

Figure 2: Superposition method of heat sink with embedded heat pipes

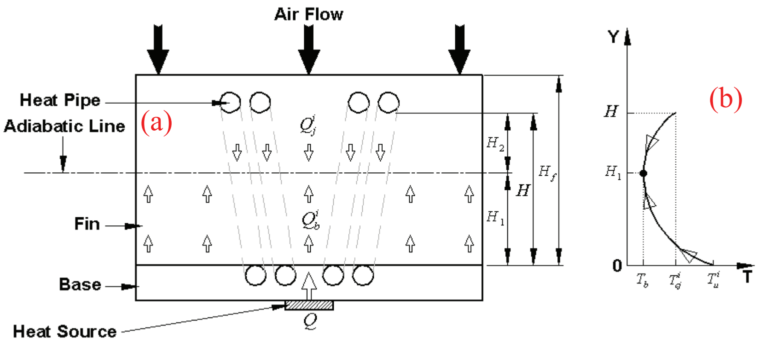

Figure 3: (a) Heat sink with embedded heat pipes heat flow pathways, (b) Fin temperature distribution

The heating power Q_j^i is carried away through the heat pipes laid in a parallel fashion to the left and right of the heat source; the base plate is the adiabatic boundary condition, and Q_j^i is transferred downward to the fins. Consequently, Q equals the sum of Q_b^i and Q_j^i from the superposition method. Because of measuring the thermal performance by separately testing the heat sink with and without the function of heat pipes, Q_b^i can be found from comparing the same temperature differences corresponding to the input heating power. Then Q_j^i equals to Q minus Q_b^i.

Assuming that Q_b^i and Q_j^i transfer heat as one-dimension steady heat flow model, and Q is divided into two pathways transferring heat from Q_b^i upward and Q_j^i downward to the fins as shown in Fig. 3(a). The region where temperature gradient equals to zero appearing between these two heat transfer pathways is called adiabatic line. The fins in this adiabatic position will not have heat transfer. The distance from the upper surface of the base plate to the condensation section of the heat pipes is H, and those from the adiabatic position to the upper surface of the base plate and to the condensation section of the heat pipes are H_1 and H_2 respectively. Figure 3(b) shows temperature distribution graph for the surface of the fins, where T_b is adiabatic temperature, T_{cj}^i is the temperature of the condensation section of the heat pipes, and T_u^i is the temperature of the upper surface of the base plate. Assuming these temperatures are uniform both on the upper surface of the base plate and on the condensation section of the heat pipes, the steady one-dimensional energy balance equation for fins is[12]

$$\frac{d^2T^i}{dY^2} - m^2\left(T^i - T_a^i\right) = 0 \tag{1}$$

and

$$m = \sqrt{\frac{2h}{k_j t_f}} \tag{2}$$

where h represents the convective heat transfer coefficient, k_f is the fin conductivity , t_f is the fin thickness and T_a^i is the ambient temperature. The specified boundary conditions can be expressed as

$$T^i = T_u^i \ \ at \ \ Y = 0 \ \ and \ \ T^i = T_{cj}^i \ \ at \ \ Y = H \tag{3}$$

The temperature profile for the fins can be obtained from Eq.(1) as

$$T^i(Y) = T_a^i + \left[\frac{\left(T_u^i - T_a^i\right)e^{mH}}{e^{mH} - e^{-mH}} - \frac{\left(T_{cj}^i - T_a^i\right)}{e^{mH} - e^{-mH}}\right]e^{-mY} + \left[\frac{\left(T_{cj}^i - T_a^i\right)}{e^{mH} - e^{-mH}} - \frac{\left(T_u^i - T_a^i\right)e^{-mH}}{e^{mH} - e^{-mH}}\right]e^{mY} \quad (4)$$

From the definition of adiabatic line,

$$\frac{\partial T^i}{\partial Y} = 0 \;\; at \;\; Y = H_1 \quad (5)$$

The location of adiabatic line can be shown as

$$H_1 = \frac{1}{2m}\ln\left[\frac{\left(T_u^i - T_a^i\right)e^{mH} - \left(T_{cj}^i - T_a^i\right)}{\left(T_{cj}^i - T_a^i\right) - \left(T_u^i - T_a^i\right)e^{-mH}}\right] \quad (6)$$

Figure 4 shows an analysis of the thermal resistance network of the heat sink with embedded heat pipes. When the superscript i equals 2 or 4, it represents, respectively, that the heat sink has a total of two or four embedded heat pipes. The heat sink with two embedded heat pipes has base plate thermal resistance R_b^2 and fin-base convective resistance R_n^2 in the Q_b^2 pathway, and base to heat pipes resistance R_{h1}^2, heat pipes resistance R_{p1}^2 and fin-pipe convective resistance R_{f1}^2 in the Q_1^2 pathway when i equals to 2. When i is 4, the heat sink with four embedded heat pipes has a base plate thermal resistance R_b^4, fin-base convective resistance R_n^4 in the Q_b^4 pathway, base to inner heat pipes resistance R_{h1}^4, inner heat pipes resistance R_{p1}^4, inner fin-pipe convective resistance R_{f1}^4, base to outer heat pipes resistance R_{h2}^4, outer heat pipes resistance R_{p2}^4 and outer fin-pipe resistance R_{f2}^4 in Q_1^4 and Q_2^4 pathway, respectively.

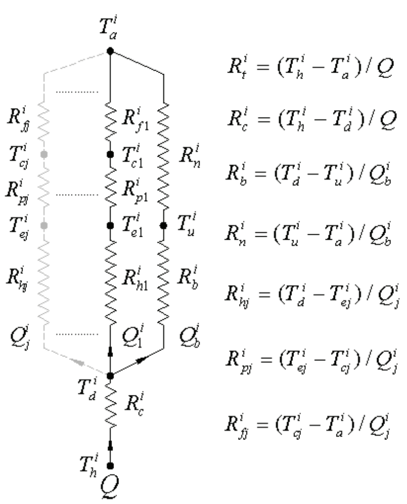

Figure 4: Thermal resistance analysis network

The total thermal resistance R_t^i can be expressed as the sum of the thermal contact resistance R_c^i and the thermal resistances on the pathways of Q_b^i and Q_j^i, which is

$$R_t^i = R_c^i + \frac{1}{\frac{1}{\left(R_b^i + R_n^i\right)} + \sum_{j=1}^{i/2}\frac{1}{\left(R_{hj}^i + R_{pj}^i + R_{fj}^i\right)}} \quad (7)$$

In Eq. (7), R_t^i is defined as the temperature difference (the temperature of heat source T_h^i minus the ambient temperature T_a^i) divided by total heating power Q. R_c^i is defined as the effective temperature difference at the interface (T_h^i minus the temperature at the center of the lower surface of the base plate T_d^i) divided by Q. R_b^i is defined as the temperature difference (T_d^i minus the average temperature at upper surface of the base plate T_u^i) divided by Q_b^i. R_n^i is defined as the temperature difference (T_u^i minus T_a^i) divided by Q_b^i. R_{hj}^i is defined as the temperature difference (T_d^i minus the temperature of evaporation section of heat pipes T_{ej}^i) divided by Q_j^i. R_{pj}^i is defined as the temperature difference (T_{ej}^i minus the temperature of condensation section of heat pipes T_{cj}^i) divided by Q_j^i. R_{fj}^i is defined as the temperature difference (T_{cj}^i minus T_a^i) divided by Q_j^i.

3. Experimental Investigation

The experimental methods stated in this paper are mainly aimed at testing the thermal performance of the heat sink with embedded heat pipes as shown in Fig. 5. The heat pipes are bending pipes with a diameter 6 mm and a total length 170 mm. The length of evaporation section and condensation section is 65 mm respectively, and the insulated length is 40 mm. The materials of heat pipe's container and wick type are copper metal and sintered structure of pure copper powder respectively. According to the superposition method for the heat sink with embedded heat pipes, the first step is to measure the entire thermal performance of the heat sink with embedded heat pipes, then measure that of the heat sink with losing the function of embedded heat pipes at positions where j is equal to $1, 2 \ldots i/2$, successively. The heat capacity transference from the base plate and the heat pipes to the fins can be obtained by comparing the individual results in the same temperature differences respectively.

The experimental test includes the experiments of heat sinks with two and four embedded heat pipes respectively. The upper surface of the dummy heater is coated with thermal grease to reduce contact resistance.

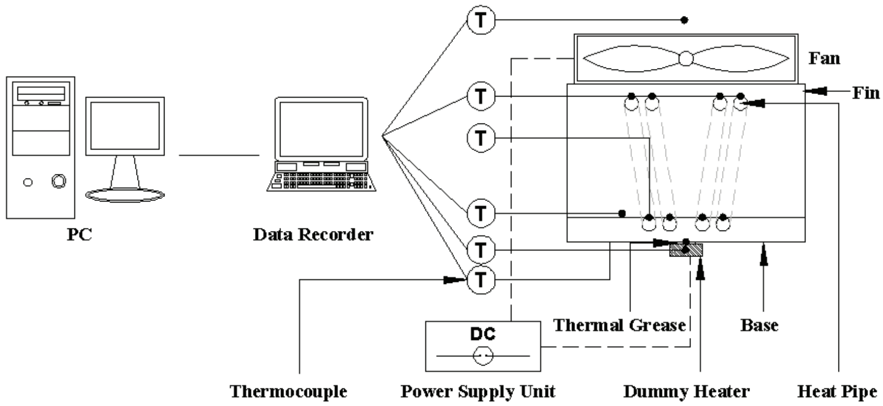

Figure 5: Experimental apparatus for Heat sink with embedded heat pipes

A T-type thermocouple is attached to the upper surface of the dummy heater to measure the temperature (T_h^i). Six thermocouples are attached to the center of the lower surface of base plate and five points along the diagonal of the upper surface of base plate, measuring the temperatures at the center of the lower surface of the base plate (T_d^i) and the average temperature of the upper surface of the base plate (T_u^i). Computational Fluid Dynamic commercial software (Icepak) is used to calculate the average temperature of T_u^i, which is compared with the experimental measurement of five-point average value and develops a correlation between them within an error of ±3%. A fan is placed on the top of heat sink to disperse heat through forced convection. A thermocouple is placed on the top of the fan to measure the ambient temperature (T_a^i). Thermocouples are attached to the evaporation and condensation sections of heat pipes to measure the temperatures of T_{ej}^i and T_{cj}^i. This experiment starts with a heating power of 40W and increases it up to 240W by increments of 20W.

After separately testing the full thermal performance of the above two experiments for the heat sink with function of embedded heat pipes, let all heat pipes in the heat sink with two embedded heat pipes fail to function ,and allow the inner (j = 1) and outer (j = 2) heat pipes in the heat sink with four embedded heat pipes to fail to function successively. The heat sink experiments without the function of heat pipes are then performed, and the corresponding thermal resistances can be determined.

The thermocouples used in the experiment have a measurement error of ± 0.5 ºC. The cooling circulator manufactured by Firstek Scientific Co., Ltd., has a measurement error of ± 0.5 ºC. The data recorder manufactured by Yokogawa Co., Ltd., has a measurement error of ±1 %. The power supply unit has a measurement error of ±0.5 %. The maximum error for the thermal resistance is within ±5 %.

4. Results and Discussions

Figure 6 shows the experimental results of thermal performance lines for a heat sink with and without the function of two embedded heat pipes. As the heating power is increasing, the temperature difference ($T_u^2 - T_a^2$) between the upper surface of the base plate and the surrounding air also increases whether with or without the function of two heat pipes. The slopes of these two lines represent the thermal resistances. Because the slope of the upper line is greater than that of the lower, the thermal resistance without function of heat pipes is greater than that with function of two heat pipes. It means that the temperature difference ($T_u^2 - T_a^2$) is higher without the function of two heat pipes than that with the function of two heat pipes.

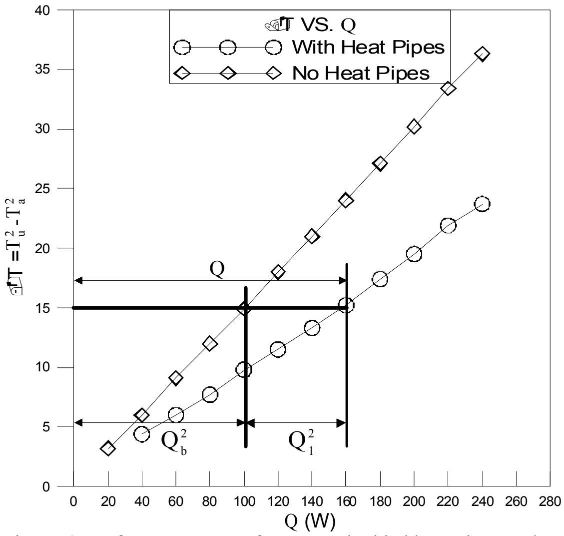

Figure 6: Performance curve for two embedded heat pipes under various heating power

This is because having an extra path transfers heat from heat pipes to surrounding and thus reduces the temperature difference. As the temperature difference for the two lines is fixed as shown in Fig.6, it reaches the thermal performance lines with two points at the power input with and without function of two heat pipes. The corresponding heating power represents the Q_b^2 in the heat sink without the function of two heat pipes and the total Q with the function of two heat pipes. The heat transfer rate Q_1^2 is equal to the total Q minus the Q_b^2. As indicated in Fig.6, the temperature difference is 15.2ºC, the heating power for Q is 160W, and the power for Q_b^2 is 102.6W. Therefore Q_1^2 equals 57.4W. Table 1 shows the ratio of bypass heating power to total heating power. The ratio (Q_b^2 / Q) is 64% and the ratio (Q_1^2 / Q) is 36%.

Table 1. Ratio of bypass heating power to total heating power of heat sink with two embedded heat pipes

Q (W)	Q_b^2/Q (%)	Q_b^2 (W)	Q_1^2/Q (%)	Q_1^2 (W)
40	67	26.9	33	13.1
60	67	40	33	20
80	64	51.4	36	28.6
100	65	65	35	35
120	63	76	37	44
140	63	88.6	37	51.4
160	64	102.6	36	57.4
180	64	116	36	64
200	65	129.5	35	70.5
220	66	146	34	74
240	66	157.4	34	82.6

Figure 7 shows the experimental results of thermal performance lines for a heat sink with and without the function of four embedded heat pipes. As is the case in Fig.6, the temperature difference of heat sink without function of embedded heat pipes is the same in the heat sink with embedded heat pipes, which is fixed the temperature difference of three curves in the Fig.7. The corresponding heat transference rate is equal to Q_b^4. Let the temperature difference of the inner embedded heat pipes be the same in the heat sink with four embedded heat pipes : Q_1^4 is equal to the corresponding heat transferring rate minus Q_b^4, and Q_2^4 is equal to Q minus Q_b^4 adding Q_1^4. As indicated in Fig.7, the temperature difference is 14.8ºC, the heating power for Q is 200W, the power for Q_b^4 is 104.4W, the power for Q_1^4 is 53.9W, and the power for Q_2^4 is 41.7W. Table 2 shows the ratio of bypass heating power to total heating power. The ratio (Q_b^4/Q) is 52%, the ratio (Q_1^4/Q) is 27%, and the ratio (Q_2^4/Q) is 21%.

Table 2. Ratio of bypass heating power to total heating power of heat sink with four embedded heat pipes

Q (W)	Q_b^4/Q (%)	Q_b^4 (W)	Q_1^4/Q (%)	Q_1^4 (W)	Q_2^4/Q (%)	Q_2^4 (W)
40	52	20.8	27	11	21	8.2
60	52	31.2	27	16.5	21	12.3
80	50	39.9	29	23.1	21	17
100	51	50.6	27	27.2	22	22.2
120	51	61.4	27	32.5	22	26.1
140	52	72.1	27	37.9	21	30
160	52	82.9	27	43.2	21	33.9
180	52	93.6	27	48.5	21	37.9
200	52	104.4	27	53.9	21	41.7
220	52	114.2	27	60.2	21	45.6
240	52	125.6	27	64.9	21	49.5

Figure 8 indicates the relationships of the base plate resistance R_b^i and the fin-base convective resistance R_n^i toward the heating power Q_b^i. These thermal resistance curves on the paths Q_b^i are a horizontal trend line as shown in Fig.8. R_b^2 and R_n^2 are approximately 0.25ºC/W and 0.15ºC/W respectively when Q_b^2 is between 26.9 and 157.4 W. R_b^4 and R_n^4 are approximately 0.28ºC/W and 0.14ºC/W respectively when Q_b^4 is between 20.8 and 125.6 W. They do not change as heating power increases. Thus, R_b^i and R_n^i in this experiment can be considered constants.

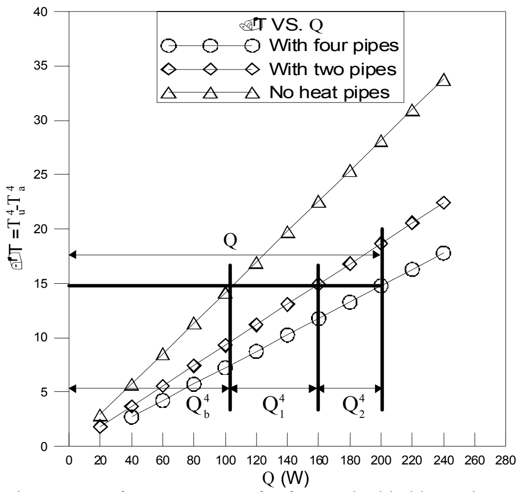

Figure 7: Performance curve for four embedded heat pipe under various heating power

The reason is that the components transferring heat through this path of heating power Q_b^i transferred from the base plate without function of heat pipes to the fins are all solid. The thermal physical properties of these components are the same when there is not much change in temperature. Thus R_b^i and R_n^i should remain constant. R_b^i and R_n^i obtained in this experiment are both constant, corroborating the correctness of the experimental results. The experimental results of R_b^4 is larger than that of R_b^2, resulting from the distortion effect of heat sink with four embedded heat pipes larger than that of heat sink with two embedded heat pipes. From above-mentioned experimental results, R_b^i increases and R_n^i decreases as i increases.

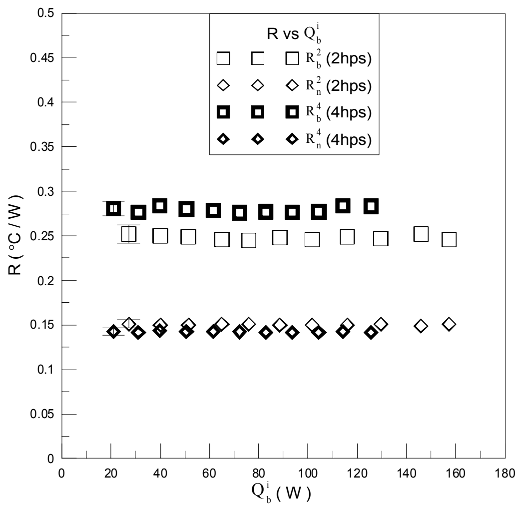

Figure 8: Relationships of base plate resistance R_b^i and fin-base convective resistance R_n^i with the heating power Q_b^i

Figure 9 indicates the base to heat pipes resistance R_{hj}^{i}, heat pipes resistance R_{pj}^{i} and fin-pipe convective resistance R_{fj}^{i} with heating power Q_{j}^{i}. R_{h1}^{2} drops from 0.43ºC/W to 0.33ºC/W under heating power of 13W to 40W. When Q_{1}^{2} is 51.8W, it reaches a minimum value of 0.32ºC/W. R_{h1}^{2} rises from 0.33ºC/W to 0.39ºC/W under heating power of 57.6W to 82.6W. R_{h1}^{4} drops from 0.38ºC/W to 0.35ºC/W under heating power of 11W to 27.2W. When Q_{1}^{4} is 37.9 W, it reaches a minimum value of 0.34ºC/W. R_{h1}^{4} rises from 0.36ºC/W to 0.41ºC/W under heating power of 43.2W to 64.9W. R_{h2}^{4} drops from 0.58ºC/W to 0.53ºC/W under heating power of 8.2W to 22.2W. When Q_{2}^{4} is 30 W, it reaches a minimum value of 0.52ºC/W. R_{h2}^{4} rises from 0.58ºC/W to 0.61ºC/W under heating power of 37.8W to 49.6W.

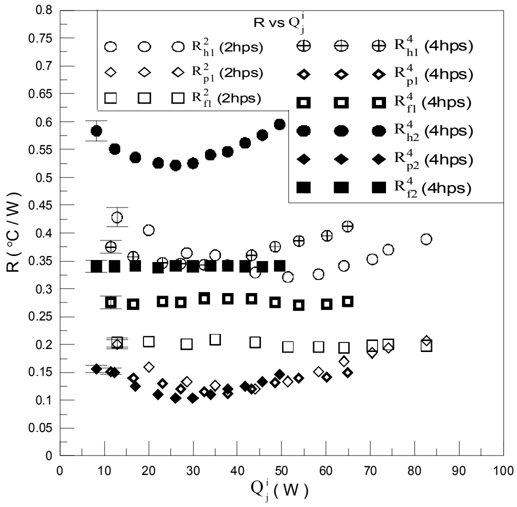

Figure 9: Relationships of the base to heat pipes resistance R_{hj}^{i}, heat pipes resistance R_{pj}^{i} and fin-pipe convective resistance R_{fj}^{i} with heating power Q_{j}^{i}

The fin-pipe convective resistance R_{fj}^{i} do not change much as the heating power increases, so they can be considered a constant in this experiment. When the Q_{1}^{2} is 13W to 82.6W, R_{f1}^{2} is approximately 0.20ºC/W. R_{f1}^{4} is approximately 0.28ºC/W while Q_{1}^{4} is 11W to 64.9W. R_{f2}^{4} is approximately 0.34ºC/W when the Q_{2}^{4} is 8.2W to 49.6W. R_{p1}^{2} drops from 0.20ºC/W to 0.13ºC/W when Q_{1}^{2} is between 13W and 44W. It reaches its minimum value of 0.12ºC/W when Q_{1}^{2} is 51.8W. R_{p1}^{2} rises from 0.15ºC/W to 0.21ºC/W when Q_{1}^{2} is between 57.6W and 82.6W. The R_{p1}^{4} drops from 0.15ºC/W to 0.12ºC/W when Q_{1}^{4} is between 11W and 32.5W. It reaches its minimum value of 0.11ºC/W when Q_{1}^{4} is 37.9W. The R_{p1}^{4} rises from 0.12ºC/W to 0.15ºC/W when Q_{1}^{4} is between 43.2W and 64.9W. The R_{p2}^{4} drops from 0.16ºC/W to 0.11ºC/W when Q_{2}^{4} is between 8.2W and 22.2W. It reaches its minimum value of 0.10ºC/W when Q_{2}^{4} is 30W. The R_{p2}^{4} rises from 0.12ºC/W to 0.15ºC/W when Q_{2}^{4} is between 37.8W and 49.6W. They change as the heating power changes.

Figure 10 shows the relationships of the total thermal resistance and thermal contact resistance to the total heating power Q. The contact thermal resistance is approximately 0.03ºC/W when the heating power is between 40W and 240W. Therefore the contact thermal resistance in this experiment can be seen as a constant. The total thermal resistance R_{t}^{2} drops from 0.32ºC/W to 0.27ºC/W when the heating power is between 40W to 140W and reaches its minimum of 0.27 ºC/W at 140W. R_{t}^{2} rises from 0.27ºC/W to 0.29ºC/W under 140W to 240W. This is because of the heating power increasing to the point that the embedded heat pipes are starting to function, and the total thermal resistance shows a decreasing trend. The heat pipes are unable to bear excessive higher heat at heating powers of above 240W, causing the evaporation section to produce more amounts of vapor than that of condensed liquid, resulting in the heat pipes losing performance, thereby increasing total thermal resistance. The total thermal resistance R_{t}^{4} is 0.24 ºC/W when the heating power is 40 to 240 W and does not change much as the heating power increases. This is because the four embedded heat pipes carry away 48% of the total heat, and the two outer heat pipes can share the load of the two inner heat pipes load, not causing R_{t}^{4} to increase.

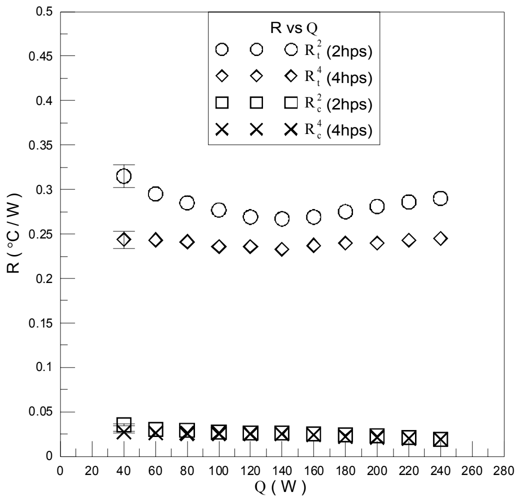

Figure 10: Relationships of the total thermal resistance and thermal contact resistance with heating power Q

Figure 11 indicates the temperature of heat source with total heat transference rate Q. The temperature of heat source T_{h}^{i} of heat sink with two (i = 2) and four (i = 4) embedded heat pipes can be calculated by Eq. (8) and Eq. (9) at heating power 40W to 240W respectively. When the T_{h}^{i} is 70ºC, the corresponding heating power Q of the heat sink with two and four embedded heat pipes is 131W and 164W individually. This means that the temperature of heat sink with four embedded heat pipes rises more slowly than that of two embedded heat pipes in the same heating power. The reason is that outer heat pipes of the heat sink with four embedded heat pipes can bear and carry away an additional 33W of heat capacity from the heat source when the T_h^i is 70º. Furthermore, with respect to CPUs that emit high heat flux, a heat sink with four embedded heat pipes is able to carry away heat capacity faster than a heat sink with two embedded heat pipes, thereby attaining a lower CPU operating temperature.

$$T_h^2 = 0.30 \times Q + 30.6 \quad (8)$$

$$T_h^4 = 0.24 \times Q + 30.6 \quad (9)$$

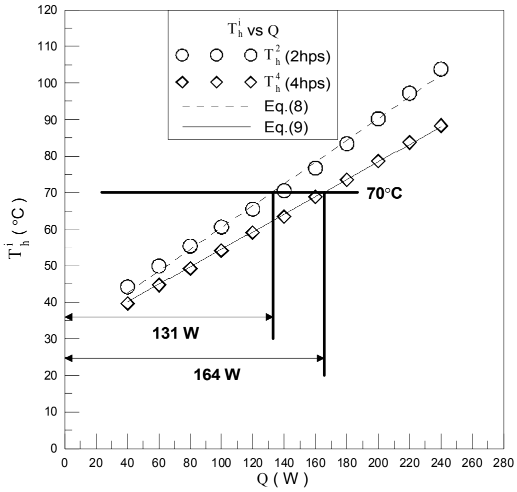

Figure 11: Relationships of the temperature of heat source with total heat transferring rate Q

5. Conclusions

Through these experiments in this study, it has been found that heat transfer rate Q_1^2 and Q_b^2 of heat sink with two embedded heat pipes occupy 36% and 64% of the total Q respectively, and Q_2^4, Q_1^4 and Q_b^4 of the heat sink with four embedded heat pipes account for 21%, 27% and 52% of the total Q individually. Moreover, the total thermal resistance of the heat sink with two embedded heat pipes is only affected by changes in the base to heat pipes thermal resistance and heat pipes thermal resistance over the heat flow path of the Q_1^2; that is, the total thermal resistance varies according to the functionality of the heat pipes. As for the total thermal resistance of heat sink with four embedded heat pipes, at 40W to 240W, the two outer heat pipes can carry away more heat, so the total thermal resistance is a constant. If the temperature of the heat source is not allowed to exceed 70º, the total heating powers of heat sink with two and four embedded heat pipes will not exceed 131W and 164W respectively. Finally, the superposition principal analytical method for the thermal performance of the heat sink with embedded heat pipes is completely established in the present paper.

References

[1] Bar-Cohen, A. D. Kraus, and S. F. Davidson, "Thermal frontiers in the design and packaging microelectronic equipment". Mechanical Engineering, Vol. 105, No. 6, 1983, 53-59.

[2] Ralph L. Webb, "Next Generation Devices for Electronic Cooling with Heat Rejection to Air". ASME J. Heat Transfer, Vol.127, 2005, 2-10.

[3] Zhipeng Duan, and Yuri S. Muzychka, "Impingement air cooled plate fin heat sinks Part II- Thermal resistance model". IEEE Inter Society Conference on Thermal Phenomena, 2004.

[4] S. C. Lin, F. S. Chuang, and C. A. Chou, "Experimental study of the heat sink assembly with oblique straight fins". Experimental Thermal and Fluid Science, Vol. 29, 2005, 591–600.

[5] G.. P. Peterson. An introduction to heat pipe - modeling, testing, and applications. New York: John Wiley & Sons Inc.; 1994.

[6] Taxiong Wang, and G. P. Peterson, "Investigation of a Novel Flat Heat Pipe". ASME J. Heat Transfer, Vol. 127, 2005, 165-170.

[7] Faghri, Heat Pipe Science and Technology, Taylor and Francis Ltd., 1995.

[8] H. Xie, A. Ali, and R. Bhatia, "The use of heat pipes in personal computers". Inter Society Conference on Thermal Phenomena, 1998.

[9] Jaroslaw Legierski, and Boguslaw Wiecek, "Steady state analysis of cooling electronic circuits using heat pipes". IEEE Transactions on Components and Packing Technologies, Vol.24, No.4, 2001, 549-553.

[10] N. J. Gernert, J. Toth, and J. Hartenstine, "100 W/cm^2 and higher heat flux dissipation using heat pipes". 13th International Heat Pipe Conference, 2004.

[11] J.C. Wang, H.S. Huang, and S.L. Chen, "Experimental investigations of thermal resistance of a heat sink with horizontal embedded heat pipes". International Communications in Heat and Mass Transfer, Vol. 34, 2007, 958-970.

[12] W. M. Rohsenow, J. P. Hartnett, and Y. I. Cho. Handbook of heat transfer .3 rd ed. McGraw-Hill; 1998.

JJMIE

Volume 2, Number 1, Mar. 2008
ISSN 1995-6665
Pages 31 - 44

Jordan Journal of Mechanical and Industrial Engineering

Future Policies and Strategies for Oil Shale Development in Jordan

Jamel O. Jaber [a], Thomas A. Sladek [b,*], Scott Mernitz [c], T. M. Tarawneh

[a] *Faculty of Engineering Technology, Al-Balqa' Applied University, Amman, Jordan*
[b] *Ockham Energy Services, 8820 W. Francis Place, Lakewood, Colorado 80215, U.S.A*
[c] *Behre Dolbear & Company (USA), Inc., 999 18th Street, Suite 1500, Denver, Colorado 80202, U.S.A*
[e] *Department of Civil Engineering, Jordan University, Amman, Jordan*

Abstract

Indigenous oil shale deposits could satisfy Jordan's demand for liquid and gaseous fuels as well as electricity for many centuries. Markets also exist for raw and retorted oil shale, spent shale, and for sulfur recovered during the upgrading and refining of crude shale oil. Although the potential benefits of oil shale development are substantial, complex and expensive facilities would be required, and these have serious economic, environmental, and social implications for the Kingdom and its people. In January 2006, the United States Trade and Development Agency (USTDA) awarded a grant to the Jordanian Ministry of Planning and International Cooperation to support the analysis of current oil shale processing technologies and the application of international expertise to the development of a oil shale industry in Jordan. The goal of the technical assistance project was to help the Governement of Jordan (GoJ) establish short- and long-term strategies for oil shale development and to facilitate the commercial production of shale oil in the country. This paper discusses the results of the project. The Kingdom's current energy situation and its previous work on oil shale are summarized, and the incentives and restraints on oil shale commercialization are described. Impediments to development are identified, and possible governmental responses are assessed.

Keywords: Oil Shale; Jordan; Retorting; Electricity; Environment; Economic Analysis;

1. Background

The Hashemite Kingdom of Jordan is about the size of Indiana in the United States of America or Portugal or Hungary in Europe. Jordan is landlocked except for about 26 km of shoreline on the Gulf of Aqaba in the Red Sea. Most of the land is on an arid desert plateau. Precipitation is sparse. Less than 4% of the land is capable of growing crops. The scarce surface water is fully utilized, and the large groundwater resources are being depleted.

Jordan is a "lower middle income country" according to the World Bank. There are about 6 million Jordanian citizens and about one million Iraqi refugees and/or visitors. The largest cities are the capital Amman (1.9 million people), Zarqa (0.5 million), and Irbid (0.28). Major economic activities are agriculture, light manufacturing, mining and quarrying, commercial services and tourism. The exchange rate for Jordanian Dinar is about USD 1.41. In 2006, the average gross domestic product per capita was about US$ 2500; inflation rate approximately 6.25%; and unemployment reached 12.5% of the total workforce [1, 2].

In 2006, the average daily energy consumption was about 107,000 barrels of liquid fuels, and electricity demand peaked at about two GW. Except for a small amount of natural gas, in the northeastern corner near the Iraqi border, almost all of needed primary energy is imported. This caused a heavy burden on the national economy, with an energy bill of more than three billion US$, in 2006 [3]. Crude oil and some refined products are imported from neighboring Arab countries through Aqaba port, and then transported to the only refinery, nearby Zarqa. Natural gas comes in a pipeline, from Egypt and runs up to the Syrian border, which at present supplies main power stations. The huge cost of imported energy, because of prevailing high prices of crude oil in the international market, has encouraged GoJ to exploit its vast resources of oil shale and renewable sources, such as solar and wind energy.

* Corresponding author. e-mail: tasladek@msn.com

2. Oil Shale Resources and Their Quality

Oil shale is a rock that contains kerogen, which is a complex organic substance that breaks down when retorted (heated) to form crude shale oil, gases, and char. Four of Jordan's best-known deposits, i.e. El Lajjun, Sultani, Jurf Ed-Darawish, and Attarat Um Ghudran, are located about 100-120 km south of Amman, close to the town of Qatrana - see Fig. 1. These contain more than 22 billion tonnes of raw oil shale [4]. Tables 1 and 2 summarize estimated reserves and characteristics of main oil shale deposits in Jordan [5]. At average oil yield of about 9.0% (roughly 22 gallons per ton (gal/t)) the potential oil yield, from the previous four deposits only, is approximately 14 billion barrels, which could satisfy Jordan's liquid fuel and electricity needs for centuries. It is clear that the all deposits have acceptable stripping ratio of about unity, which makes open-cast mining attractive, with relatively low cost.

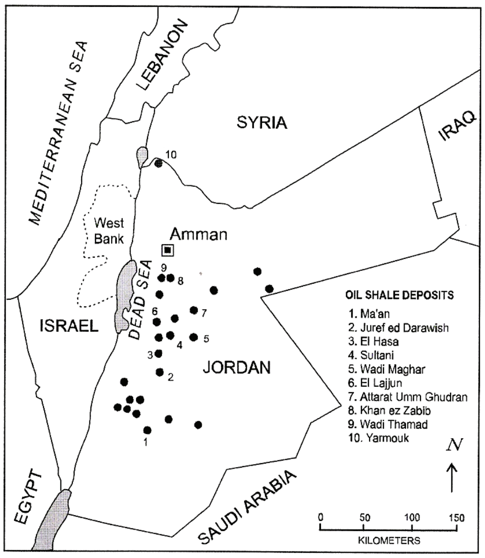

Fig. 1. Oil shale occurrences in Jordan

Nevertheless, the sulfur content is high and the ash yield is about four times that of a medium grade of bituminous coal with similar sulfur content. This makes oil shale a difficult and expensive solid fuel. Compared with Colorado shale oil (see Table 3), oil from El Lajjun deposit has (i) less nitrogen, which is good for refining, (ii) a lower pour point, i.e. flows at lower temperatures, and (iii) a lower initial boiling point: it may contain lighter hydrocarbons, which is generally good [6]. It is also heavier, which is considered relatively bad, and it contains about 15 times as much sulfur.

The high sulfur content is a very serious defect, because it makes the oil corrosive and unstable, increases the cost of refining, and it is almost impossible for the finished products to meet modern quality standards. Sulfur also inhibits the potential use of the crude shale oil as a fuel for industrial or utility applications [7, 8]. When the crude shale oil is distilled, the sulfur is distributed through all of the fractions produced, especially in heavy cuts. This, would require further treatment, upgrading and special configuration in refineries in order to meet more stringent specifications of refined products, consequently associated costs are escalated [9].

3. Development Factors

The principal factors that could affect commercialization of Jordan's vast oil shale resources are the readiness and costs of available extraction and processing technologies, the quality of the markets for the products and byproducts, the implications of development for the Kingdom's social and physical environments, and the compatibility of Jordan's laws and regulations including those related to health and environment.

Table 1. Estimated reserves of the oil shale deposits

	El-Lajjun	Sultani	Attarat Um Ghudran	Wadi Maghar	Jurf Ed Darawish	Eth-Thamad
Area (km^2)	20.4	24	348	660	90.6	66
Av. thickness oil shale OS (m)	29.6	31.6	45	40	63.8	72-200
Av. thickness of overburden (m)	28.8	69.3	53.2	40.5	47.3	142-400
Av. Stripping Ratio	1	1.6	1.2	1	-	-
Geological reserves (Mt)	1196	1130	24500	31600	8000	11400
Calculated & Indicated reserve (Mt)	1170	989	(24500)*	21600	2500	-

* NRA current investigation.

Table 2. Summary of chemical and physical properties of main oil shale deposits

	El-Lajjun	Sultani	Attarat Um Ghudran	Wadi Maghar*	Jurf Ed Darawish	Eth-Thamad*
Av. oil content (wt %)	10.5	7.5	8	6.8	5.7	10.5
Total organic content (Wt %)	22.1	21.5	23.16	20.8	18	-
Calorific value (kcal/kg)	1590	1210	--	780-1270	864	-
$CaCO_3$ (wt %)	54.3	46.96	52.2	48	69.1	-
S (wt %)	3.1	2.4	2.6	2.6	2.2	3.2
Density (g/cm^3)	1.81	1.96	1.8	2.03	2.1	1.8
Moisture (wt %)	2.43	2.6	1.71	2.7	2.8	2.5

* Information is from few boreholes drilled in the area.

Table 3. Fischer assays of oil shale from El-Lajjun and Colorado

Item	El Lajjun	Colorado
Oil yield (wt. %)	10.5	10.34
Oil yield (gal/ton)	26.0	26.7
Oil yield (bbl/ton)	0.62	0.64
Properties of shale oil		
Specific gravity (g/cm^3)	0.968	0.920
Gravity (°API)	14.7	22.3
Nitrogen (wt. %)	0.66 - 0.9	1.96
Sulfur (wt. %)	8.5 to 10.2	0.61
Pour point (°F)	30	75
Pour point (°C)	-1.1	24
Initial boiling point (°F)	171	192
Initial boiling point (°C)	77	89

4. Technology

4.1. Power Generation

Tests with Jordanian oil shale, mainly from El Lujjun and Sultani, indicate that circulating fluidized bed combustion boilers (CFBC) are more suitable than traditional pulverized fuel power boilers because they can burn larger fuel particles more completely; they tolerate variations in fuel properties and operating rates; they are less susceptible to fouling; and they produce less air pollution. CFBC boilers, in a wide range of sizes, are now used commercially for various fuels. They are used to generate electricity from oil shale in Estonia, and their use with Jordanian oil shale has been examined by several firms [10]. Jordanian oil shale has burned well in pilot-scale CFBC plants, despite the levels of ash and sulfur, and the technical risk is low. However the estimated costs for commercial plants are high [11, 12]. A large power plant (e.g. 400 MW) might be practical if low-cost financing is obtained and the Kingdom can tolerate higher power prices. Small power plants (50 MW or less) would be too expensive. Subsidies would probably be required for any plant, and these may be difficult to justify, since low-cost natural gas is available for power generation. In a previous paper, it was reported that the unit electricity produced from oil shale powered plant would far exceed those generated from traditional thermal power stations fired by heavy fuel oil or combined cycle plants supplied with imported natural gas [13]. Moreover, when environmental costs are taken into consideration natural gas represents the best option, because there is no need for pollution abatement technologies. Additional costs will incur in other types of power plants due to the combustion of heavy fuel oil or oil shale.

4.2. Liquid Fuels Production

In the retorting area, Jordan is presently engaged with five potential project developers under memoranda of understanding (MOUs) initiated in 2006 and early 2007 [14]. Four firms are considering aboveground processing, in which oil shale is mined and crushed and then heated in vessels, and one firm is considering heating the oil shale in situ (i.e. in place). If an MOU study produces encouraging results, the GoJ could negotiate a production sharing agreement with the developer. The developer would then construct a small mine and a pilot processing plant containing a single production module. Experiments would be conducted with that module to ensure that the employed technology is practical and beneficial. A commercial-scale plant, containing many modules, could then be built. The leading technologies available to the developers are discussed below.

4.3. Petrosix Retorting

The Petrosix process was developed by Petrobras, the national oil company of Brazil, beginning in 1956. The intent was to exploit the huge Irati oil shale deposits and thereby reduce Brazil's absolute dependency on imported petroleum. Today Brazil produces most of its liquid fuels from offshore oil wells, ethanol plants, and its two Petrosix retorts. The Petrosix process heats coarse oil shale in a vertical cylindrical vessel. Oil shale enters through the top and is heated with reheated recycled gases as it moves down, and is discharged from the bottom. Oil vapors and gases are discharged through the top. Part of the gas is burned to heat the other part, which is returned to the vessel to heat the oil shale. Oil recoveries are high and produced shale oil quality is good – see Fig. 2. Fine oil shale and the solid pyrolysis product are currently discarded, but they could be exploited in other projects [15, 16].

Fig. 2. Petrosix Complex in Brazil

One retort, built in 1981, can process 1600 tonnes per day. The other was completed in 1991 and could process 6200 tonnes per day. The facility's total production capacity is about 3870 barrels per day (bbl/d) of shale oil (480 t/d of fuel oil and 90 t/d of industrial naphtha, 120 t/d of fuel gas, 45 t/d of liquefied petroleum gases, and 75 t/d of sulfur). Waste vehicle tires are also retorted to recover fuels and materials [17]. The Petrosix technology is advanced and efficient. It has been operated at near-commercial scale for more than two decades. Irati oil shale has high sulfur, as does oil shale in Jordan, so the Brazilian experience is relevant to Jordan's resources.

4.4. Estonian Retorts

Estonia has a diverse and vigorous industry that exploits the Kukersite oil shale to generate electricity and produce liquid fuels as well as manufacture alternative and new materials. About 1.5 million tonnes per year of oil shale are retorted to produce 8000 bbl/d of shale oil. Utilities burn approximately 10.5 million t/yr of raw oil shale to produce almost 90% of Estonia's electrical demand, and 200 thousand t/yr of oil shale is used in cement industry – see Fig. 3 - [18-20].

Fig. 3. Oil shale plant at Narva, Estonia

Two retorting technologies are used. The Kiviter retort is a vertical cylindrical vessel that heats coarse oil shale with recycled gases, steam, and air. Oil shale enters through the top and is heated with recycled gases flowing across the moving bed. Pyrolysis is completed in the lower section of the retort, where the oil shale is contacted with more hot gas, steam and air to gasify and burn the residual carbon, i.e. char. Processed shale is discharged from the bottom. Oil recoveries are relatively low, but the equipment is rugged and its availability is high. Thermal efficiency should be slightly higher than in the Petrosix retort. Fine oil shale and some of the solid pyrolysis products are currently wasted. Viru Chemistry Group Ltd. (VKG) runs two plants that use Kiviter retorts, and it is planning to increase shale oil production, but with a different retort. Eesti Energia AS (the national utility) uses two TSK140 or Galoter retorts in its shale oil factory. The Galoter was first built in early 1980s. It pyrolyzes fine oil shale particles by mixing them with hot spent shale in an inclined rotary kiln. Oil vapor is withdrawn and condensed to yield liquid fuel and non-condensable fraction is considered a medium-energy fuel gas. Retorted shale is burned, and the hot ash is returned to the retort as a heat carrier. Surplus gases and some of the heavier oil fractions, e.g. tar, are burned to produce electric power. Oil quality is good, thermal efficiency and oil recovery ratios are high. However, the equipment is complicated and capacity factors are relatively low. Both the Kiviter and Galoter retorts have been operated at large scale for more than 20 years [21]. Their performance characteristics should be well understood; therefore, expected technical risk should be low.

4.5. Alberta-Taciuk Retorting Process (ATP)

The ATP was developed primarily to process Canadian tar sands. The processor consists of two horizontal concentric tubes, rotating together. Oil shale is charged into one end of the inner tube, moves horizontally to the other end of that tube, and then it is transferred to the outer tube (where it burns in air), moves backwards between the tubes, and is discharged when it reaches the feed end. Retorting heat is provided by transferring part of the hot-burned shale into the inner tube where it contacts the incoming fresh oil shale. The wall between the tubes is heated by contacting the retorted oil shale and the hot pyrolysis gases. This heat also is transferred to the feed material [22-24].

The ATP was first used in 1989 to clean contaminated soils. Its first, and, so far, only use in the mining industry was in the Stuart oil shale project at Queensland, Australia – see Fig. 4. Stuart was developed by Suncor, the Canadian tar sands firm, and Southern Pacific Petroleum (SPP), an Australian firm. Stuart's single ATP retort was designed to produce 4500 bbl/d of shale oil from 6000 t/d of oil shale. Commissioning began in July 1999. There were problems with the retort and other equipment, especially the oil shale dryer. Although operations were difficult throughout the life of the of the Stuart project, by the end of 2003 the plant had run for more than 500 days (up to 96 days without stopping) and produced more than 1.3 million barrels. Production rates reached about 82% of the nominal capacity, and oil recovery ratio touched 94% of targeted design [25]. The high quality oil was sold as feed to refineries and as heating oil.

Fig. 4. 210 ton per hour Alberta Taciuk Process (ATP) Retort

There were many complaints from neighbors about odor and noise, and Greenpeace Australia launched a persistent campaign to stop the project, citing its environmental effects and especially the release of greenhouse gases [26]. Suncor withdrew and SPP continued until February 2004, when SPP's secured creditor, Sandefer Capital Partners, placed the project into receivership. Sandefer acquired the project's assets through a new company, Queensland Energy Resources Limited. The plant has been shut down since mid-2004. Just before the shutdown, a large quantity of oil shale was carefully crushed and dried to the plant's design specifications. When processing this feed material, the ATP retort did achieve its design capacity as well as expected oil recovery efficiency.

4.6. Paraho Retort

The Paraho retort is a vertical shaft kiln in which coarse oil shale moves downward through the vessel and is gradually heated to the desired retorting temperatures in a rising stream of hot gases. Paraho has two configurations: direct heating and indirect heating retorting systems. In a directly heated retort, the heat-carrier gas is generated by burning recycled pyrolysis gas and the retorted shale in the lower portion of the vessel. The indirectly heated configuration has a similar mechanical design but uses an external furnace to heat the heat carrier gas and does not burn the retorted shale – see Fig. 5. It is similar to the Petrosix retort. In the 1970s, a 25-ton per day pilot plant and a 250-ton per day semi-works plant were built in Colorado and tested with Green River oil shale [27-30]. The semi-works plant was demolished in 1980s, but the pilot plant has been used to make additives for asphalt and to process oil shale from different countries, such as Morocco, Australia, and the United States. Although the Paraho technology has not been demonstrated at commercial scale, it has been used in extended operations, with oil shales from several countries, for more than 30 years. A detailed engineering design study was completed for the retorting section of a commercial plant that would use the technology. A preliminary design for a commercial mine and the balance of the processing plant was completed. These are important steps towards preparing the technology for commercial application. However, the project remained on paper.

Fig. 5. The Paraho 250 t/d Semiworks Plant in Colorado, ca. 1979

4.7. In Situ Processing

With in situ retorting, oil shale is heated underground, and the oil is drawn to the surface through wells. "True" in situ processes do no mining but may fracture the oil shale or drill boreholes into it to accelerate the rate of heating. "Modified" in situ (MIS) processes mine some of the shale, break the rest, and retort the broken material underground. MIS processing was tested in 1970s and 1980s, but results were inconsistent and not encouraging [27-30]. Three true in situ processes are currently being developed in Colorado. The most advanced is the In-Situ Conversion Process (ICP) of Shell Oil Company. Shell's process involves drilling holes into the oil shale, inserting heaters, and gradually heating the entire zone to retorting temperatures. Oil and gas are drawn to the surface for processing [31, 32]. Shell uses a wall of ice to exclude groundwater from the zone to be retorted – see Fig. 6. A ring of boreholes is drilled around the zone, and a refrigerated liquid is circulated through the holes to freeze the water between the boreholes into a barrier wall. Water is pumped out, and heating commences. The ICP technology is not ready for commercial applications, yet. Its potential advantages include the avoidance of mining and the aboveground disposal of processing wastes and very high quality of produced oil. Potential disadvantages include high demand for electricity and water, surface subsidence, groundwater contamination, and difficulty reaching the underground waste disposal areas in case something goes wrong.

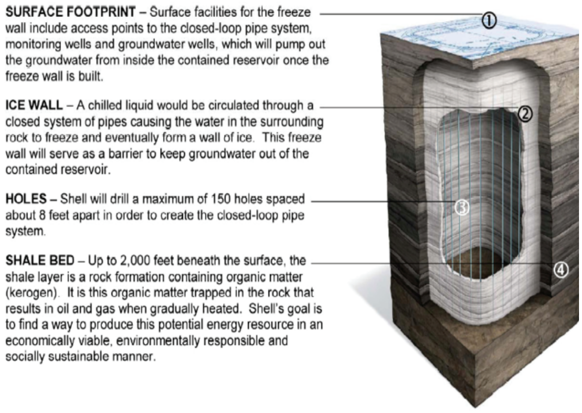

Fig. 6. In-Situ Conversion Process of Shell Oil Company

5. Economic Analysis

The cost of building chemical plants has soared since 2001, especially in terms of the U.S. dollar. Most important reasons behind this are (i) general inflation, and (ii) deterioration of the dollar, which has lost 47% of its value compared with a basket of other tradable currencies (50% against the Euro; and about 59% against the Australian dollar). Equally important is the unprecedented demand for materials, goods, and services by China, India, the energy industry, and the oil exporting countries. High capital costs impede the feasibility of capital-intensive projects, as has been well demonstrated for gas-to-liquids plants in the Middle East. Oil shale's situation may be even more precarious, because the technologies have not been proven at commercial scale, and operating problems are likely. Shale oil will have to compete with conventional crude oil, which costs much less to produce.

To assess the implications of capital cost escalation and financing strategies, the authors updated previous cost estimates for oil shale power plants and syncrude facilities in Jordan and for an oil shale syncrude project in the United States [27-30,33,34]. The product prices needed to cover operating expenses and debt service were calculated and compared to prices with current and forecast prices of energy products in Jordan. The results suggest that electricity production is not practical right now, because the breakeven power cost would be much larger than the present wholesale price of electricity. Aboveground retorting to produce synthetic crude oil does seem promising, so that technology was chosen for further study. An economic model was developed for a plant to produce 50,000 barrels per day of high quality synthetic crude, i.e. shale oil, from the El Lajjun oil shale deposit. The model was used to test the sensitivity of the plant's performance to the following key parameters:

- Facility cost
- Equity share of investment
- Debt interest rate
- Debt tenure
- Plant capacity factor
- Syncrude price
- Price of byproduct sulfur
- Cost of mining
- Other operating costs

- Rates of taxation and tax relief schemes
- Inflation

A simpler plant, which would ship crude shale oil rather than syncrude, was also examined. This would work only if the oil were destined for low-price markets (such as cement kilns) or if a robust refinery, capable of processing the poor-quality crude, will be available in Jordan. Tables 4, 5, and 6 summarize the results of the sensitivity studies.

- Efficient aboveground mining can be used in Jordan, which should reduce the syncrude price by about $5 per barrel, compared with underground mining of oil shale in the U.S.A.
- Based on previous estimates, it might cost $3.2 billion to engineer and build a syncrude plant with a design capacity of 50,000 barrels per day. If the project takes 42 months to complete, the total investment cost might reach $4 billion, including interest during construction, financing fees and expenses, taxes, and initial working capital.
- At a high availability factor of about 90.3% (330 days per year at design capacity), the facility would mine 68,000 t/d of oil shale and ship 43,500 bbl/d of syncrude and 675 t/d of elemental sulfur. Mining might cost $4.48 per tone ($4.06 per ton), and other operations and maintenance activities could cost $284 million per year.
- If the investment were financed 30% with equity and 70% with a 10-year loan earning 11%, the breakeven price of the syncrude would be around US$ 53 per barrel. If the oil were sold for $61.48 per barrel, which is the average price forecast through 2030 by the U.S. Energy Information Agency, the after-tax cash flow would generate approximately 14% internal rate of return (IRR) on the invested equity. With a 10% annual discount rate, the present value of the equity cash flow, which includes the original equity investment plus dividends to the owners, is around US$ 512 million over 20 years. The present value of royalties and other taxes collected by GoJ is estimated to be about $589 million. The minimum coverage of the debt service by operating profit is 1.29.
- IRR is most sensitive to syncrude revenue, which is determined by syncrude price and the plant's capacity factor. IRR is less sensitive to the capital cost and the non-mining operating costs. It is least sensitive to mining costs and to the price of the sulfur byproduct. IRR is very sensitive to the terms of the debt: with 10-year loan tenure, it varies from 18% with a 5% interest rate to 10% with 17% interest. With 11% interest, the IRR varies from 14% with a 10-year term to 17% with a 20-year term.
- Returns are also sensitive to the size of the equity share. Both dividends and taxes rise with equity share, but IRR declines. With 10% equity, the IRR is 21%. With 50% equity, the IRR is 12%. An all-equity deal would have an IRR of only about 10.6%.
- A viable oil shale industry could convey great financial benefits to the Kingdom. A 100,000 bbl/d industry would produce about as liquid fuel as Jordan currently consumes. During the first ten operating years of that industry, GoJ would collect, on average, approximately US$114 million per year in royalties, income taxes, and other similar payments. In addition, the Government could eliminate the subsidies it pays to fund energy price equalization pool. For 2007, paid subsidies to that pool are expected to be JD 170 million, equivalent to US$239 million [35]. The total benefit of a 100,000 bbl/d industry (taxes plus reduced subsidies) might reach US$ 353 million per year, or nearly US$ 11 for each barrel of syncrude that would be produced. Even if Jordan paid the same for the syncrude as it would otherwise have to pay for imported crude, US$ 11 per barrel of those payments would stay in the Kingdom. Much more would be retained in the form of salaries for the workers, satellite businesses, taxes on those salaries, purchases of goods and services to supply the industry and the satellite businesses, taxes on those purchases, and so on.
- The tax relief offered by Jordan's Investment Promotion Law (IPL) could enhance returns. The maximum incentive–exemption from up to 75% of income taxes for 10 years would increase IRR from 14% to 15%. To raise IRR to about 16% would cost Jordan US$ 926 million in lost taxes over 20 years, the equivalent of $2.80 per barrel of syncrude shipped. Exemption from all taxes would raise IRR to nearly 17.4%.
- Jordan has initiated MOUs with five developers and has released a document that suggests terms for production sharing agreements. That document proposes to replace existing taxes with a "petroleum tax" of up to 65% of profits and a production royalty of up to 7% of revenues. Compared with the IPL scheme, the Government would have to give up more tax revenues to induce the same increase in IRR. However, the Government could share any windfall profits. Incentives apply for the full life of a project and not just the first 10 years.
- Inflation could help a project, but only if revenues inflate as quickly as expenses. This may not happen, because oil prices do not respond to inflation. If uniformly applied, inflation of 3.5% per year would increase the IRR from 14% to 19.5%. Jordan's 2006 inflation rate of 6.5% would raise it to 24%. If oil prices did not rise as rapidly as operating costs, a project could soon collapse. If oil remained at US$ 55 per barrel while costs rose by 6.5% per year, the project would have to survive 14 years of negative cash flow. This vulnerability is troublesome, because Saudi Arabia has indicated a preference for a steady price of about $50 per barrel.
- Jordan's need for an oil refinery offers an interesting opportunity. If the new refinery could process crude shale oil, much of the market risk would be removed from an oil shale project. Capital and operating costs would be substantially reduced for the project, and it might obtain cheaper financing. However, revenues would also decrease, because less oil would be sold and at a lower price. A robust refinery for Jordan should be investigated, because even without oil shale, Jordan could reduce its energy costs by shopping for inexpensive refinery feedstocks.

Table 4: Summary Results of Sensitivity Studies

		Unit	Base Value	New Value	IRR Value	IRR Change	PV of AT Cash	Minimum DSCR
Base Case Results:			–	–	***14.0%***	–	***512***	***1.29***
Decrease by 10%	Syncrude price	$/bbl	61.48	55.33	9%	-33%	(73)	1.08
	Capacity factor	–	90.3%	81.3%	10%	-29%	(13)	1.10
	Facility cost	M$	3,220	2,898	17%	23%	816	1.43
	Non-mining O&M	M$/yr	284	255	17%	19%	836	1.41
	Debt interest rate	%/yr	11.0%	9.9%	15%	6%	603	1.35
	Equity share	–	30%	27%	14%	2%	528	1.24
	Debt tenure	years	10	9	14%	-2%	507	1.21
Increase by 10%	Syncrude price	$/bbl	61.48	67.63	19%	34%	1,100	1.50
	Capacity factor	–	90.3%	99.4%	18%	31%	1,038	1.48
	Facility cost	M$	3,220	3,542	11%	-18%	209	1.18
	Non-mining O&M	M$/yr	284	312	11%	-20%	155	1.16
	Debt interest rate	%/yr	11.0%	12.1%	13%	-6%	420	1.23
	Equity share	–	30%	33%	14%	-2%	497	1.35
	Debt tenure	years	10	11	14%	2%	518	1.36
Notes:		–	–	–	**a**	**a**	**b**	**c**

a. Internal rate of return (IRR) on equity investment from dividends
b. Present value (PV) of after-tax (AT) cash flow at 10% discount rate
c. Minimum debt service coverage ratio (DSCR): operating profit divided by debt service payment

Table 5: Threshold Values for Project Failure (a)

	Units	Value	Value	Change from Base	IRR	Years with Negative Cash Flow	PV of AT Cash, M$	Minimum DSCR	PV of Taxes, M$
		Base Case	**Worse Cases**						
Base Case		**--**	**--**	**--**	**14%**	**0**	**512**	**1.29**	**589**
Oil price	$/bbl	61.48	53.02	Down 14%	8%	10	(252)	1.00	324
Capacity factor	--	90.3%	76.5%	Down 15%	8%	10	(252)	1.00	322
Investment	M$	4,027	5,190	Up 29%	8%	10	(326)	1.00	408
Non-mining O&M	M$/yr	284	345	Up 21%	8%	10	(251)	1.00	338
Debt term	Years	10	6	Down 4 years	15%	6	778	0.93	681
Debt interest	%/yr	11.0%	17.5%	Up 59%	10%	10	(27)	1.00	405
Notes:	**--**		**--**	**--**	**b**	**a**	**c**	**d**	**e**

a. Project fails when one or more operating years has negative cash flow
b. Internal rate of return (IRR) on equity investment from dividends
c. Present value (PV) of after-tax (AT) cash flow at 10% annual discount rate
d. Debt service coverage ratio (DSCR) : operating profit divided by debt service payment
e. Present value (PV) of Government taxes and other collections at 10% annual discount rate

Table 6: Sensitivity Cases

		Value	Change from Base	IRR	Years with Negative Cash Flow	PV of AT Cash, M$	Minimum DSCR	PV of Taxes, M$
Pessimistic Case	–	–	–	9%	9	(99)	0.95	378
Oil price	$/bbl	58.81	Down 4.35%	–	–	–	–	–
Capacity factor	–	86.4%	Down 4.35%	–	–	–	–	–
Investment	M$	4,203	Up 4.35%	–	–	–	–	–
Non-mining O&M	M$/yr	296	Up 4.35%	–	–	–	–	–
Debt term	years	9	Down 1 year	–	–	–	–	–
Debt interest	%/yr	11.5%	Up 4.35%	–	–	–	–	–
Base Case	–	–	--	14%	0	512	1.29	589
Oil price	$/bbl	61.48	None	–	–	–	–	–
Capacity factor	–	90.3%	None	–	–	–	–	–
Investment	M$	4,027	None	–	–	–	–	–
Non-mining O&M	M$/yr	284	None	–	–	–	–	–
Debt term	years	10	None	–	–	–	–	–
Debt interest	%/yr	11.0%	None	–	–	–	–	–
Optimistic Case	–	–	--	22%	0	1,329	1.71	831
Oil price	$/bbl	64.15	Up 4.35%	–	–	–	–	–
Capacity factor	–	94.3%	Up 4.35%	–	–	–	–	–
Investment	M$	3,852	Down 4.35%	–	–	–	–	–
Non-mining O&M	M$/yr	271	Down 4.35%	–	–	–	–	–
Debt term	years	11	Up 1 year	–	–	–	–	–
Debt interest	%/yr	10.5%	Down 4.35%	–	–	–	–	–
Notes:	–	–	–	**a**	–	**b**	**c**	**d**

a. Internal rate of return (IRR) on equity investment from dividends
b. Present value (PV) of after-tax (AT) cash flow at 10% annual discount rate
c. Debt service coverage ratio (DSCR) : operating profit divided by debt service payment
d. Present value (PV) of taxes and other Governmental collections at 10% annual discount rate

In summary, the economic outlook for an oil shale syncrude project in Jordan is cautiously optimistic. There is optimism because conservative modeling suggests the project could be economically feasible. There is caution because the feasibility is delicate, and a project could collapse if substantial but conceivable changes occur in investment cost, oil price, capacity factor, or operating costs; or if the debt is unfavorably structured. A project could also be destroyed if several key variables changed by small increments in the wrong direction at the same time. An adverse shift of less than 4.5% in capital cost, oil revenue, operating costs, and debt payments could transform a good if not spectacular business into a project that cannot pay its bills and has a present value of minus US$ 99 million.

6. Environmental and Legal Issues

6.1. The Environment

Jordan's renewable natural water resources are 800 to 850 million m^3 per year. The water is provided by precipitation, by the in-flowing Yarmuk and Jordan rivers, and by renewable and fossil aquifers. Priorities for water use are human needs first and then followed by municipal, tourism, industries, and irrigated agriculture. Despite its low priority, agriculture used 64% of Jordan's water supply in 2006. Agricultural use is declining as well drilling is restricted, water meters are mandated, and farmland is converted to other uses. At the same time, water use by municipalities and tourism is rising rapidly. Although Jordanians use little water, the Kingdom has a serious water problem: water master plan expects consumption in 2020 to be nearly twice the available supply of renewable natural water, so supply shortfalls are likely [36]. A deficit of 320 million m^3 is forecasted at year 2010, when the first small oil shale plants may appear in the country. Possible mitigation methods include water reclamation, use of more treated wastewater in industries and for irrigation, desalination of seawater and brackish water, and development of new sources of groundwater and of surface water, including increased deliveries from Syria [37]. Despite these efforts, shortfalls are likely, and large investments will be needed to reduce them.

Oil shale facilities will use water in mining, retorting, upgrading, refining, power generation, waste disposal, site reclamation, and in the cities where new workers and their families will live. They will also produce water, by draining wet mines and from drying and retorting the oil shale. Both water production and water consumption vary with scale of operation and the nature of the extraction and processing technologies. Large plants to produce electric power from oil shale will use about 35% more water to produce the same amount of energy as a shale oil plant. However, electricity may be considered more useful and therefore entitled to more water. There is essentially no surface water in the oil shale areas, except during flash floods. There are two large aquifers, which are already important water sources for cities, farms, mines, and industries. If an oil shale industry emerges in Jordan in the near future, it will probably use surface mining and heated aboveground retorts. The average net water usage could be approximately 3.2 barrels of water per barrel of upgraded shale oil produced. A 100,000 barrel per day industry might consume approximately 18.9 million m^3 per year: as much as 0.5 million Jordanians, as many as lived in the city of Zarqa. If this industry happens, it could raise Jordan's water supply deficit in 2020 by 5%, at least.

A commercial-scale oil shale project would reshape the social, economic, and political life of the communities in the oil shale region. Development will occur in remote, sparsely populated, and non-industrialized areas with only limited infrastructure in place. If development is rapid, the local communities may suffer from inadequate utility services and insufficient public services, such as public transportation, education, health care, and police and fire protection. The GoJ and the developers should provide resources, such as planning assistance and money, in advance of development. Oil shale development could also have negative effects on air, land, and water in the oil shale region. Specific concerns include [38]:

- Mining – release of silica, metallic and organic salts, mercury, methane, carbon monoxide, nitrogen oxides (NOx), unburned fuels, and nuisance dusts during blasting, crushing, transportation, and materials handling. Leaching of salts and organic compounds from disturbed overburden and oil shale.
- Retorting and upgrading – release of hydrogen sulfide, carbonyl sulfide, carbon disulfide, sulfur dioxide, polycyclic organic matter, trace metals, NOx, and particulate matter, especially from the retorts during discharging and maintenance. Accidental discharge of process water condensates. Venting and loss of hydrocarbon vapors from poorly sealed storage tanks and pipelines. Discharge of heavy metals during catalyst regeneration.
- Thermal energy and power systems – emissions of sulfur dioxide, NOx, and particulate matter in stack gases. Discharge of blow downs and water treatment chemicals.
- Waste management – disposal of retorted oil shale, spent shale, spent catalysts, process waters and sludge, chemicals from treatment of water and wastewater, fly ash, and domestic wastes from worker facilities and related municipal growth.

Severity of the impacts will vary with employed technology, scale of operation, and types and efficiencies of environmental control systems. The most obvious concerns are air pollution from mining and processing the high-sulfur oil shale, as well as the potential leaching of contaminants from waste disposal areas. Both air-borne releases and leaching could threaten the aquifers that are Jordan's principal source of potable water [39]. Control methods are available for all of the areas of concern. For example:

- Dust – water sprays, wetting agents, paving, enclosures, filters, wet and dry scrubbers, precipitators
- Gases – combustion controls and selective catalytic reduction for NOx. Oxidation and chemical and physical absorption processes for sulfur compounds. Catalytic thermal oxidation for hydrocarbons and floating head tanks for product storage.

- Liquid and solid wastes – conventional wastewater treatment systems, evaporation ponds, landfill liners, filters, leachate collection and treatment systems, compaction, and solidification.

Except for high sulfur content, there is nothing particularly difficult about managing oil shale wastes, because they are similar to those produced in other industries. Scarcity of water and the scale of operations will complicate matters. Although standard control technologies may work well, they have not been validated with Jordanian oil shale at commercial scale. This concern should be addressed during pilot plant and modular testing programs. Another important issue is the quality of final products from the shale oil, which usually have high contents of aromatics, constitute, especially the light cut, i.e. mainly gasoline and kerosene produced from shale oil [40-43]. Many researchers reported that high levels of nitrogen, sulfur, ash, and toxic inorganic matter in the derived shale oil by pyrolysis, particularly if they are present in high concentration, might limit the use of this fuel as a direct substitute for petroleum-derived commercial fuels, since the fuel would represent a health hazard [44-46]. For example, polycyclic aromatic hydrocarbons containing sulfur and nitrogen are important because of their carcinogenic and/or mutagenic activity. Also, increased concentrations of such compounds have been shown to give increased soot and pollutant emissions in combustion systems, therefore, it requires more extensive refining, e.g. cleaning and hydro-treatment, than crude oil [8].

Jordan has endorsed many of the international conventions that promote environmental protection and sustainable development. The Ministry of Environment has central responsibility for environmental protection, in cooperation with the Ministry of Energy and Mineral Resources and the Ministry of Health. A long series of laws has established criteria for protecting the environment. For oil shale, the most relevant of these are the Air Protection By-Law No. 28 (2005), the Environment Impact Assessment (EIA) By-Law No. 37 (2005), and the Jordanian Emissions Standards for Electricity Generation (1999). By-Law No. 37 is particularly important because it requires a comprehensive EIA for large projects such as oil shale plants. The framework for Jordan's EIA process is in keeping with global standards. Regulations have evolved which will likely require extensive study of the baseline conditions in the area to be affected by oil shale development. They will also require thorough definition of the expected range of gross emissions, evaluation of proposed control technologies, analysis of alternatives, atmospheric dispersion modeling, evaluation of water requirements and impacts on water quality, consultation with concerned stakeholders and the public at large, and evaluation of archaeological, social, and natural values. Although the assessment process has been unevenly applied, progress is apparent. The inclusion of non-governmental organizations (NGOs), which can represent broad-based community concerns, is especially significant. The Stuart oil shale project in Australia was subjected to an intense campaign by an activist organization because of greenhouse gas releases and their implications for global warming [26]. Oil shale projects in Jordan may also be troubled by such activities. GoJ should pay attention to monitoring the effects of industrial developments and enforcing regulations where monitoring exposes violations. Bonding to guarantee adequate reclamation and closure at the end of a project's life is also needed. Although there are no international standards, many governments require an irrevocable letter of credit, full cash bond, or bond insurance policy.

International mining and energy companies are becoming increasingly involved in Jordan's minerals businesses. Their involvement in Jordan's oil shale industry is very likely, because of the complexity, long lead times, and investment requirements. This is significant, because good governance is a priority for many of these companies, and they have the technical and financial resources to provide for environmental and social sustainability. Their participation, and the support of multilateral financial institutions, may depend on compliance with the Equator Principles. These are voluntary guidelines for evaluating the social and environmental risks associated with the financing of projects to develop natural resources. The Principles evolved from practices of the World Bank and, as of May 2007, had been adopted by 51 global financial institutions, including the great majority of lenders that might be drawn to oil shale projects in Jordan. Although there are no specific standards for oil shale activities, the general standards for social and environmental assessment, analysis of labor and working conditions, waste management, pollution prevention and abatement, occupational health and safety, indigenous peoples, and other topics would certainly apply. If an oil shale project does not comply with the Equator Principles, the participating financial institutions will not issue loans. Those 51 institutions comprise approximately 90% (i.e. about $28 billion in 2006) of the private global project finance capacity for natural resources projects.

6.2. Legal Framework

Jordan's emerging oil shale industry will be shaped by mandates covering mining, environmental protection, land ownership, property rights limitations, financial subsidies and other incentives. The companies that will constitute this industry, including foreign investors, will be organized and registered under the Companies Law No. 22 of 1997, as amended. The standard corporate structures can be accommodated under this law and its amendments, and other arrangements could probably be negotiated if in the mutual interest of the developers and the Kingdom. The mining sector is governed by the Organization of Natural Resources Affairs Law (Law No. 12 for the year 1968) and Mining Regulation No. 131 for the year 1966. These establish that all minerals in Jordan are owned by the Government and may be used in trade only with the consent of the Government. Limits are imposed on the geographical extent of an extraction activity. Procedures are defined for accessing and using a site and for protecting water resources, holy sites and other special areas, and the health and safety of workers as well as the public.

Two new draft laws, (i) the Law for the Minerals and Petroleum Regulatory Commission and (ii) the Law for the

Jordanian Geologic Survey Commission, are under development. The first commission will regulate and monitor the industry and facilitate the establishment of projects, including those that have MOUs with the GoJ. The second commission will be responsible for research, surveys, and the promotion of mineral products. These laws are intended to overcome regulatory weaknesses and to clarify the framework under which projects will be developed. The principal environmental mandates are provided under the Environmental Protection Law No. 1 for the year 2003. In which the Ministry of Environment is designated to be the responsible authority in the area of environmental protection and the competent reference for permitting, monitoring, and regulating the industry, specifically as related to waste management, hazardous materials, and protection of the quality of soils and water resources.

An oil shale project is very likely to be affected by the Equator Principles. Jordan's existing laws and regulations do comply with the Principles, except in the areas of cumulative impacts and the efficient production, delivery, and use of energy. Thus, the GoJ should correct this deficiency. The mining sector is important to Jordan's economy. Foreigners are allowed to invest in the industry under "special agreements" which provide secure title and rights and assure stability of the fiscal regime over a project's lifetime. That regime offers relatively low tax rates, competitive royalties, and profit sharing on an equitable basis. The principal concerns of many investors (foreign exchange, repatriation of capital and profits, ownership rights, assignation, rights to operate and market, arbitration of disputes, and regulatory stability) are included in the regime, which should provide a reasonable level of comfort to investors in the oil shale industry. Jordan's laws also cover labor and employment matters, arbitration, protection of intellectual property, and public and occupational health.

7. Conclusions and Recommendations

Jordan's domestic recoverable energy resources are limited and lag far behind the demands of increasing population and economic growth. Thus, the country currently relies, and will continue to do so in the near future, almost solely on the combustion of imported fossil fuels in order to satisfy its national energy demand. This adds on pressure on government to act swiftly and adopt wise plans in order to ensure a reliable and secure energy supply for economic and social developments with serious considerations to minimize adverse environmental consequences associated with oil shale development [47].

7.1. Technology

Currently, the GoJ is engaged with five potential oil shale developers. Its approach to enlisting external help to create local oil shale industries appears sound. This should result in the evaluation of a broad range of aboveground retorting technologies for Jordan's near-surface deposits, and in the positioning of a leading in situ technology for the deeper and thicker ones. The modular progression, where a developer uses one retort to generate essential data and then scales up if appropriate, is sound and prudent. However, it will introduce delays and probably will increase costs. It also may result in production of a difficult waste product: small quantities of crude shale oil. The GoJ could ease this waste problem by providing a refinery capable of converting that material into useful products. Jordan should also build its technical capacity to facilitate and monitor the industry. It may be difficult to add staff, improve facilities, and enhance training, given Jordan has limited resources. Many of Jordan's neighbors in the Middle East and North Africa face similar challenges, in that they have oil shale resources but lack the expertise and capacity to benefit from them. The GoJ should consider leading an international effort to overcome the constraints, by creating an international oil shale commercialization center. The primary aims of such center are (i) to enhance understanding of the world's oil shale resources, (ii) to improve the commercial practicality of existing conversion technology, and (iii) to explore and perfect new, beneficial, and sustainable ways to extract useful energy and materials from oil shale in Jordan and elsewhere.

7.2. Economics

Oil shale retorting and power plants will be expensive, and their energy products are likely to cost more than what can be obtained from conventional sources which Jordanians are accustomed to paying. Feasibility of a retorting facility will be strongly sensitive to oil prices, availability and capacity factors, which the Government cannot control. However the Government can do other things to influence a project's feasibility, principally by participating in the emerging industry and helping it to secure a place in Jordan's energy economy and, most importantly, to obtain low cost financing. Specifically, the GoJ could:

- Install a refinery capable of handling a plant's output, thereby reducing costs and market risk.
- Reduce investment cost by helping developers secure debt and equity, thereby reducing fund-raising fees and expenses.
- Take positions in the projects (as done in the phosphate mining and potash industries), thereby providing access to inexpensive multilateral financing, with lower interest rates and longer terms.
- Solicit grants from concerned nations and foundations to pay for planning, infrastructure construction, and training programs.
- Provide appropriate forms of tax relief to encourage efficient, profitable operations without removing technical and managerial risks, which should be retained by the developers.

7.3. Water

A sizable shale oil industry would substantially aggravate the water supply problem in Jordan. Diversion of water to oil shale development will influence current users and increase the expected supply shortfalls. The following activities are recommended to ease this problem:

- For planning purposes, the GoJ should obtain water use estimates for Jordanian conditions. Existing estimates were developed for the U.S.A. and Estonia. Even if the same technologies were used in Jordan, substantially different amounts of water would be required.

- Water conservation should be emphasized in the Government's negotiations with developers. Rates of water use should be weighed when evaluating competing proposals. Design changes could substantially reduce water consumption.
- Water should be priced appropriately. A tiered pricing structure that discourages waste may be an acceptable solution.
- Developers should be encouraged to cooperate with each other and with other users to develop non-conventional water resources, such as treated wastewater. Sharing of resources would provide economies of scale and could make water reclamation and reuse much more practical.

7.4. Environment

The framework and nature of laws regarding environmental and social sustainability issues is good. Needed agencies and institutional framework exist to administer the laws. Proper regulations to supply details for administering the laws appear to exist as well. However, improvements are still needed in the following areas:

- Give more attention to the monitoring and enforcement of environmental regulation of major industrial projects.
- Strengthen agency staffing, training, capacity building, data, and tools for effective regulation.
- Improve baseline studies and impact modeling, which are of uneven quality.
- Standardize procedures to bond projects for reclamation and closure, security, health and safety, and enforcement.
- Carefully consider the Equator Principles in structuring environmental management programs for oil shale projects.

7.5. Strategic Implementation Plan

The Government has taken an important step by inviting private firms to participate as developers of oil shale projects and suppliers of energy to the Kingdom. Accomplishing the rest of the Government's goals will require a large number of discrete tasks, which can be arranged into any number of strategic plans. This study divided the tasks into five categories and forty tasks, as shown in table 7. The overall process is estimated to take 120 months, from the start of the regulatory reforms and studies in January 2008 until the first commercial shale oil is produced at the end of 2017. The time could be reduced by about four years by eliminating the intermediate modular phase, but substantial risks of technical and economic failure and social and environmental damage would result.

Acknowledgements

This paper is based on work performed in 2007 by the authors under a contract entitled "Technical Assistance on Oil Shale Resources Development in Jordan." The contract was between the Ministry of Energy and Mineral Resources of the Hashemite Kingdom of Jordan and Behre Dolbear & Company (USA), Inc. The contract was administered by the Jordanian Ministry of Planning and International Cooperation. The contract was funded by the U.S. Trade and Development Agency (USTDA), an agency of the U.S. Government, under Grant Number GH062127073. The opinions, findings, conclusions or recommendations expressed in this paper are those of the authors and do not necessarily represent the official position or policies of USTDA, Behre Dolbear & Company (USA), Inc., Interdisciplinary Research Consultants, Al-Balqa Applied University, or the Government of the Hashemite Kingdom of Jordan and its ministries. Those parties make no representation about, nor accept responsibility for, the accuracy or completeness of the information contained in this paper.

Table 6: Schedule for the Strategic Implementation Plan

YEARS FROM 1 JANUARY 2008		1		2		3		4		5		6		7		8		9		10	
MONTHS FROM 1 JANUARY 2008	6	12	18	24	30	36	42	48	54	60	66	72	78	84	90	96	102	108	114	120	126
START DATE	Jan-08	Jul-08	Jan-09	Jul-09	Jan-10	Jul-10	Jan-11	Jul-11	Jan-12	Jul-12	Jan-13	Jul-13	Jan-14	Jul-14	Jan-15	Jul-15	Jan-16	Jul-16	Jan-17	Jul-17	Jan-18

A. CAPACITY BUILDING & REGULATORY REFORM
1. Align regulations with Equator Principles (12-18 months)
2. Standardize bonding procedures (12-18 months)
3. Add staff for permits, regulation, management (12-18 mos
4. Initiate international oil shale center (18 months)
5. Operate international oil shale center (Continues)

B. ENVIRONMENTAL INITIATIVES
1. Develop practices for baseline studies (6 months)
2. Conduct baseline studies & publish results (18 months)
3. Conduct Environmental Impact Assessment (18-36 mos)
4. Permit modular phase (18 months)
5. Permit commercial phase (24 months)
6. Accelerate vehicle conversion to CNG (24 months)
7. Monitor industry (Continues)

C. ECONOMICS AND FINANCING
1. Plan participation in oil shale projects (6 months)
2. Arrange module financing (6 months)
3. Arrange commercial financing (6 months)
4. Refinance & exit (12 months after commercial startup)

D. TECHNOLOGY IMPLEMENTATION
1. Evaluate robust refinery (12 months)
2. Implement refinery (24 months)
3. Complete MOU studies & select developers (18 mos)
4. Design modular plants (12 months)
5. Acquire water supplies (12 months)
6. Construct modular plants (24 months)
7. Operate modular plants (24 months)
8. Assess modular plants (12 months)
9. Design commercial plants (12 months)
10. Acquire water for commercial plants (12 months)
11. Design & build utility & pipeline networks (18 mos)
12. Construct commercial plants (36 months)
13. Operate commercial plants (Continues)

E. IMPACT MITIGATION
1. Assess water needs for oil shale (12 months)
2. Plan response to modular phase (18 months)
3. Fund planning, infrastructure, training (18 months)
4. Implement response to modular phase (30 months)
5. Plan response to commercial phase (18 months)
6. Implement response to commercial phase (18 mos)

References

[1] Central Intelligence Agency, 2007. The World Fact Book. Washington, DC.

[2] Department of Statistics, Annual Statistical Book 2660, Amman, Jordan, 2007

[3] Ministry of Energy and Mineral Resources, 2007, Annual Report 2006, Amman, Jordan.

[4] Natural Resources Authority, 2007, Annual Report 2006, Amman, Jordan,.

[5] Y. Hamarnah, 1998, Oil Shale Resources Development in Jordan, updated and revised by J. Alali and S. Sawaqed, 2006, Natural Resources Authority, Amman, Jordan.

[6] T. Sladek, S. Mernitz, J.O. Jaber, "Strategies for Oil Shale Development in the Hashemite Kingdom of Jordan". Proceedings of the 27th Oil Shale Symposium, , Colorado School of Mines, Golden, USA, 2007.

[7] J.O. Jaber, S.D. Probert, P.T. Williams, " Evaluation of oil yield from Jordanian oil shales". Energy, Vol. 24, 1999, 761-781.

[8] P.T. Williams, H. M. Chishti, " Reaction of nitrogen and sulphur compounds during catalytic hydro treatment of shale oil".Fuel, Vol. 80,2001, 957–963.

[9] B. Akash, J.O. Jaber, " Characterization of shale oil as compared to crude oil and some refined petroleum products, Energy Sources". Vol. 25, 2003, 1171-1182.

[10] J.O. Jaber, S.D. Probert, " Oil shale integrated tri-generation system: the technology and predicted performance".Oil Shale, Vol.15,1998,3-30.

[11] Ots, "Oil Shale Fuel Combustion". Eesti Energia, Tallinn, Estonia, 2004.

[12] Petersen,"The unique experience of oil shale utilization at Narva power plants". Proceedings of the International Oil Shale Conference Recent Trends in Oil Shale: Research and Applications, Amman, Jordan, 2006.

[13] J.O. Jaber, A. Al-Sarkhi, B. Akash, M. Mohsen, "Medium-range planning economics of future electrical power generation".Energy Policy, Vol. 32, 2004, 357-366.

[14] Natural Resources Authority Annual Report 2006, Amman, Jordan, 2007

[15] Petróleo Brasileiro SA, 2007, “Six: Schist Industrialization Business Unit.” Retrieved on (date)? From http://www2.petrobras.com.br/minisite/refinarias/petrosix/ingles/processo/index.asp

[16] W.P. Martignoni, W.J.B. Rodriguez, "Oil shale industrialization in Brazil-Petrosix Technology". Retrieved on Date? From http://aiche.confex.com/aiche/2006/techprogram/P77492.HTM.

[17] Antonio C.L.Lisbˆoa, Carla F.S. Rombaldo, Washington J.B. Rodriguez, " Adding tires to the feedstock of the Petrosix oil shale processing plant". Retrieved on Date from http://dpi.eq.ufrj.br/ciaiq_22/CD/formCrCongreso/papers/07c/07c_371.pdf.

[18] Opik, " Scenarios for Shale Oil, Syncrude and Electricity Production in Estonia in the Interim 1995-2025".Oil Shale, Vol. 9, 1992, 81-87.

[19] V. Liblik, H. Kundel, " Pollution Sources and Formation of Air Contamination Multicomponential Concentration Fields of Organic Substances in North-Eastern Estonia".Oil Shale, Vol. 13, 1995, 43-64.

[20] E.P. Volkov," New developments in oil shale technology, Proceeding of the 17th Congress of the World Energy Council Energy and Technology: Sustaining World Development into the Next Millennium, , Houston, Texas, USA, 1998.

[21] J. Purga, "Oil shale business-opportunity for smart and strong".Proceedings of the International Oil Shale Conference Recent Trends in Oil Shale: Research and Applications.Natural Resources Authority, Amman, Jordan, 2006.

[22] R. Koszarycz, R. Padamsey, L.R. Turner, R.M. Ritcey, The AOSTRA Taciuk Process Heading into Commercialization Phase, Technical Report, Alberta Oil Sands Technology and Research Authority, Calgary, Alberta, Canada, 1992.

[23] SUNCOR Energy, Presentation about Jordanian Oil Shale Project: Conceptual Design, Amman, Jordan, March 1999.

[24] J. Qain, "World oil shale retorting technologies".Proceedings of the International Oil Shale Conference Recent Trends in Oil Shale: Research and Applications, Amman, Jordan, 2006.

[25] J. Schmidt, "Technology selection for an oil shale deposit". Proceedings of the International Oil Shale Conference Recent Trends in Oil Shale: Research and Applications,Amman, Jordan, 2006.

[26] Green-Peace, " Stuart oil shale project: a toxic experiment". Report published by Green Peace, Goldstone, Queensland, Australia (ISBN 1-876221-12-7), 2003.

[27] Sladek, T. A., and others, "An Assessment of Oil Shale Technologies". U. S. Office of Technology Assessment, Congress of the United States, Washington DC, 1980

[28] Allred, V.D. Oil Shale Retorting Phenomenology.in V.D. Alfred, editor. Oil Shale Processing Technology. , New Jersey,: The Center for Professional Advancement;1982, p.?.

[29] Hunt, V.D. Synfuels Handbook,., New York: Industrial Press, Inc; 1983.

[30] Speight, J.G. Fuel Science and Technology Handbook, New York: Marcel Dekker, Inc., 1990.

[31] Murphy, "Sustainable development of Jordan oil shale". Proceedings of the International Oil Shale Conference Recent Trends in Oil Shale: Research and Applications, Natural Resources Authority, Amman, Jordan, 2006.

[32] Shell Exploration & Production, “Mahogany Research Project – The In Situ Conversion Process.” Retrieved on Date, MM/dd/2007 from http://www.shell.com/us/mahogany.

[33] J.O. Jaber, M. Mohsen and M. Amr, " Where to with Jordanian oil shales".Oil Shale, Vol. 18, 2001,401-421.

[34] Lurgi GmbH, and Natural Resources Authority, Technical and Economic Feasibility of a Large-Scale Oil Shale Retorting Complex, Natural Resources Authority, Amman, Jordan, 1986.

[35] Ministry of Energy and Mineral Resources, Facts and Figures Amman, Jordan, 2007.

[36] Ministry of Water and Irrigation.Annual Report 2006, Amman, Jordan, 2007.

[37] Ministry of Water and Irrigation, National Water Master Plan, Amman, Jordan,2007.

[38] J.O. Jaber, S.D. Probert, "Environmental impact assessment for the proposed oil shale integrated tri-generation plant".Applied Energy, Vol. 62, 1999, 169-209.

[39] J. Soone, "Environmentally sustainable use of the energy and chemical potential of oil shale". Proceedings of the International Oil Shale Conference Recent Trends in Oil Shale: Research and Applications, Natural Resources Authority, Amman, Jordan, 2006.

[40] E. Putun, A. Akar, E. Ekinci, and K. Bartle. 1988, Chemistry and geochemistry of Turkish oil shale kerogens, Fuel, Vol. 67, 1998, 1106–1110.

[41] P.T. Williams, J.M. Nazzal, " Polycyclic aromatic compounds in oils derived from the fluidized bed pyrolysis of oil shale".Journal of Analytical and Applied Pyrolysis, Vol. 35, 1995, 181–197.

[42] H.M. Chishti, P.T. Williams, " Aromatic and hetero-aromatic compositional changes during catalytic hydrotreatment of shale oil". Fuel, Vol. 78, 1999, 1805–1815.

[43] J.M. Nazzal, " The presence of polycyclic aromatic hydrocarbons (PAH) in the oil derived from the pyrolysis of Jordan oil shale". Oil shale, Vol. 24, 2007, 465-475.

[44] J.J. Schmith-Collerus, F. Bonomo, K. Gala, L. Leffler.Polycondensed aromatic compounds (PAC) and carcinogens in the shale ash of carbonaceous spent shale from retorting of oil shale. In T.F. Yen (Ed.), Science and Technology of Oil Shales. MI: Ann Arbor Science Publishers; 1976

[45] C.E. Rovero, P.T. Crisp, J. Ellis, P.T. Bolton, " Chemical characterization of shale oil from Condor, Australia". Fuel, Vol. 62, 1983, 1274–1282.

[46] H. Okutan, D. Dilek, M. Citiroglu, E. Ekinci" Polycyclic aromatic compounds detected in pyrolysis residues of seyitomer oil shale and lignite". Environmental Technology, Vol. 15, 1994, 333–342.

[47] J.O. Jaber, O.O. Badran, N. Abu-Shikhah, " Sustainable energy and environmental impact: role of renewable as clean and secure source of energy for the 21^{st} century in Jordan". Clean Technologies and Environment Policy, Vol. 6,2004, 174-186.

JJMIE

Volume 2, Number 1, Mar. 2008
ISSN 1995-6665
Pages 45 - 52

Jordan Journal of Mechanical and Industrial Engineering

Selection of Metal Casting Processes: A Fuzzy Approach

Kasim M. Daws [a], Zouhair I. AL-Dawood [a,*], Sadiq H. AL-Kabi [b]

[a] Mechanical Engineering Department, University of Baghdad, Bagdad, Iraq
[b] Technical Institute, Samawa, Iraq

Abstract

Choosing the right manufacturing process for making a component is an important consideration at the early stages of design. In metal casting process, there are over forty different processes with different capabilities. A designer can benefit from knowing the manufacturing process alternatives available to him. Inaccurate process selection can lead to financial losses and market share erosion. In this paper, an automated advisory casting process selection system is designed. The designed system named (CACPS) the objectives of this system to solve the problems of process selection and evaluation (PS&E) activities. The designed system depends on methodology for selection and evaluation of process that based on a number of user-specified criteria or requirements. The decision model enables the representation of the designer's preferences over the decision factors it is based on weighted property index (W.P.I) algorithms to determine the relative importance of each criterion. A compatibility rating between product profile requirements and the alternatives stored in the database for each decision criteria are generation using fuzzy logic (F.L) methodology. These requirements were matched with the capabilities of each process the compatibility ratings are aggregated into single rating of that alternative's compatibility. A ranked set of compatible alternative processes is out put by the system. This approach has advantages over the existing systems, which are equipped with a decision module or a database.

Keywords: Metal Casting; Process Selection; Fuzzy logic; Design for Manufacturing; and Decision-Making;

1. Introduction

The designer needs a systematic and rousts way of evaluating the available options and identifying which might be the best. Manufacturing process selection is the task of choosing a method for transforming a set of material into a given shape using one or more processes. The best process is normally considered to be the economic, subject to it meeting the technical constraints. [1]. The material and manufacturing process selection problem is a multi-attribute decision-making problem. These decisions are made during the preliminary design stages in an environment characterized by and uncertain requirements, parameters, and relationships. Material and process selection (MPS) decisions occur before design for manufacturing (DFM) can begin [2]. Studies have indicated that although the cost of product design is only around 5% of the total product cost, decisions made during the design stage affect (70 – 80 %) of the final product cost [3].

In this paper a development of an advisory system called Computer Aided Casting Process Selection (CAMS) that aids the designer in decision-making (D.M). The objectives of the designed system are to evaluating and selecting the optimal and alternatives process that satisfied the design specifications. The (CACPS) system indicate to the designer the compatibility degree between the selected processes to all the specified criteria and capabilities then these selected processes are ranked according to its compatibility's.

2. Classification of Manufacturing Processes

For the purpose of selection, a rigorous definition of a process is not required. It is sufficient to consider it manufacturing step that alters the characteristics of one or more materials in some way in order to produce or modify a component or components. By this measure, a large number of processes exist at all levels of complexity and scale. To help compare the various processes for selection purposes it is helpful to find some means of classification them [4]. A process taking a broad view is a method for shaping or finishing or joining a material as shown in Figure 1. The kingdom of processes contains broad families such as casting, deformation, molding, machining, etc. each family contains many classes; casting contains sand –casting, die-casting, and investment casting, for

* Corresponding author. e-mail: ziaa04@yahoo.com

instance. These in turn have many members; there are many variants of sand –casting, some specialized to give greater precision, other modified to allow exceptional size, still others adapted to deal with specific materials [5].

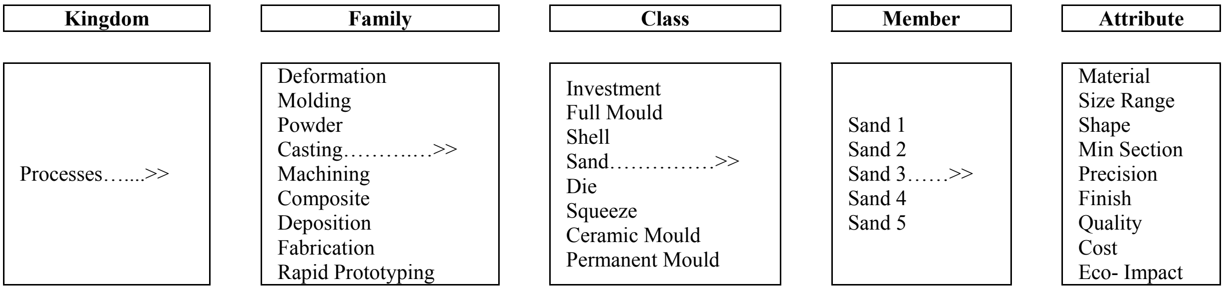

Figure 1: A schematic illustrating the taxonomy of the manufacturing processes [5].

3. Fuzzy Logic Methodology

Fuzzy logic (F.L.) is one of the elements of artificial intelligence that is gaining in popularity and applications in control systems and pattern recognition. It is based on the observation that people make decisions based on imprecise and numerical information. Fuzzy models or sets are mathematical means of representing vagueness and imprecise information, hence the term fuzzy [6]. These models have the capability of recognizing, representing, manipulating, interpreting, and utilizing data and information that are vague and lack certainty. The concept of fuzzy can be illustrated in Figure 2.

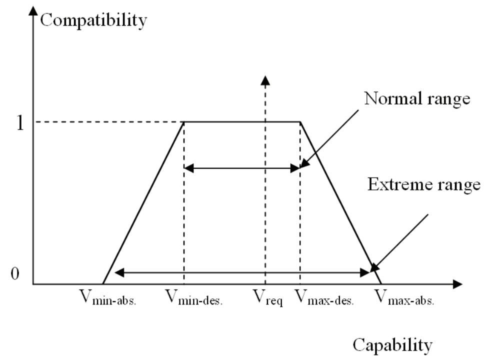

Figure 2: Fuzzy mapping of process capability [7].

Where:

$V_{min\text{-}abs}$ = the absolute minimum value
$V_{min\text{-}des}$ = the desire minimum value
V_{req} = the requirement value
$V_{max\text{-}des}$ = the absolute maximum value
$V_{max\text{-}abs}$ = the desire maximum value

In fuzzy logic methodology, the part process compatibility value will gradually grow from zero to one, instead of suddenly jumping from zero (incompatible) to one (fully compatible). For analysis the process of compatibility the range of capability are needed the previous values to mapped on a normalized scale as in the previous figure. If the value of part requirement falls within $V_{min\text{-}des}$ and $V_{min\text{-}abs}$ the compatibility is considered fully compatible. If the part requirement value is between $V_{min\text{-}abs}$ and $V_{min\text{-}des}$, or between $V_{max\text{-}des}$ and $V_{max\text{-}abs}$, then the compatibility is considered less than one but more than zero. If the part requirement value is less than $V_{min\text{-}abs}$ or more than $V_{max\text{-}abs}$, then the compatibility is considered zero.

The compatibility $P(x_i)$ for a value x_i of an attribute i can be calculated by using the following equations [7]:

$$P(x_i) = 1 \quad \text{if } V_{min\text{-}des} < x_i < V_{max\text{-}des} \qquad (1)$$

$$P(x_i) = (x_I - V_{min\text{-}abs}) / (V_{min\text{-}des} - V_{min\text{-}abs}) \quad \text{if } V_{min\text{-}abs} < x_i < V_{min\text{-}des} \qquad (2)$$

$$P(x_i) = (V_{max\text{-}abs} - x_i) / (V_{max\text{-}abs} - V_{max\text{-}des}) \quad \text{if } V_{max\text{-}des} < x_i < V_{max\text{-}abs} \qquad (3)$$

$$P(x_i) = 0 \quad \text{if } x_i < V_{min\text{-}abs} \text{, or } x_i > V_{max\text{-}abs} \qquad (4)$$

Fuzzy technologies and devices can be applied successfully in areas such as robotics and motion control, evaluation of design alternatives, decision making, and the design of intelligent systems, in materials selection involving multi-criteria, image processing and machine vision [6].

4. Casting Process Selection

Casting process selection influences other major decisions such as the type of tooling, process parameters, and extent of machining, heat treatment, and quality control procedures. These in turn affect the economic quantity, tooling, labor costs, and lead time forecasting. Casting process combination is characterized by different range of geometric features that can be produced (minimum section thickness, minimum core size, etc), achievable quality (surface finish, porosity…etc) and production parameters (sample lead-time, economic lot size…etc).

To select a feasible casting process, the part requirements or attributes with the corresponding capabilities of the process must be considered. For example if an aluminum alloy sand cast part has a minimum wall thickness of 3.75mm, in comparison to the process capability range of 3.5 to 4.5 mm, then the part and process are compatible with respect to minimum wall thickness criterion. Similarly, other requirements can be checked and other process that satisfies all the requirements of the part is considered as a feasible process.

The above approach is simple and easy to apply in order to select a set of feasible processes. However, the approach does not capture the real situation of process capabilities, and secondly, it is difficult to compare two different feasible processes with respect to a given part in a quantitative manner. For example, it is difficult to accept that a wall thickness of 3.49mm would imply complete incompatibility where as 3.51 mm would imply complete compatibility. To overcome this difficulty and reflect real-life situations more realistically, fuzzy logic (F.L) is applied. In this approach an introduction of two, more limits: minimum desirable and maximum desirable values of process characteristics. Thus if take minimum desirable value of minimum wall thickness 4 mm then a value of 3.75 indicates 50% compatibility with respect to the wall thickness criterion.

For example, if surface finish capability of sand casting process is taken as (6, 12, 25 and 50 µm) indicating $V_{min-abs}$, $V_{min-des}$, $V_{max-des}$ and $V_{max-abs}$ respectively, the part process compatibility for surface finish criterion will be zero (i.e.-applying equation 8). Taking into account that the requirement falls outside even the absolute range

If an alternative process such as investment casting with four limits as (0.8, 1.6, 3.2, and 6.4 µm), then the part process compatibility will be 0.75 (applying equation 6) implying that it would be possible to achieve the requirement, but the process control has to be tighter. The other way to achieve part-process compatibility would be to modify the surface finish requirement of the part to more than six µm so that it falls within the range of the limits of sand casting. The overall compatibility of a part and process can be computed by taking a weighted average of the part-process compatibility with respect to different criteria.

Four limits for each criterion is considered because in practice the process characteristics also depend on the equipment, manpower, skill, quality management practices and other company decisions. This can be captured in a band of values for each process capability characteristics.

5. Assignment of Compatibility to Selected Casting Process

Usually at the beginning of the conceptual design, designers are given functional requirements and relevant business requirements such as time to market, likely production volume, and total production quantity. During the conceptual design stage designers identify critical design requirements such as size, material requirements, gross shape, form features, tolerances, surface finish requirements…etc. at this stage there exist sufficient information to start preliminary process planning (e.g. material and process selection). A selection of optimal and alternative casting process with compatible alloy that can meet these critical requirements with the minimum cost is considered.

5.1. Problem Statement

The technique is dependent on the selection consist of two phases or steps these are Screening phase and Ranking phase. They can be summarized as the following:

5.1.1. Screening Phase

This phase consists of the following criterion.

5.1.1.1. Type of Materials:

Materials are treated as go-no-go decision and any casting process that cannot cast the material is eliminated. As example die-casting cannot cast steel alloys or cast-iron successfully. In the designed (CACPS) system, aluminum and steel alloys are considered in database materials, with about 95 alloys with different conditions and chemical composition.

5.1.1.2. Shapes:

Shapes also are treated as go-no-go decision and any casting process cannot cast the required shape is eliminated. As example, centrifugal casting can cast only shapes that are cylindrical parts or shapes that are symmetrical about axis of rotations. In the designed (CACPS) system there are total of seven shapes are considered dependent:

1. Planar
2. Surface of revolution
3. Prismatic
4. Constant cross section
5. Thin wall
6. Free from drape
7. Free from general

5.1.1.3. The Required Quantity:

The quantity required affects process selection to a considerable extent. The cost of a process has break-even point over the economic production quantities. The die design and fabrication costs take a significant percentage of the production cost of the part. This percentage differs from process to process. For example the die design and fabrication cost for die-casting differ from the cost of mold in sand casting because the die is used to produce thousands of parts, but a preparation of one mold for each part produce in sand casting. Therefore, the number of the required parts must be economical to cover the costs of design and fabrication of the mold [8]. These are differing from process to process as illustrated in Table 1.

Table 1: Storing economical region for some Casting Processes.

Process	Lower quantity	Upper quantity
Shell	100	No upper limit
Gravity die	100	No upper limit
Pressure die	1000	No upper limit
Lost foam	5000	20000

Therefore, any number of required parts does not fall in the economical region of the process will be eliminated. For example, the economical region for die-casting is above 1000 units and the economical region for sand casting is above 1. If the user wants to produce 500 castings then the sand casting will be economical and the die-casting will be uneconomical method.

5.1.2. Screening and Ranking Phase

This phase contains the specification requirements, which consist of four main groups of criterion, some of these criterions working as screening phase and others working as ranking phase these are shown in Table 2.

Table 2: : Specification requirements

Geometric Attributes	Economic Considerations
Size	Tooling cost
Weight	Cost per unit
Section Thickness	Relative cost in quantity
Hole Size	Relative cost in small No.
Tolerance	Labor cost
Quality Requirements	**Production Requirements**
Surface Finish	Production Volume
Mechanical Properties	Production Rate
Complexity	Flexibility
Porosity	Lead time

5.1.2.1. Geometric Attributes

Size*:*Size of the casting part is the maximum dimensions in length in millimeter units. The size of the candidate designs limits the selection of the casting process. For example size capability of die casting is limited to 500 mm (i.e. size larger than 500 mm cannot be casted by using die casting method) but the capability to sand casting to cast part unlimited in size. Therefore, any size does not fall within the capability of the process will be eliminated. To clear the compatibility of the different processes to cast the required size, four limits are specified as it is shown in Table 3. below which specifies some of casting method with different limits in size.

Table 3: Size limits for some casting processes [9].

Process	$V_{min-abs.}$ (mm)	$V_{min-des.}$ (mm)	$V_{max-des.}$ (mm)	$V_{max-abs.}$ (mm)
Sand	5	10	Unlimited	unlimited
plaster	5	10	10	50
Die	5	10	450	500
Vacuum	10	20	1500	20000

Part Weight:Each casting process has a range of casting weights that it can produce under normal conditions. While handling part weights, it may be incorrect to simply. Consider the upper and lower bound of each process regarding the maximum and minimum weight that can be casted. With the increasing pace of technology improvements, larger parts are being casted with processes earlier kwon for casting only parts with a small or medium weight. However, it is still true that every casting process is most advantageous over a certain weight range. Outside this range, the process will be infeasible. The designed consider this by defining the typical and extreme limits for each casting process as show in Table 4.

Section Thickness:When evaluating the feasibility of casting processes to manufacture a given section thickness, the following uncertainties are encountered [11]: The capabilities to manufacture thin sections vary from foundry to foundry, even with a given casting process. For example, some sand foundries may be able to manufacture thinner sections than others may.

The ability to make a thin wall section also depends on the metal to be casted and the foundry capabilities. As example investment, castings can cast thin walls ranges from 0.22 mm. to 0.98 mm. These two are internally defined as lower thin section and upper thin section. To calculate the compatibility for each process we specify four limits to section thickness criterion in Table 5.

Table 4: Part weight limits for some casting process [10].

Process	$V_{min-abs.}$ (kg)	$V_{min-des}$ (kg)	$V_{max-des}$ (kg)	$V_{max-abs.}$ (kg)
1- Shell	0.03	0.05	50	100
2-Plaster	Very small	Small	30	50
3-Squeeze	Very small	small	10	15
4-Investment	0.001	0.005	90	100

Table 5: Limits for section thickness criterion [11].

Process	$V_{min-abs.}$ (mm)	$V_{min-des}$ (mm)	$V_{max-des}$ (mm)	$V_{max-abs}$ (mm)
Die casting	0.5	1	8	12

***Hole Size*:**Hole size is the minimum or maximum diameter for hole that can be made in the casted part. Casting processes are different capabilities in making the hole size from process to process. For example in the sand casting the hole size depend on the core size, while other process don't uses core. This has differences in hole size such as lost foam casting. To calculate the compatibility for each process by using fuzzy logic technique four limits are required for applying (F.L).

***Tolerance*:** Tolerance is defined as the acceptable variation to the ideal or nominal dimension. These are described by the system of geometric dimensioning and tolerance (GD&T) and are based on the ASME standard 1994. Tighter tolerances than normal will lead to increased cost and lead-time. Generally, tolerances depend on the geometry of the part. However, foundries generally state the tolerances that can be obtained by using its processes and provide guidelines to the designer to work towards these tolerances. These tolerances are called *as cast* tolerances because they are obtained without any additional processes such as machining or using additional equipment. Table 6. specify four limits for tolerances to calculate process compatibility.

Table 6: Limits for dimensional tolerance criterion [9].

Process	$V_{min-abs.}$ (mm)	$V_{min-des}$ (mm)	$V_{max-des}$ (mm)	$V_{max-abs}$ (mm)
Sand casting	0.55	0.65	6	6.5

Casting tolerances greatly depend on both the metal and the process. (CAPP-CT) uses a database of casting tolerance to suggest an appropriate casting process. Tighter linear tolerance than available in the chosen casting process can be obtained by secondary processes such as machining. For example in investment casting there are several ways to obtain a tolerance tighter than what can be commonly obtained. Some of the methods displayed on the investment casting foundry are:

1. Part redesign including addition of tie bars, ribs, and gussets to certain shapes.
2. Tuning of wax injection tooling after the first sample to meet the nominal dimensions.
3. Straightening after casting.
4. Gauging and hand fitting.
5. Machining.
6. Other secondary operations.

5.1.2.2. Quality Requirements

Surface Finish:The surface finish of a part determines its appearance affects the assembly of the part with other parts and may determine its resistance to corrosion. The surface roughness of a part must be specified and controlled because of its influence on fatigue failure, friction, wear, and assembly with other parts. In metal casting processes, each casting process has the ability to produce surface finish different to other process and this depending on the molding material used. The (CACPS) system considers only as cast surface finishes. It does not favor processes that need secondary processes that can be used to give a better surface finish. For example investment casting typically provide as cast surface finish that vary from 0.8 µm to 6.4µm. Process overlap with regard to finish that can be obtained from them. Suppose the designer wishes to obtain an as cast finish of 1.5 µm. neglecting other considerations such as weight, tolerance etc. and considering surface finish, the designer is faced with several processes which can give the desired finish such as pressure die casting, investment casting, plaster casting, shell casting, and ceramic casting. To determine the degree of compatibility for each process, four limits are considered as illustrated in Table 7. below:

Table 7: Limits for surface finish criterion [12].

Process	$V_{min\text{-}abs.}$ (µm)	$V_{min\text{-}des}$ (µm)	$V_{max\text{-}des}$ (µm)	$V_{max\text{-}abs}$ (µm)
Sand casting	6	12	25	50
shell casting	1	3	6	8
plaster casting	0.75	1.3	2.5	4
Investment casting	0.8	1.6	3.2	6.4

The calculations of compatibility for each process in Table 10. to surface finish criterion by using fuzzy logic approach as in the following:

1. Sand casting process compatibility P (1.5) to produce finish (1.5 µm) is 0 by applying eq. [$P(x_i) = 0$ if $x_i < V_{min\text{-}abs}$] (i.e. this process incapable to produce this finish) . This case be can represent in figure 3.
2. Shell casting process compatibility P (1.5) to produce finish 1.5 µm is 25 % , which can be represented in figure (7). $P(x_i) = (x_I – V_{min\text{-}abs}) / (V_{min\text{-}des} - V_{min\text{-}abs})$ if $V_{min\text{-}abs} < x_i < V_{min\text{-}des}$.
   $P(1.5) = (1.5 –1) / (3- 1) = 0.5 /2 = 0.25$
3. Plaster casting process compatibility P (1.5) to produce finish 1.5 µm is 100 % (fully compatible). Figure 5. show this case.
   $P(x_i) = 1$ if $V_{min\text{-}des} < x_i < V_{max\text{-}des}$ …(5)
   $P(1.5) = 1$ because $1.3 < 1.5 < 2.5$

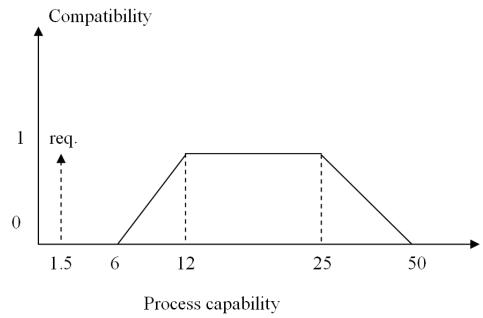

Figure 3: Sand casting surface finish capability

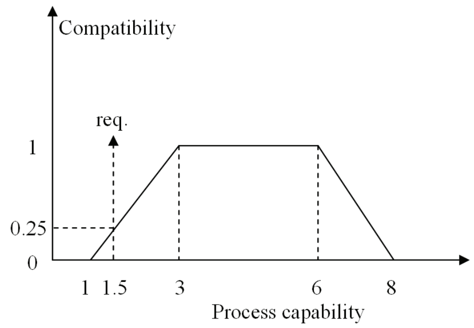

Figure 4: Shell casting surface finish capability

4. Investment casting process compatibility P (1.5) to produce finish (1.5 µm) is 87.5 % as shown in figure (6).
   $P(x_i) = (x_I – V_{min\text{-}abs}) / (V_{min\text{-}des} - V_{min\text{-}abs})$
   if $V_{min\text{-}abs} < x_i < V_{min\text{-}des}$ (-6)
   $P(1.5) = (1.5 – 0.8) / (1.6 – 0.8) = 0.7 / 0.8 = 0.875$

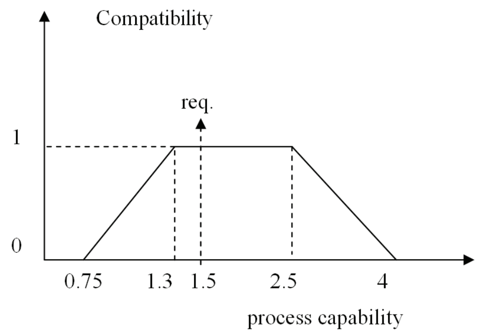

Figure 5: Plaster casting surface finish capability

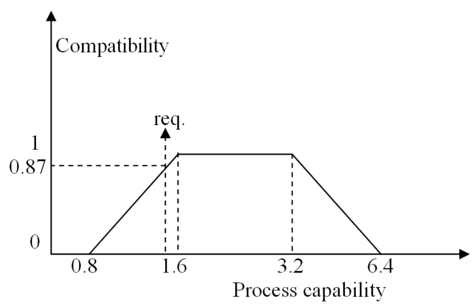

Figure 6: Investment casting surface finishes capability

Then it can be concluded from the previous calculations the process that preferred to produce surface finish (1.5 µm) is the plaster casting which is considered as the optimal process for this criterion.

Complexity:The complexity of a part refers to its shape, size, and number of feature that it contains. For geometrically simple parts such as bolt or straight shafts, the most economical method of manufacturing is relatively apparent. As the shape of part become more complex, selection of suitable process becomes important. Casting processes are more suitable to the intricate and nonsymmetrical shapes. In addition, the capabilities of each process are different to other process such as sand casting used to produce small and large intricate shapes, while die-casting is used to produce small and simple shapes.

Mechanical Properties: Mechanical properties such as strength and hardness have the biggest influence on part size and shape but they also have bearings on the process choose. The type of casting process selected is affected to the quality of mechanical properties of the part such as plaster casting has poor mechanical properties but squeeze casting has excellent mechanical properties. Then if the mechanical properties are important criterion then a suitable casting process is chosen. Table 8. shows some of casting process with mechanical properties that is produced from it.

Table 8: Casting methods with mechanical properties [12].

Casting process	Mechanical property
1- Sand	Good
2- Shell	Good
3- Plaster	Poor
4- Pressure die	Very good
5- Squeeze	Excellent

Porosity: Defects may be internal to the part or concentrated mainly at the surface. Porosity is one of the internal defect in the casting part, the degree of porosity differ from casting process to another. Table (9) below illustrates some of casting processes and their degree of porosity.

Table 9: Casting process and porosity [13].

Casting process	Porosity (Quality)
1- Sand	Bad
2- Investment	Medium
3- Squeeze	Best
4- Centrifugal	Good to best

5.1.2.3. Economic Consideration

Tooling includes pattern and core box for sand casting, and metal mould for die-casting as well as investment casting (for wax patterns). Their cost is driven by the material and manufacturing (mainly machining) of the tooling. The material is decided depending on the tool life required, which is in turn influenced by the order quantity. The tool manufacturing cost is driven by its geometric complexity. Then the tooling costs of casting processes are different from process to process. Table 10. illustrated some of processes with their cost considerations such as tooling cost, cost per unit, relative cost in quantity, relative cost in small number, and labor cost are different from process to process.

5.1.2.4. Production Considerations

Production Rate: Each casting process has its own possible production rate or an economical range of production rates although individual rates will differ depending on process capability. For example die casting can produce parts at a rate of thousands per hour while the cycle time for sand casting is typically take long time to produce limited parts than die casting. Table 11. illustrates some of casting process with their production rates.

Table 11: Production rates for some casting process [12].

Casting process	Production rate (unit / hour)
Sand casting	(50-150)
Plaster casting	(1-50)
Die casting	(> 1000)

Lead Time: Lead-time is the time required to preparation and setup tooling and equipment that needed for casting process before production. Each casting process required tools and equipment's differ to other process and these depending on the method used. Therefore, the lead-time is different from process to process such as lead-time for preparation and setup die-casting is longer than lead-time required to sand casting. Then lead-time also affects in selection of a process in Table 12. show some casting processes with the required lead-time.

Table 12: Casting process lead-time [13].

Casting process	Lead-time (week)
Sand casting	(1-4)
Die casting	(12 – 16)
Investment casting	(8-12)

Process Flexibility: Process flexibility is the capability of process to change the design of the casting part. Some of casting processes have a high flexibility to cast different parts such as reusable mold while other processes have limited flexibility to cast different parts such as permanent mold. Therefore, process flexibility affected in selection of casting process. Table (13) illustrates the degree of flexibility of some casting processes.

Table 10: Cost considerations for casting method [14, 15].

Casting process	Tooling Cost	Cost per	Cost in Unit	Cost in small Quantity	Labor Cost No.
Sand casting	Low	Low	Low	Very Low	Low-Medium
Lost foam Casting	High	Medium	Low	High	High
pressure die Casting	High-Highest	Highest	Very Low	Highest	Low

Table 13: Degree of flexibility for some casting processes [12].

Casting Process	Degree of Flexibility
Sand casting	Excellent
Shell casting	Fair
Lost Foam	Good
Die casting	Poor

6. Methodology of Process Selection

The process selection module assesses the degree of compatibility between a process alternative and the product requirements. process compatibility is performed via selection queries on the database for each product specifications. The queries are based on the application of fuzzy logic approach to determine the degree of compatible for each process. In this paper we selected twelve casting process as a database in material selection database. There are about seventy alloys of aluminum and steel with different chemical composition. Then each alloy gave properties different to other alloy. To select the optimal alloy from alternative alloys the user or designer can inter the range of values for mechanical properties with degree of accuracy required or named fuzzy limit. Then by using fuzzy logic approach (FLA) as mention in previous section any alloy that have values out of the range of absolutely limits will be eliminated. The (CACPS) has been designed by using visual basic language version (6) which links with Microsoft Access system in building database for casting process capabilities. The system interacts with user or designer to specify the specifications of required criteria. Then the selected process that satisfies design requirements will inter to the next step of determining the optimal casting process and this process can be determined according to the degree of compatibility between product specifications and the capability of process

This approach is differing from the existing approaches in determining the values of compatibilities for both optimal and alternatives selection processes, and this does not existing in the other approaches. Then this method is more accrued from the other methods. The limitation of this approach is, when there is no result that can meet the initial requirement, the system does not suggest to the user how can change the input value to have results.

7. Case Study: Selection Process for Elevator Control Quadrant

The elevator control quadrant component is a part of control system for the wing-elevator of a commercial aircraft. It is to be made of a light alloy (aluminum) [14]. The required specifications as in the following:

1. Metal Type: Aluminum
2. Weight: 5kg
3. Section Thickness: 5 mm
4. Surface finish: 10 μ m
5. Tolerance: 0.5 mm

To select the optimum process for manufacturing the elevator control quadrant part that satisfied the above requirements the inputted criterion to the (CACPS) system as in figure 7.

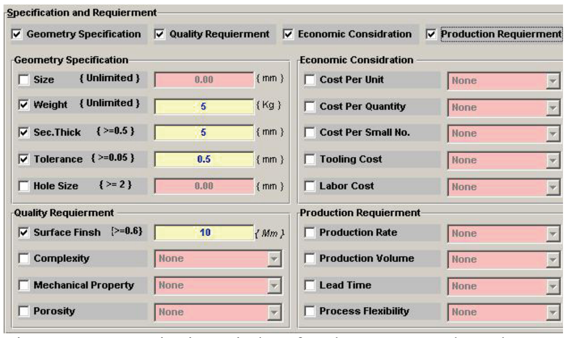

Figure 7: Input criterion window for elevator control quadrant

The results that are obtained from applying (CACPS) system can be illustrated in Figure 8.

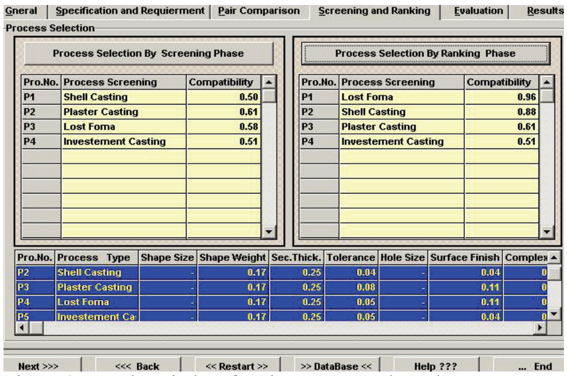

Figure 8: Results window for elevator control quadrant

From the above window, the system selected four processes. All the selected processes (Lost foam, shell, plaster, and investment casting with degree of computability's 96%, 88%, 61%, and 51% respectively) are satisfied the requirements specifications and these results compatible with the selected processes in reference [14].

8. Conclusions

In this paper fuzzy logic (F.L) technique used successfully for decision making in conceptual design phase, to select casting process. The (F.L) technique is more suitable in selection methodology for casting process because the capability of each process different from foundry to another. Also in practice, the process characteristics also depend on the equipment, labor skills, quality management practices and other company-dependent factors. This can be captured in a band of values for each process capability characteristic. then (F.L) used to calculate the degree of compatibility between requirements and process capability. The degrees of compatibility that are obtained from the system are varying from part to part and depending on the user preference to the required criterion. The system capable of drawing in diagrams for compatibility degree for both selected process and with each criterion its clear the real representation of capability for each process to the satisfied requirements. Hence the designer can benefits from these diagrams in decision making for selecting the most preferred to him. The alternatives selected processes enable the designer to make some of modifications in the design stage until reach to satisfaction the requirements of design.

If the product specification required high accuracy or surfaces finish more than the capabilities of some casting process and the part must be produced by (sand casting as example) secondary operations (such as machining) must be made on casting part to ensure these specification. The system can be extending to involve other materials and other manufacturing processes.

References

[1] Dieter, G.E. Engineering design a material and processing approach. NY: Mc Graw-Hill; 1991.

[2] Karthik S., Patwardhan H., Chung C., and Ramani K., "Rapid Application Development of Process Capability Supplier." Computer and Information in Engineering (CIE) Conference, Chicago, USA, 2003.

[3] Yusheng Chen Saty and Gupta K, "A Web-Based Process/ Material Advisory System ". ASME International Metal Engineering Proceedings, Orlando, Florida, 2000.

[4] Cebon D. and Ashby M.F. "The Optimal Selection of Engineering Entities." Technical Report, Department of Engineering, Cambridge University, Cambridge, UK, 1997.

[5] Esawi A. , Ashby M., "The Development and Use of a Software Tool for Selecting Manufacturing Process at Early Stages of Design". Conference on Integrated Design and Process Technology, Berlin, Germany, 1998.

[6] Kalpakjian, S., Manufacturing Processes for Engineering Materials, 3rd ed., Menlo Park, CA, Addison Wesley, 1997.

[7] Ravi B. Metal casting computer-aided design and analysis. New Delhi: Prentice Hall of India; 2005.

[8] Jyh-Cheng, Yu Steven and Krizan Ishii "Computer Aided Design for Manufacturing Process Selection". Journal of Intelligent Manufacturing, Vol. 4, No. 3, 1993, 199-208.

[9] Mikell P. Groover. Fundamentals of modern manufacturing materials, process, and systems. Prentice Hall.Inc;1996

[10] Energetics, Incorporated "Energy and Environmental Profile of the U.S. Metal Casting Industry" September 1999.

[11] Karthik, S. , Chung C.W, Ramani K. & Tomovic M. "Methodology for Metal-Casting Process Selection" Society of Automotive Engineers, Inc., 2002

[12] EPA, Office of Compliance Sector Notebook Project "Profile of the Metal Casting Industry." October 1988.

[13] Schey, J. A. Introduction to manufacturing process.3 rd ed. NY: McGraw Hill ; 2000.

[14] Giachetti R. E.,"A Decision Support System for Material and Manufacturing Process Selection." Journal of Intelligent Manufacturing, Vol. 9, No. 3, 1998, 265-276.

JJMIE

Volume 2, Number 1, Mar. 2008
ISSN 1995-6665
Pages 53 -63

Jordan Journal of Mechanical and Industrial Engineering

An Application of Finite Element Method and Design of Experiments in the Optimization of Sheet Metal Blanking Process

Emad Al-Momani, Ibrahim Rawabdeh *

Industrial Engineering Department, University of Jordan, Amman, Jordan

Abstract

Metal blanking is a widely used process in high volume production of sheet metal components. The main objective of this paper is to present the development of a model to predict the shape of the cut side. The model investigates the effect of potential parameters influencing the blanking process and their interactions. This helped in choosing the process leading parameters for two identical products manufactured from two different materials blanked with a reasonable quality on the same mold. Finite Element Method (FEM) and Design of Experiments (DOE) approach are used in order to achieve the intended model objectives. The combination of both techniques is proposed to result in a reduction of the necessary experimental cost and effort in addition to getting a higher level of verification. It can be stated that the Finite Element Method coupled with Design of Experiments approach provide a good contribution towards the optimization of sheet metal blanking process.

Keywords: Blanking process; Finite Element Method; Design of Experiments; Optimization; Burrs height;

1. Introduction

Metal blanking is a widely used process in high volume production of metal components. General guidelines for this process exist but they are not sufficient to overcome the difficulties in designing blanking processes, where requirements for less cycle time and accurate product dimensions become more demanding. The design of blanking processes in industrial practice is still based largely on experimentations and it is often governed by time-consuming and expensive trial and-error iterations caused by limited, mostly empirical, knowledge of these processes. There is a need for a new method that allows for the reduction of trial and error option in designing a blanking process. Therefore, appropriate modeling and understanding of the blanking process could be beneficial to reduce the lead-time and to control the product specifications, especially the shape of a blanked (sheared) edge.

Current research on the control of blanking operations aims to improve the monitoring and control of the quality of components. The motivation is the reduction of reject volume, the reduction of manual quality control, and the high cost of replacing tools after catastrophic failure [1]. Optimizations of manufacturing processes and parameters control are known to have direct impact on the production line maintenance and operations [2]. Among the most important tools for manufacturing processes optimization are the design of experiments (DOE) approach and the finite element method (FEM).

In this paper, a combination of both techniques is used in order to achieve a higher level of verification and to reduce the cost of the necessary experimental effort. Design of experiments will aid in guiding the selection of the proper combination of the process parameters at their specified levels in such a way that costly dies will not be manufactured until the finite element method shows the best set of the process parameters.

1.1. The Blanking Process

Blanking is a manufacturing operation as old as the technology itself. Its applications range from components of very light to heavy appliances and machineries [3]. Blanking is defined as the cutting of a work piece between two die components to a predetermined contour [4]. During blanking, the part is subjected to complex solicitations such as deformation, hardening and crack initiation and propagation. The theoretical modeling of such processes is very difficult due to the complexity in describing the different stages of the whole shearing process starting with the elastic stage and ending with the total separation of the sheet metal [5].

* Corresponding author. e-mail: rawabdeh@ju.edu.jo

The behavior of the blank material during the blanking process can be divided into five stages. During the start of the process, the sheet is pushed into the die and the blank material is deformed, first elastically. The process continues and the yield strength of the blank material is reached, first at the outer fibers and later at all the fibers in the zone between the punch and the die. Normally, the material underneath the punch is subjected to thinning. The plastic deformation causes rounding of the edge of the blank. During this stage, or possibly as early as during the plastic deformation stage, damage initiation followed by the nucleation and growth of cracks takes places. In most of the conventional blanking situations, ductile fracture occurs after shear deformation. This causes rough, dimpled rupture morphology on the fractured surface of the product. Finally, the work due to friction is dissipated when forcing (pushing) the slug through the die hole [6].

1.2. Finite Element Method (FEM) and Design of Experiments (DOE)

Numerical methods provide a general tool to analyze arbitrary geometries and loading conditions. Among the numerical methods, Finite Element Analysis (FEA) has been extensively used with success; however, this kind of analysis requires the generation of a large set of data in order to obtain reasonably accurate results and consumes large investment in engineering time and computer resources [7]. FEM is a good choice for the analysis of sheet metal processes since it helps in eliminating the need for time-consuming experiments to optimize the process parameters [3]. The FEM simulations are increasingly used for investigating and optimizing the blanking processes. Many time-consuming experiments can be replaced by computer simulations. Therefore, highly accurate results of sheet metal forming may be obtained by using the FEM simulation [8]. The finite element method gives an approximate solution with an accuracy that depends mainly on the type of element and the fineness of the finite element mesh.

In the manufacturing area, Design of Experiments (DOE) is found to be an efficient statistical technique that can be used for various experimental investigations. The design of experiments is one of the powerful tools used to investigate deeply hidden causes of process variation [9]. It is a systematic, rigorous approach to engineering problem solving that applies principles and techniques at the data collection stage to ensure the generation of valid, defensible, and supportable conclusions. In the blanking process, experimental design is considered a powerful approach for product and process development, and for improving the yield and stability of an ongoing process. Hambli *et al.*, [10] found that the design of experiments technique is an efficient and cost-effective way to model and analyze the relationships that describe process variations.

The sheet metal industry is highly interested in knowing if two identical products manufactured of two different materials, can be blanked with a reasonable quality without the need to build two separate setups. This will increase the efficiency of the production processes and reduce the level of wasted materials, time, cost, and effort involved in the production stages. In addition, the industry needs a suitable model to overcome the long cycle time in developing a particular blanking process. This can be achieved by combining the Finite Element Method and Design of Experiments techniques aiming at identifying opportunities to increase efficiency and productivity as well as eliminating waste and reducing production cost associated with the blanking process. The main objective of this paper is to construct a finite element model to predict the shape of the cut side of a blanked product, and to investigate the effect of potential parameters influencing the blanking process and their interactions using the design of experiments approach in order to choose the process leading parameters in an optimal way.

2. Relevant Literature

Numerical simulation of the problems associated with sheet metal forming using the Finite Element Method (FEM) can help in process design by reducing the number of trial steps. Although process modeling using FEM simulation is already used in industry in a wide variety of forming operations, no commercially available FEM code is capable of simulating, with the required degree of precision, the blanking process, and fracture formation [11]. Hambli [5] presents industrial software called BLANKSOFT dedicated to sheet metal blanking processes optimization. Several researches have emphasized different aspects of the blanking process. Through literature, it is clear that many methods are used to study the blanking process to achieve the optimal combination of its parameters. This includes analytical approaches [6, 12]; Finite Element Method [13, 14, and 5]; Design of Experiments [10, 15] and Neural Networks Modeling [15, 16]. Literature shows that the mechanical characteristics of the blanking process and the geometrical aspect of the sheared edge are affected by different parameters. These parameters include clearance, wear state of the tool, tool radii and geometry, thickness of the sheet, blank geometry, or layout, material prosperities such as hardness and ductility, friction, tools surface finish or lubricant type, sheet metal coating, and stroke rate or blanking speed [10-16].

Using a combination of techniques in analyzing the blanking process and its parameters and conducting comparisons are widely common in literature. Klingenberg and Singh [6] have compared two existing analytical models of blanking while Biglari *et al.* [13] have performed a comparison between fine and conventional blanking. Hambli [15] has combined predictive finite element approach with neural network modeling of the leading blanking parameters in order to predict the burr height of the parts for variety of blanking conditions. Brokken *et al*. [17] presented a set of interrelated numerical techniques resulting in a finite element model of the metal blanking process, focusing on the prediction of the shape of the cut edge of the blanked product. In addition, Rachik *et al*. [18] presented a comprehensive experimental and numerical study of the sheet metal blanking process.

The clearance impact on the blanking processes has consumed a significant amount of research. This concern about the clearance factor is because the structure of the blanked surfaces is influenced by both the tooling (clearance and tool geometry) and the properties of the work piece material (blank thickness, mechanical properties, microstructure, etc.). The selection of the clearance influences the life of the die or punch, the blanking force, the unloading force and the dimensional precision [19]. Hambli and Guerin [16] have developed a methodology to obtain the optimum punch–die clearance for a given sheet material by the simulation of the blanking process. The proposed approach combined predictive finite element and neural network modeling of the leading blanking parameters. Miguel and Jose [20] have proposed a general framework for numerical simulation of blanking process using FEM, and analyzed the influence of clearance on stress distribution prior to material separation.

Clearance parameter impact on the blanking process is widely tested. Fang *et al.* [19] investigated the punch–die clearance values for a given sheet material and the thickness are optimized by using a finite element technique in which the shearing mechanism was studied by simulating the blanking operation. Goijaerts *et al.* [21] performed finite element simulations and experiments on both blanking and tensile testing to evaluate the validity of both approaches with corresponding criteria for five different metals. Maiti *et al*. [3] analyzed the blanking of thin sheet of mild steel using an elastic plastic finite element analysis based on the incremental theory of plasticity. The study has helped to evaluate the influence of tool clearance, friction, sheet thickness, punch/die size, and blanking layout on the sheet deformation. Hambli *et al.* [10] investigated the blanking process using tools with four different wear states and four different clearances and studied the effects of the interaction between the clearances, the wear state of the tool and the sheet metal thickness on the evolution of the blanking force and the geometry of the sheared profile. The results of the proposed experimental investigation show that there is no universal optimal clearance value. Whether clearance should be set at 5% or 10% ultimately depends on the priorities of the practitioners.

Simulation techniques applied for the blanking process are beneficial to the understanding of the process behavior. Shim *et al*. [14] investigated the blanking operation of very thin sheet metals like membranes. Klingenberg and Singh [12] investigate the behavior of the blank material during the process through finite element simulations, analytical modeling, and experimental work. They have found that the quality of blanking process output is the determinant factor in assessing the goodness of the tool and parameters design. The quality of sheet metal blanking processes part can be assessed by the burr height of the sheared edge after blanking [15]. Thomas *et al.* [22] presented results from a numerical model validated by experiment, which illustrate the effects of some process parameters on blanking forces and edge quality of aluminum sheets.

A review of the literature on the blanking process shows that while a large number of analytical techniques have been used to study the process, the amount of theoretical and practical work done is relatively insufficient and thus further investigation is still needed. One reason for this may be the difficulty of simulating the shearing process because of the narrowness of the shear band formed and the lack of an appropriate fracture criterion. The most recent studies in the field of manufacturing processes show that, despite the increasing progress in blanking process analysis, there is still a lack of models allowing for the optimal design of sheet metal shearing processes [10].

3. Methodology

Finite Element Method (FEM) and Design of Experiments (DOE) techniques are used to achieve the study objectives. The combination of both techniques is proposed to result in a reduction of the necessary experimental cost and effort in addition to receiving a higher level of verification. Design of Experiments provides the guidance in the selection of the proper combination of the process parameters at their specified levels, in such a way that costly dies will not be manufactured until the finite element simulations show the best set of process parameters. The methodology that is followed to attain the research objectives is divided into the following work phases:

- Classify the blanking parameters into controllable and uncountable. A summary of the blanking parameters with their classification is presented in Figure 1. The identified controllable parameters are clearance, blank holder force, sheet metal thickness, and material type. While, the uncountable parameters are material prosperities inconsistency and conditions (shape, defects and internal stresses), friction and wear state of the tool, stroke rate or blanking speed, and punch-die alignment.

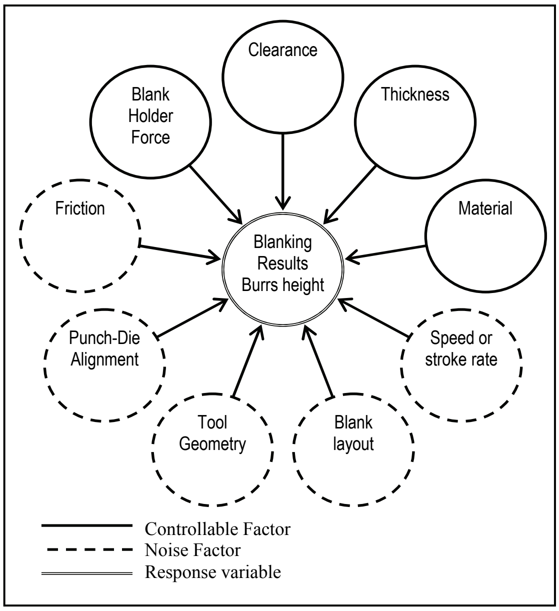

Figure 1. Summary of the blanking parameters situation in this research

- Choose the controllable factors that influence the blanking process as the interest domain.
- Select an appropriate working range for each potential factor. It is found that the working range of clearance fall within the range (0-25)% of the sheet metal thickness, the working range of the blank holder force fall within the range (0-30)% of the shearing force and

the working range of the thickness of their used material fall within the range (0.5-0.8) mm.

- Prepare to use of Design of Experiments (DOE) technique by selecting the experimental levels for each selected factor, i.e. the clearance to be in five levels (5, 10, 15, 20, 25) % of the sheet metal thickness, blank holder force to be in two levels (0, 3000N) and sheet metal thickness to be in four levels (0.5, 0.6, 0.7, 0.8) mm.
- Perform a factorial experimental design in order to take high-level interactions based on the findings of the previous steps.
- Develop a Finite Element Model (FEM) that represents the existing process in order to evaluate the quality of the inputs.
- Compare the two techniques (FEM and DOE) and analyze the results to get the proposed optimal set of parameters.

4. Finite Element Simulation

The problem studied in this work involves simulating of an axis-symmetric blanking operation of sheet metal. The simulation is designed to study a configuration that includes two types of materials (AISI-Steel 12 and AISI-Stainless Steel 480); five values of clearances (C= 5, 10, 15, 20, and 25 percent of sheet metal thickness); two values of the blank holder force (BHF = 0, and 3000 Newton); and four values of thickness of the sheet (t = 0.5, 0.6, 0.7, and 0.8 mm). Eighty simulations are performed for the above configuration according to the whole combinations of parameters. Simulations are conducted on the commercial finite element software package ABAQUS/Explicit.

The process is simplified by using a two-dimensional situation, under plane-strain conditions, since in a normal blanking operation the punch-die clearance is usually very small in relation to the blank diameter, otherwise, the deformation will be in a 3-D form. In all simulations, a circular disc with a diameter of 55 mm has been used as the blank. Only half of the blank was modeled because the blanking process is symmetric about a plane along the center of the blank. Figure 2 shows part of the finite element mesh used to model the plate in the shear zone.

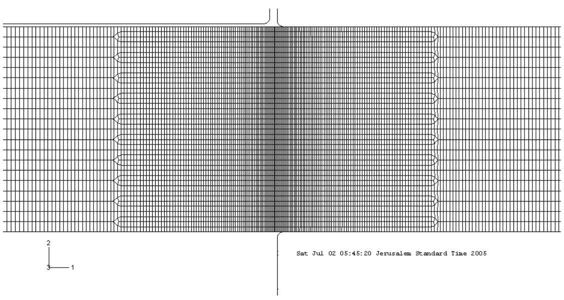

Figure 2. A part of the finite element mesh used to model the plate in the shear zone.

In the blanking operation, deformation is concentrated along very narrow shear band. The width of the shear band is a few microns, thus, the number of elements used is critical for every simulation since a large number of elements increases the accuracy of the result, but also substantially increases the calculation time. Therefore, a very dense mesh is defined in the shearing region and relatively large elements for the remainder. The blank is modeled using twenty layers of four-node axi-symmetric elements (ABAQUS type CAX4R). This number is doubled to be forty layer in the cutting region, one thousands axi-symmetric elements are used in the radial direction. The mesh is designed to be smaller as the cutting region is approached to get accurate results. A total of (23020) elements and (24041) nodes have been used in the model and the smallest element size is 3.324E-3 mm after testing different meshes. The tools are modeled with rigid surfaces and contacts are defined between the top of the blank and the punch, the top of the blank and the blank holder, and the bottom of the blank and the die. The friction coefficient between the blank and the other tools is assumed 0.1. The contact between components is established in a reasonably gentle manner to avoid large over-closures and rapid changes in contact pressure. This approach, although requires one more step, minimizes the convergence difficulties, and makes the solution more efficient.

For the materials aspects, most materials of engineering interest initially respond elastically. If the load exceeds some limit (the “yield load”), the deformation is no longer fully recoverable. However, a portion of the deformation will remain when the load is removed. Plasticity theories model the material's mechanical response as it undergoes such non-recoverable deformation in a ductile fashion. As a first approximation, the blanking process is simulated using two-dimensional plane-strain model. The specimen is modeled using isotropic material properties. The plastic material behavior is described by the Von Misses yield condition and isotropic hardening in which the strain-hardening behavior described using tabulated data (stress versus effective plastic strain). The classical metal plasticity model is used with isotropic hardening which is available in ABAQUS/Explicit. Stress-strain data representing the material hardening behavior are necessary to define the model and the mechanical characteristics of the material are obtained from tensile tests. A shear failure model offered in ABAQUS/Explicit is used to limit the subsequent load carrying capacity of an element (up to the point of removing the element) once a stress limit is reached.

Two separate tensile tests were performed to provide information on the properties of materials under uni-axial tensile stresses. The purpose of the first test is to get the stress-strain diagram while the purpose of the second test is to get the modulus of elasticity and Poisson’s ratio. The results are presented in Table 1.

4.1. Model Verification

In order to assess the quality of the model, a comparison with experiments is made. A company that deals with dies and tools manufacturing and steel sheets forming, is selected for conducting the experiments. The blanking experiments were carried out using a blanking machine at a local industrial company.

Table 1. Material characteristics of Steel 12 and Stainless steel 480 obtained from the load-elongation diagrams.

Material	Yield stress [MPa]	Ultimate tensile stress [MPa]	Ductility as % elongation	strain-hardening exponent n	strength coefficient K [MPa]	Modulus of Elasticity [GPa}	Poisons ratio
Steel 12	201	296	37.6	0.2354573	524.448	201	0.31
Stainless steel	296.54	475	24.4	0.20651387	816.44	187	0.29

A die of a 20 mm in diameter and a punch of 19.9 mm in diameter, which gives a clearance of 10% for the 0.5 mm thick stainless steel specimen and 7% for the 0.7 mm thick steel specimens, were selected for conducting the experiments. The capability of controlling the blanking velocity is limited; as a result, one value is selected for the blanking velocity that is 0.1 m/s. The steps in executing the blanking process are shown in Figure 3.

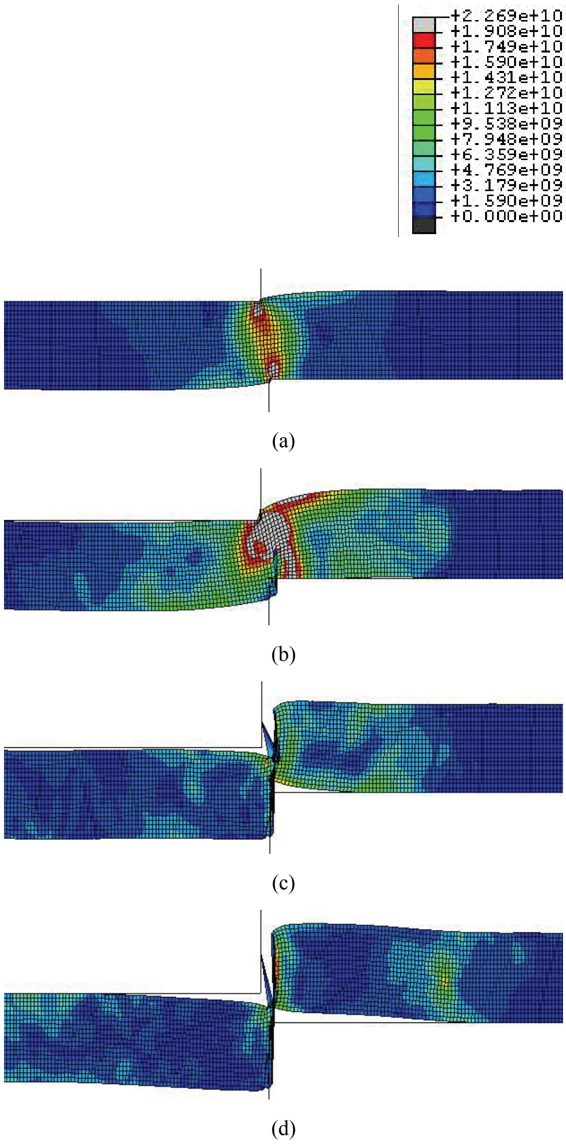

Figure 3. Crack propagation in the mesh for Steel 12

The FEA model was validated through the compression of the experimental and the simulated punch load-penetration curves and the experimental and the simulated burrs height that were developed off line. Figure 4 shows the experimental and the simulated punch load-penetration curves for stainless steel. The agreement between both curves is good with a percent error in blanking force of 7.6%. Figure 5 shows the burs height in the mesh for Steel 12 with 7 % clearance and 3000 N applied blank holder force. The burrs appear clearly and its height is 0.0811 mm. In the experiment, the average burrs height for five blanked specimens was 0.085 mm measured by a digital V-Caliper with ±0.005 accuracy, which seems to be in good agreement with the simulation results with an error of about 5%.

It was determined that the four inputs (factors) that are considered important to the blanking process are material type; clearance; sheet metal thickness and blank holder force. To ascertain the relative importance of each of these factors on burrs height, a set of experiments are conducted for different factors levels combinations. Table 2 represents these factors and their level values.

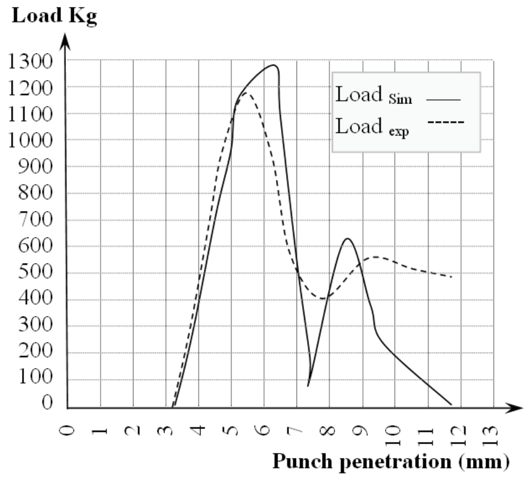

Figure 4. The experimental punch load-penetration curve and the ABAQUS result of the simulated punch load-penetration curve for stainless steel where Load $_{Simulation}$ = 12.75 kN, and Load $_{exp}$ = 1200 Kg * 9.81 N/m^2 = 11.772 kN.

The analysis is based on a full factorial experimental design. Running the full complement of all possible factor combinations means estimating all main and interaction effects. The specific statistical objectives of the experiment are to determine the important factors that affect burrs height of the blanked edge, the settings that minimize burrs height of the blanked edge, and a prediction equation that functionally relates burrs height to various factors. The FEM simulations were run with 80 different settings and their results are shown in Table 3. The response data is plotted in several ways to see if any trends or anomalies appear that would not be accounted for by the standard linear response models.

Table 2. Blanking process factors and their corresponding level values.

Factor	Number of levels	Level Values				
		Level 1	Level 2	Level 3	Level 4	Level 5
Material type	2	Steel 12	Stainless steel			
Clearance	5	5	10	15	20	25
Thickness	4	0.5	0.6	0.7	0.8	
Blank holder force	2	0	3000			

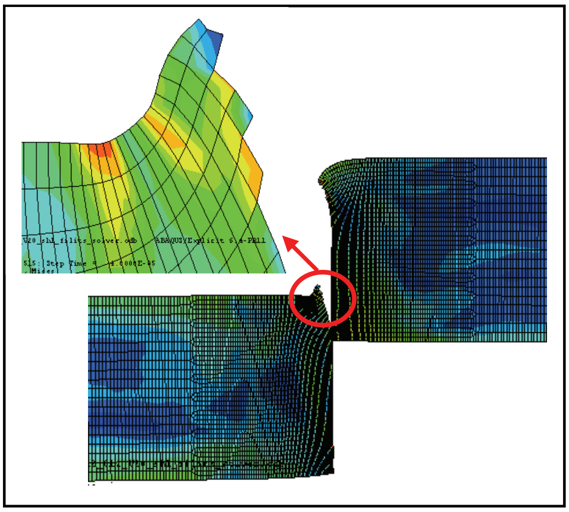

Figure 5. FEM result for Steel 12 with 7 % clearance and 3000 N blank holder force.

5. Blanking Process Modeling

The basic steps of the model building process are model selection, fitting, and validation. In the model selection step, plots of the data, process knowledge, and assumptions about the process are used to determine the form of the model to be fit to the data. Then, using the selected model and possible information about the data, an appropriate model-fitting method is used to estimate the unknown parameters. When the parameters are estimated, the model is then carefully assessed to see if the underlying assumptions of the analysis appear plausible. If the assumptions seem valid, the model can be used to estimate, predict, and optimize the burrs height value of the blanked product. If the model validation reveals problems with the current model, then the modeling process is repeated using information from the model validation step to select and/or fit an improved model.

With a full factorial experiment, a model containing a mean term, four main effect terms, six 2-factor interaction terms, 3-factor interaction term and a 4-factor interaction term (15 parameters) can be fitted. However, to eliminate the least impact factors, it is assumed that the three factor interaction terms and more are non-existent since it is very rare for such high-order interactions to be significant, and they are very difficult to interpret from an engineering viewpoint. Because of eliminating the high order interactions, a theoretical model with eleven unknown constants is obtained, and the analysis of the experimental data will clarify which of these are the significant main effects and interactions needed for a final model. The analysis of variance (ANOVA) is used to test the following hypotheses:

H_{o1}: There is no main effect for material type, clearance, thickness, and blank holder force

H_1: There is a main effect for material type, clearance, thickness, and blank holder force.

H_{o2}: There is no interaction effect among any of the material type, clearance, thickness, and blank holder force parameters.

H_2: There is an interaction effect among any of the material type, clearance, thickness, and blank holder force parameters.

The MINITAB-14© results for fitting the eleven-parameter model are displayed in Table 4. The table shows that both of the null hypotheses are rejected since many factor-mean effects and interactions are significant. This fit has a high R^2 and adjusted R^2, but the large number of high p-values (>0.05) makes it clear that the model has many unnecessary terms. Starting with these eleven terms, a stepwise regression option is used to eliminate unnecessary terms. By a combination of a backward elimination stepwise regression and the removal of remaining terms with a *p*-value higher than 0.05, a formula is achieved with an intercept and five significant effect terms where the thickness and all its interactions are removed from the model in addition to the material-blank holder force interaction. Equations (1) and (2) are the final equations resulting from Design Expert© for Steel 12 and Stainless Steel 480, respectively.

<u>Steel 12: Burrs Height =</u>

$$\begin{aligned}&0.05174\\&+2.8766X^{-3}*C\\&-3.3695X^{-6}*BHF\\&+1.0111X^{-6}*C*BHF\end{aligned} \quad (1)$$

<u>Stainless Steel 480: Burrs Height =</u>

$$\begin{aligned}&0.05533\\&+1.7944X^{-3}*C\\&-3.3695X^{-6}*BHF\\&+1.011X^{-6}*C*BHF\end{aligned} \quad (2)$$

Where: C: Clearance as a percent of sheet metal thickness, and BHF: Blank holder force measured in Newton.

The Design Expert© software is used for fitting the new model where only sixteen combinations are used. The obtained ANOVA results are shown in Table 4. At this stage, the model appears to account for most of the variability in the response, achieving an adjusted R^2 of 0.9914. All the remaining main effects with two 2-factor interactions are significant. Values of less than 0.05 indicate model terms are significant. In this case Material type, Clearance, Blank holder force, and the multiplication of the Material type by Clearance and the multiplication of the Clearance by Blank holder force are significant model terms.

Table 3. Design of experiment matrix with the corresponding burrs height

Material									
ST12					Stainless				
Exp #	Clearance (mm)	Thickness (mm)	BHF (N)	Height (mm)	Exp #	Clearance (mm)	Thickness (mm)	BHF (N)	Height (mm)
1	5	0.5	0	0.06795	41.	5	0.5	0	0.0633
2	5	0.5	3000	0.07075	42.	5	0.5	3000	0.07065
3	5	0.6	0	0.06794	43.	5	0.6	0	0.06332
4	5	0.6	3000	0.07076	44.	5	0.6	3000	0.07064
5	5	0.7	0	0.06746	45.	5	0.7	0	0.06319
6	5	0.7	3000	0.07026	46.	5	0.7	3000	0.07054
7	5	0.8	0	0.06656	47.	5	0.8	0	0.06304
8	5	0.8	3000	0.06936	48.	5	0.8	3000	0.07032
9	10	0.5	0	0.0843	49.	10	0.5	0	0.0733
10	10	0.5	3000	0.0913	50.	10	0.5	3000	0.09155
11	10	0.6	0	0.08426	51.	10	0.6	0	0.07328
12	10	0.6	3000	0.09128	52.	10	0.6	3000	0.09158
13	10	0.7	0	0.08328	53.	10	0.7	0	0.07299
14	10	0.7	3000	0.09028	54.	10	0.7	3000	0.09133
15	10	0.8	0	0.08168	55.	10	0.8	0	0.07256
16	10	0.8	3000	0.08864	56.	10	0.8	3000	0.09088
17	15	0.5	0	0.0996	57.	15	0.5	0	0.08485
18	15	0.5	3000	0.1116	58.	15	0.5	3000	0.11605
19	15	0.6	0	0.09962	59.	15	0.6	0	0.08486
20	15	0.6	3000	0.11156	60.	15	0.6	3000	0.11606
21	15	0.7	0	0.09833	61.	15	0.7	0	0.08447
22	15	0.7	3000	0.1103	62.	15	0.7	3000	0.11569
23	15	0.8	0	0.09616	63.	15	0.8	0	0.08384
24	15	0.8	3000	0.1202	64.	15	0.8	3000	0.11504
25	20	0.5	0	0.1128	65.	20	0.5	0	0.09515
26	20	0.5	3000	0.1651	66.	20	0.5	3000	0.14075
27	20	0.6	0	0.11282	67.	20	0.6	0	0.09512
28	20	0.6	3000	0.16508	68.	20	0.6	3000	0.14072
29	20	0.7	0	0.11135	69.	20	0.7	0	0.09462
30	20	0.7	3000	0.16364	70.	20	0.7	3000	0.14026
31	20	0.8	0	0.10888	71.	20	0.8	0	0.09384
32	20	0.8	3000	0.1612	72.	20	0.8	3000	0.13952
33	25	0.5	0	0.1235	73.	25	0.5	0	0.10315
34	25	0.5	3000	0.1937	74.	25	0.5	3000	0.1644
35	25	0.6	0	0.1235	75.	25	0.6	0	0.10316
36	25	0.6	3000	0.1937	76.	25	0.6	3000	0.16442
37	25	0.7	0	0.12192	77.	25	0.7	0	0.1026
38	25	0.7	3000	0.19213	78.	25	0.7	3000	0.16385
39	25	0.8	0	0.11936	79.	25	0.8	0	0.10168
40	25	0.8	3000	0.18952	80.	25	0.8	3000	0.16296

Table 4. The analysis of variance (ANOVA) for the modified linear model, height versus material type, clearance, and blank holder force.

Response: Heihgt ANOVA for Selected Factorial Model Analysis of variance table [Partial sum of squares]					
Source	**DF**	**Sum seq.**	**Mean Sq.**	**F**	**Prob > F**
Model	**5**	0.03400000	6.708E-003	939.85	< 0.0001 sign.
Material	**1**	6.401E-004	6.401E-004	89.68	< 0.0001
Clearance	**4**	0.02400000	0.02400000	3326.41	< 0.0001
Blank holder force	**1**	5.010E-003	5.010E-003	701.90	< 0.0001
Material * Clearance	**4**	4.685E-004	4.685E-004	65.64	< 0.0001
Clearance * Blank holder force	**4**	3.680E-003	3.680E-003	515.62	< 0.0001
Residual	**10**	7.137E-005	7.137E-006		
Cor Total	**15**	0.03400000			
Std. Dev.	2.672E-003		R-Squared	0.9979	
Mean	0.11		Adj R-Squared	0.9968	
C.V.	2.51		Pred R-Squared	0.9946	
PRESS	1.827E-004		Adeq Precision	6.4550	

Figures 6 and 7 show the mean and the interaction effects for burr heights. The slope of the line is an indication of the variable effect degree on the burr height - the higher the slope the higher the interaction effect. It is clear that the material type has an effect on burrs height and, in general, the Steel 12 gives a higher burr height than Stainless Steel 480 in general. The clearance effect on the burr height is large - the higher the clearance the higher the burrs height for both materials. It is also clear that as the clearance increases more than 15%; its effect starts to be higher for Steel 12 than for Stainless Steel. The thickness effect is insignificant since a horizontal line appears. However, the blank holder force has a clear effect, the lower the blank holder force the lower the burr height.

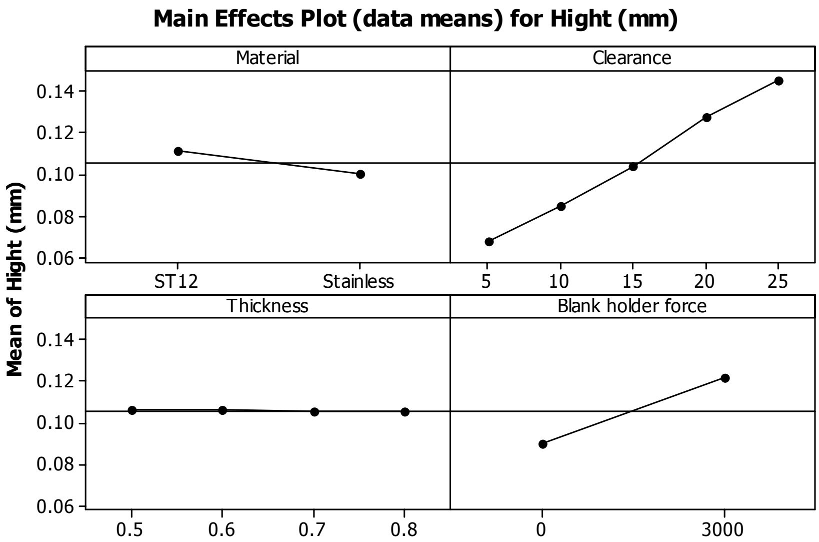

Figure 6. Mean effect plot for bur height

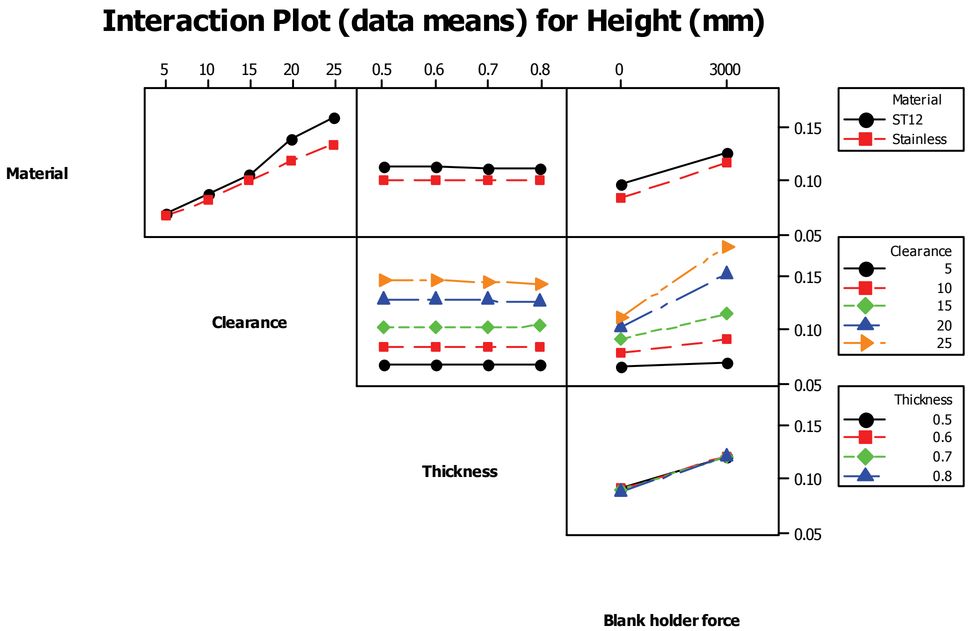

Figure 7. Interaction plot for bur height

The developed burrs height model is used for the prediction and optimization purposes. While prediction is used to determine the value of a new observation of the burrs height for a particular combination of the values of the blanking process significant parameters, optimization, on the other hand, is performed to determine the values of the blanking process inputs that should be used to obtain the desired burrs height output. Optimization is used to minimize the burrs height of the process and to increase the opportunity of using the same blanking setup for both materials (Steel 12 and Stainless Steel 480). Figure 8 shows the graphical representation of equations (1) and (2) which relate the burrs height to clearance and blank holder force, respectively. It is clear from Figure 8 (a and b) that the height increases with the increase in clearance and the blank holder force. The effect of clearance is higher than the effect of blank holder force; this is clear from the surfaces slope. As clearance increases, the effect of blank holder force on increasing the burrs height also increases.

In order to minimize burrs height, it is obvious that the clearance must be small. Since the blank holder force effect is not very significant at small clearance values, the small blank holder force is preferable. Figure 9 shows the burrs height as a function of clearance for both materials when no blank holder force is applied. It is clear that the optimum clearance that gives minimum burrs height for both materials simultaneously, in this case, is about 3 % that is the intended intersection point of the two lines. These readings can be seen in an easier and more obvious way through the contour plot shown in Figure 10. This plot is used to determine the settings that minimize the burrs height value for both materials. It shows that the contour curves are linear and start to have some curvature at the combination of high clearance and high blank holder force, which in turn imply that the interaction term is more significant at this condition. To get small burrs height, it is better to have a small clearance. For approximately the same burrs height, a small blank holder force makes the system more robust to the changes in clearance, where a clearance range up to about 12% exists, whereas, a limited range up to about 7 % exists at high blank holder force.

(a)

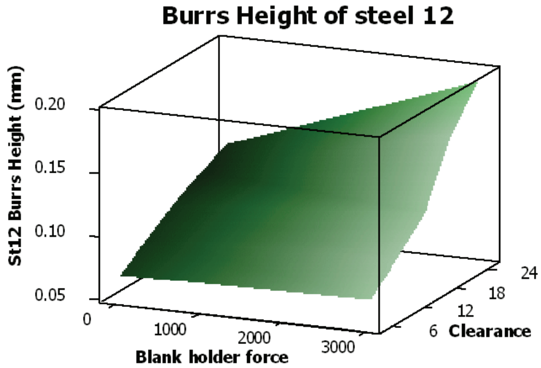

(b)

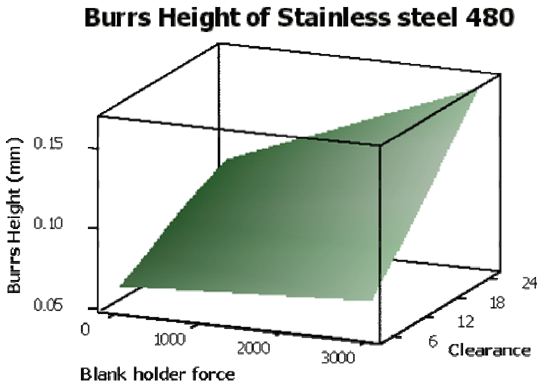

Figure 8. Surface plot burr height versus clearance and blank holder force a) Steel 12 and b) Stainless Steel 480

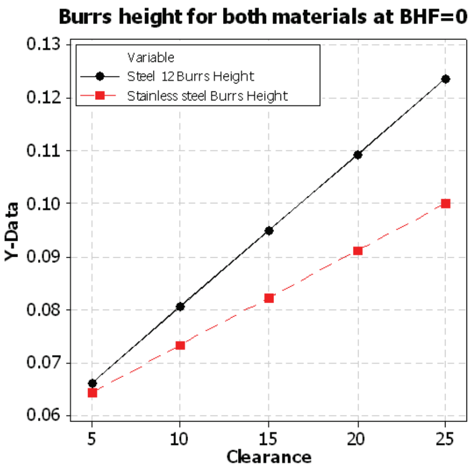

Figure 9. A plot for the burrs height of Steel 12 and Stainless steel 480 at no blank holder force and different clearances.

5.1. Model Validation

In order to validate the results of the model, a comparison was made with experiments carried out in actual work environment in the selected company. Since the thickness parameter is found to be insignificant, the experiments are conducted for only one thickness value using the 20-mm diameter die with 19.90 mm diameter punch for Steel 12 specimen, which has the thickness of 0.7 mm. Two cases are studied with and without blank holder force of 3000 N. The burrs height is measured for five samples then averaged. The same procedure is repeated for the Stainless Steel 480, with a thickness of 0.5 mm, and a clearance of 10% is achieved on the previous setup. Table 5 compares the burr height results from the simulation, experiments, and the model for Steel 12 and Stainless Steel 480 at zero and 3000 N blank holder force, respectively.

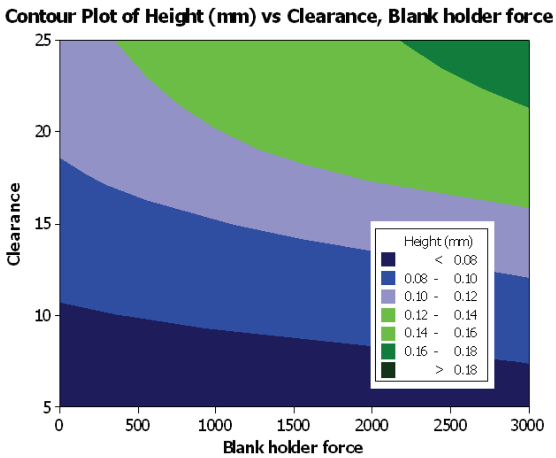

Figure 10. Contour plot of height versus clearance and blank holder force for both materials.

Table 5 shows the ability of the fitted model to predict the real burrs height with an error less than 10%. On the other hand, the experimental data validate the result of the FEM analysis, which stated that burrs height increases with increasing the blank holder force. If the objective is to find a model that is valid even when the sheet thickness is changed, then it is preferable to do not interact between thickness and the other factors. The main effect of the thickness is not important by itself, what is important is to identify the optimal clearance setting and the tool wear states that are not too detrimental to the process, regardless of the sheet thickness [15]. It is found that the thickness is not a significant factor in the developed model, which makes the experimental results robust for different sheet metal thickness.

6. Conclusions and Future Work

The developed experimental investigation of the sheet metal blanking process makes it possible to study the effects of process parameters such as the material type, the punch-die clearance, the thickness of the sheet and the blank holder force and their interactions on the geometry of the sheared edge especially the burrs height. The finite element and design of experiments methods are used in order to obtain a better understanding of the blanking manufacturing response. The process signatures indicate that the material types as well as the geometric characteristics of the tools and their configuration influence the burrs height of the sheared edge.

Table 5. Simulation, experimental and model burrs height for Steel 12 and stainless steel 480 at zero and 3000 N blank holder force.

Material Type	Simulation burrs height (mm)		Experimental burrs height (mm)		Model burrs height (mm)	
	BHF= 0	BHF= 3000 N	BHF= 0	BHF= 3000 N	BHF= 0	BHF= 3000 N
Steel 12	0.0721	0.0811	0.079	0.085	0.07188	0.0830
Stainless steel 480	0.0733	0.09155	0.076	0.095	0.07327	0.0935

This investigation shows that, in order to minimize the burrs height, the clearance should be set at about 5 % with almost no blank holder force. When blank holder force is set to zero, the process is slightly more robust to clearance changes than when a high blank holder force is used. It is not recommended to use a zero blank holder force; rather a small value in the order of about 2% of the blanking force can prevent the remaining skeleton from moving out of plane. The presented investigation of the blanking process makes it possible to predict optimum process parameters. It is possible to reduce the lead-time by using the Finite Element Analysis in conjunction with Design of Experiment technique in the design process, where computer simulations can replace many time consuming experiments. This will make the design process faster and more reliable. From another point of view, it is possible to build quality into products from the early design phases by predicting the shape of the cut edge and the burs height of a blanked product. This will improve the final products quality and reduce burrs removal rework in addition to increasing the manufacturing process flexibility and reducing its cost through building one blanking setup for different materials. In conclusion, it can be stated that the Finite Element Method coupled with Design of Experiments techniques can be used in order to contribute towards the optimization of sheet metal blanking processes. Further investigation is needed to explore more parameters and operating conditions to develop a general model for more material types. It is recommended to experimentally perform the blanking process that combines the optimal set of parameters and monitor its output quality.

Acknowledgement:

This work has been partially funded by The Deanship of Scientific Research at The University of Jordan. The authors would like to thank Rum-Aladdin for Engineering Industries Company for its help and they are grateful to Dr. Ridha Hambli from LASQUO, ISTIA, University of Angers, France, for his help and support in this research.

References

[1] I. Wadi, and R. Balendra, “An intelligent approach to monitor and control the blanking process”. Advances in Engineering Software, Vol. 30, 1999, 85-92.

[2] K. Tahboub, and I., Rawabdeh, “A Design Of Experiments Approach For Optimizing An Extrusion Blow Molding Process”. Journal of Quality in Maintenance Engineering, Vol. 10, No.1, 2004, 47-54.

[3] S. Maiti, A. Ambekar, U. Singh, P. Date, and K. Narasimhan, “Assessment of influence of some process parameters on sheet metal blanking”.Journal of Materials Processing Technology, Vol. 102, 2000, 249-256.

[4] R. Hambli, “Finite element simulation of fine blanking process using a pressure-dependent damage model”. Journal of Materials Processing Technology, Vol. 116, 2001, 252-264.

[5] R. Hambli, “BLANKSOFT: a code for sheet metal blanking processes optimization”. Journal of Materials Processing Technology, Vol. 141, 2003, 234-242.

[6] W. Klingenberg, and U. Singh, “Comparison of two analytical models of blanking and proposal of a new model”. International Journal of Machine Tools and Manufacture, Vol. 45, 2005, 519-527.

[7] H. Andruet, “Special 2-D and 3-D Geometrically Nonlinear Finite Elements for Analysis of Adhesively Bonded Joints,” Unpublished Doctoral Dissertation, Virginia Polytechnic Institute, USA, 1998.

[8] M., Samuel, “FEM simulations and experimental analysis of parameters of influence in the blanking process”. Journal of Materials Processing Technology,Vol. 84, 1998, 97-106.

[9] I. Rawabdeh, H. Hilwa, and M. Abu Hammad, “Minimizing Necking Defects in Aluminum beverage Cans Using Experimental Design Techniques”. Dirasat, Engineering science, Vol. 30, No.1, 2003, 84-97.

[10] R. Hambli, S. Richir, P. Crubleau, and B. Taravel, “Prediction of optimum clearance in sheet metal blanking processes”. International Journal of Advanced Manufacturing Technology, Vol. 22, 2003, 20-25.

[11] F. Faura, A. Garcia, and M. Estrems, “Finite element analysis of optimum clearance in the blanking process”. Journal of Materials Processing Technology, Vol.80-81, 1998, 121-125.

[12] W. Klingenberg, and U. Singh, “Finite element simulation of the punching/blanking process using in-process characterization of mild steel”. Journal of Materials Processing Technology, Vol. 134, 2003, 296-302.

[13] F. Biglari, A. Kermani, M. Parsa, K. Nikbin, and N. O’Dowd, “Comparison of fine and conventional blanking based on ductile fracture criteria”. 7th Biennial ASME Conference on Engineering Systems Design and Analysis, Manchester, UK, 2004.

[14] K. Shim, S. Lee, B. Kang and S. Hwang, “Investigation on blanking of thin sheet metal using the ductile fracture criterion and its experimental verification”. Journal of Materials Processing Technology, Vol. 155-156, 2004, 1935-1942.

[15] R. Hambli, R. “Design of Experiment Based Analysis for Sheet Metal Blanking Processes Optimization”. The International Journal of Advanced Manufacturing Technology, Vol.19, 2002, 403-410.

[16] R. Hambli, and F. Guerin, “Application of a neural network for optimum clearance prediction in sheet metal blanking processes”. Finite Elements in Analysis and Design, Vol.39, 2003, 1039-1052.

[17] D. Brokken, W. Brekelmans, and F. Baaijens, “Predicting the shape of blanked products: a finite element approach”. Journal of Materials Processing Technology, Vol.103, 2000, 51-56.

[18] M. Rachik, J. Roelandt, and A. Maillard, “Some phenomenological and computational aspects of sheet metal blanking simulation”. Journal of Materials Processing Technology, Vol. 128, 2002, 256-265.

[19] G. Fang, G., P. Zeng, and L. Lou, “Finite element simulation of the effect of clearance on the forming quality in the

blanking process". Journal of Materials Processing Technology, Vol.122, 2002, 249-254.

[20] V. Miguel, and D. Jose, "A computational approach to blanking processes". Journal of Materials Processing Technology, Vol. 125-126, 2002, 206-212.

[21] A. Goijaerts, L. Govaert, and F. Baaijens "Evaluation of ductile fracture models for different metals in blanking". Journal of Materials Processing Technology, Vol.110, 2001, 312-323.

[22] P. Thomas, J. Ralf, and H. Michael, "A finite element based model for description of aluminum sheet blanking".International Journal of Machine Tools and Manufacture, Vol. 40, 2000, 1993-200

JJMIE

Volume 2, Number 1, Mar. 2008
ISSN 1995-6665
Pages 65 - 69

Jordan Journal of Mechanical and Industrial Engineering

Expected Delays in Completing Projects under Uncertainty

Ahmed Farouk Abdul Moneim *

College of Engineering, Arab Academy of Science and technology and Maritime Transport, Alexandria, Egypt

Abstract

A method is proposed to estimate, rationally, a contingency covering probable delays in completing projects. Project completion time is assumed random variable distributed normally with given expected value and variance. Two pure strategies and a mixed strategy for decreasing expected delay, if it turns out to be unacceptable, are presented. A new function SDF(Z_C), as a function of a standard normal variable Z_C corresponding to contract time T_C, is derived and given also in a table form for calculation simplicity. The mixed strategy of compressing both expected project completion time and its variance, to achieve a desirable level of expected project delay, leads to a nonlinear program and solved by Solver/Excel.

Keywords: Project Delay Period; Time-Over-Run; Standard Delay Function (SDF); Nonlinear Minimization Problem; Consequences of Project Delay;

Nomenclature

C_T	Cost of 1 % compression of expected project completion time
C_σ	Cost of 1 % compression of standard deviation of project completion time
d	Delay period in project completion
$E(d)$	Expected value of delay period
SDF(Z_C)	Standard Delay Function.
TE	Expected (average) project time
T_C	Contract time
TC	Total cost of compression
t	Project completion time
f(t)	Probability density function of project completion time (normal distribution)
X_T	Percentages of compression of expected project completion time
X_σ	Percentages of compression of standard deviation
γ	Desired reduction ratio of the expected delay period
σ_P	Standard deviation of the project completion time
υ	Standard deviation reduction ratio
τ	Reduction ratio of reducing the expected project completion time
$\Phi(Z)$	Cumulative probability function of Normal distribution
$Z = \frac{t - T_E}{\sigma_P}$	Standard normal variable

1. Introduction

Time-over-run is one of the most important issues facing project managers and business executives in their endeavor to undertake responsibilities of completing and delivering projects .The risk of Time-over-run could be so extremely high that cannot be taken by contractors. Risk, generally is evaluated as the product of two terms: the probability of not completing the project by the time prescribed in the contract – as the risk-initiating event- and the consequences of delay.

At first, consider the second term i.e. the consequences of delay. Almost all contracts include articles prescribing delay penalties. Usually, delay penalties are prescribed as rates ($ / unit time of delay). There is an upper limit of the sum to be charged as delay penalties. This upper limit is defined by law not to exceed a specified percentage of the contract value (say 10%). As delay penalties start to exceed that limit, the contract is automatically cancelled and the remaining uncompleted work of the project could be assigned to another competent contractor (usually the next in the bidders list). Any extra costs resulting from calling a new contractor will be charged to the delayed contractor. This is just the monetary part of the consequences of the risk of time-over-run. Another part of these consequences- that is more painful- the loss of reputation of delayed contractors and hence loosing their competitive power.

* Corresponding author. e-mail: jc_wang@microloops.com

The first term of the product evaluating the risk of time-over-run is the probability of the event of completing the project in a time exceeds that prescribed in the contract (contract time). This statement implies that the completion time of a project is a random variable. This is true, since completion time of a project is completely determined by durations of its constituting activities and their precedence order. Durations of activities and tasks of a project cannot be defined as certain quantities because of the following reasons:

- All projects are unique undertakings rarely to be repeated.
- Environmental conditions- in which activities are performed - are uncertain and can be only described by parameters of random nature.
- Labor and equipment productivities cannot be assumed deterministic quantities but rather random variables because of the clear variation in their values.
- Reworks of some activities or part of activities are due to project owner refusals and/or faulty executions. The time increase in these situations is random.
- Other pertinent reasons.

Uncertainties in project planning have been recognized since the fifties of the last century. Project Evaluation and Review Technique-known as PERT- was the first model accounting for the randomness of activity durations (assuming beta distribution for activity durations). Based on the Central Limit theorem, in PERT, project completion time is assumed to be normally distributed [1]. The normality of the project completion time enables project planners to easily evaluate the probability of delay as the probability of completing a project in a time exceeding contract time.

Naturally, all contractors are concerned with avoidance or at least mitigation of the risk of time-over-run beside other risks such as cost-over-run [2]. As a method for mitigation of the risk of time-over-run is to include a rough estimate to cover such risks in the bid cost estimations. This is usually included in the estimates of contingencies.

However, problems of rational evaluation of contingencies in bidders' proposals have been considered in several researches [3], [4].

In the present work, a rational approach is proposed not only to evaluate the expected delay period and thereby the amount of expected delay penalty but also to provide a method to test different alternative strategies of reducing the expected delay period.

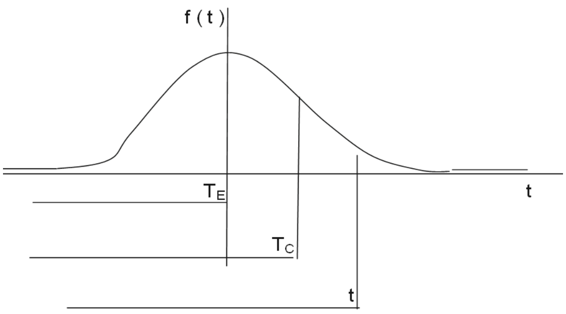

Fig. 1 Project time normal distribution and its parameters

2. Expected Delay Period

2.1. Derivation of a mathematical expression for Expected Delay Period

The delay in project completion is defined as follows

$$d = (t \mid t > T_C) - T_C$$

$$E(d) = E(t \mid t > T_C) - T_C$$

$$E(d) = \frac{\int_{T_C}^{\infty} t.f(t)dt}{\int_{T_C}^{\infty} f(t)dt} - T_C$$

$$f(t) = \frac{1}{\sigma_P \sqrt{2\pi}} .e^{-(1/2)\left(\frac{t-T_E}{\sigma_P}\right)^2}$$

$$\frac{t - T_E}{\sigma_P} = z$$

$$dz = \left(\frac{1}{\sigma_P}\right) dt$$

$$t = z.\sigma_P + T_E$$

Then,

$$E(d) = \frac{\int_{z_C}^{\infty} (z\sigma_P + T_E)\ \sigma_P\ \exp(-z^2/2)\ dz}{\sigma_P \sqrt{2\pi}[1 - \Phi(z_C)]} - T_C$$

$$E(d) = \frac{\sigma_P\ \exp(-z_C^2/2)}{\sqrt{2\pi}[1 - \Phi(z_C]} - \sigma_P\ z_C$$

$$E(d) = \sigma_P\ \mathrm{SDF}(z_C)$$

$$SDF(z_C) = \frac{\exp(-z_C^2/2)}{\sqrt{2\pi}[1 - \Phi(z_C]} - z_C$$

The Standard Delay Function $SDF(Z_C)$ is a newly introduced function of the standard normal variable Z_C. For ease and simplicity of practical calculations, $SDF(Z_C)$ is tabulated in a similar way as the cumulative normal function $\Phi(Z)$

Finally, we obtain for the expected value of delay period in completing a project with completion time normally distributed with mean T_E and standard deviation σ_P having T_C as contract time in the following form:

$$E(d) = \sigma_P\ SDF\ (Z_C) \quad (1)$$

The standard Delay function $SDF(Z_C)$ is given by

$$SDF\ (Z_C) = \frac{e^{-Z_C^2/2}}{\sqrt{2\pi}[1 - \Phi(Z_C)]} - Z_C \quad (2)$$

The table of $SDF(Z_C)$ is given in table 1

2.2. Strategies of decreasing Expected Delay Period

While preparing bids, contractors may find the expected delay period as evaluated by expression (1) and table (1) excessively large. This would entail undesirable increase in bid price in case of accounting for potential penalties in bid estimates and hence diminishing chances of winning. What could be the strategies adopted by contractors in order to reduce the expected delay period to enhance their situation in bidding?.

Consider at first two pure strategies: either by reducing expected project time by means of compressing durations of activities keeping their standard deviations unchanged, or by reducing the standard deviation of project completion time by reducing the variation in estimated activities durations keeping expected durations unchanged.

2.2.1. Pure strategy of compressing T_E only, keeping σ_P unchanged

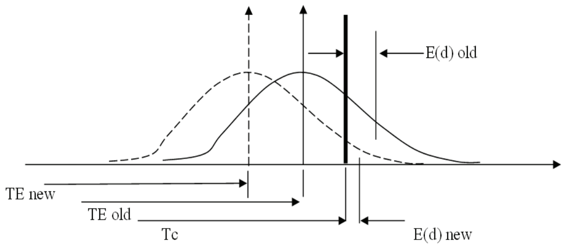

Fig. 2 Pure Strategy of decreasing delay by compressing expected project time only

Table 1. Standard Delay Function SDF (Z_C)

Zc	SDF(Zc)									
	0	0.01	0.02	0.03	0.04	0.05	0.06	0.07	0.08	0.09
0	0.798	0.794	0.791	0.787	0.784	0.780	0.777	0.773	0.770	0.766
0.1	0.763	0.759	0.756	0.753	0.749	0.746	0.743	0.739	0.736	0.733
0.2	0.730	0.726	0.723	0.720	0.717	0.714	0.711	0.708	0.705	0.701
0.3	0.698	0.695	0.692	0.689	0.686	0.683	0.681	0.678	0.675	0.672
0.4	0.669	0.666	0.663	0.661	0.658	0.655	0.652	0.649	0.647	0.644
0.5	0.641	0.639	0.636	0.633	0.631	0.628	0.626	0.623	0.620	0.618
0.6	0.615	0.613	0.610	0.608	0.605	0.603	0.600	0.598	0.596	0.593
0.7	0.591	0.588	0.586	0.584	0.581	0.579	0.577	0.575	0.572	0.570
0.8	0.568	0.566	0.563	0.561	0.559	0.557	0.555	0.552	0.550	0.548
0.9	0.546	0.544	0.542	0.540	0.538	0.536	0.534	0.532	0.530	0.528
1	0.526	0.524	0.522	0.520	0.518	0.516	0.514	0.512	0.510	0.508
1.1	0.506	0.504	0.502	0.501	0.499	0.497	0.495	0.493	0.492	0.490
1.2	0.488	0.486	0.484	0.483	0.481	0.479	0.478	0.476	0.474	0.472
1.3	0.471	0.469	0.467	0.466	0.464	0.463	0.461	0.459	0.458	0.456
1.4	0.455	0.453	0.451	0.450	0.448	0.447	0.445	0.444	0.442	0.441
1.5	0.439	0.438	0.436	0.435	0.433	0.432	0.430	0.429	0.427	0.426
1.6	0.425	0.423	0.422	0.420	0.419	0.418	0.416	0.415	0.414	0.412
1.7	0.411	0.410	0.408	0.407	0.406	0.404	0.403	0.402	0.400	0.399
1.8	0.398	0.397	0.395	0.394	0.393	0.392	0.390	0.389	0.388	0.387
1.9	0.386	0.384	0.383	0.382	0.381	0.380	0.378	0.377	0.376	0.375
2	0.374	0.373	0.372	0.370	0.369	0.368	0.367	0.366	0.365	0.364
2.1	0.363	0.362	0.361	0.359	0.358	0.357	0.356	0.355	0.354	0.353
2.2	0.352	0.351	0.350	0.349	0.348	0.347	0.346	0.345	0.344	0.343
2.3	0.342	0.341	0.340	0.339	0.338	0.337	0.336	0.335	0.334	0.333
2.4	0.333	0.332	0.331	0.330	0.329	0.328	0.327	0.326	0.325	0.324
2.5	0.323	0.323	0.322	0.321	0.320	0.319	0.318	0.317	0.316	0.316
2.6	0.315	0.314	0.313	0.312	0.311	0.311	0.310	0.309	0.308	0.307
2.7	0.307	0.306	0.305	0.304	0.303	0.303	0.302	0.301	0.300	0.299
2.8	0.299	0.298	0.297	0.296	0.296	0.295	0.294	0.293	0.293	0.292
2.9	0.291	0.290	0.290	0.289	0.288	0.287	0.287	0.286	0.285	0.285
3	0.284	0.283	0.283	0.282	0.281	0.280	0.280	0.279	0.278	0.278
3.1	0.277	0.276	0.276	0.275	0.274	0.274	0.273	0.272	0.272	0.271
3.2	0.270	0.270	0.269	0.269	0.268	0.267	0.267	0.266	0.265	0.265
3.3	0.264	0.264	0.263	0.262	0.262	0.261	0.261	0.260	0.259	0.259
3.4	0.258	0.258	0.257	0.256	0.256	0.255	0.255	0.254	0.253	0.253
3.5	0.252	0.252	0.251	0.251	0.250	0.250	0.249	0.248	0.248	0.247
3.6	0.247	0.246	0.246	0.245	0.245	0.244	0.244	0.243	0.243	0.242
3.7	0.241	0.241	0.240	0.240	0.239	0.239	0.238	0.238	0.237	0.237
3.8	0.236	0.236	0.235	0.235	0.234	0.234	0.233	0.233	0.232	0.232
3.9	0.231	0.231	0.230	0.230	0.229	0.229	0.229	0.228	0.228	0.227
4	0.227	0.226	0.226	0.225	0.225	0.224	0.224	0.223	0.223	0.223

Given the desired reduction ratio γ of reducing the expected delay period, required to evaluate the corresponding reduction ratio τ of reducing the expected project completion time.

To find τ, we proceed as follows:

$$E(d)_{New} = (1-\gamma).E(d)_{old}$$
$$\sigma_P.SDF(Z_{Cnew}) = (1-\gamma).E(d)_{old}$$
$$SDF(Z_{Cnew}) = \frac{(1-\gamma).E(d)_{old}}{\sigma_P}$$

From table 1, we find the value of Z_{Cnew} corresponding to the value of $SDF(Z_{Cnew})$

$$T_{Enew} = T_C - \sigma_P.Z_{Cnew}$$
$$\tau = \frac{T_{Eold} - T_{Enew}}{T_{Eold}}$$

T_C, T_{Eold}, σ_P, γ are given and $SDF(d)_{old}$ is found from table 1.

Illustrative Example:

Given: $T_{E\ old}$ = 300 days; σ_P = 40 days; T_C = 350 days, then Z_C = 1.25. From table 1, SDF(1.25)= 0.479, the original expected delay period is evaluated: $E(d)_{old}$ = 40 x 0.479 = 19.16 days. It is required to reduce this expected delay by 40%, what would be the corresponding percentage of compression of T_E

$$SDF(Z_{Cnew}) = \frac{(1-\gamma).E(d)_{old}}{\sigma_P} = 0.6 \times 19.16 / 40 = 0.2874$$

Again from table 1, the corresponding $Z_{C\ new}$ = 2.95, then $T_{E\ new}$ = 350 − 40 x 2.95= 232 The corresponding compression ratio τ will be τ = (300 − 232) / 300 = 0.2267.

The expected project time should be compressed by about 23% in order to reduce the expected delay period by 40%. The decision whether to adopt this strategy or not, would be taken on the basis of tradeoff between the cost of compression of the expected project completion time from 300 days to 232 days and the expected penalty of 8 days delay.

2.2.2. Pure strategy of decreasing σ_P only, keeping T_E unchanged

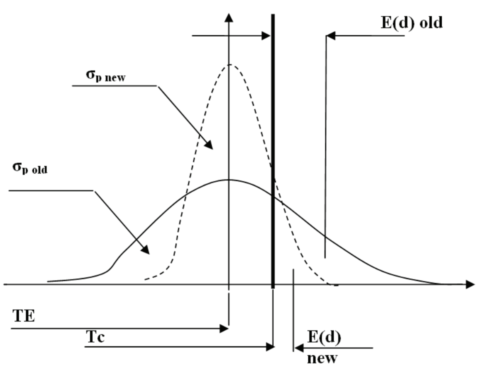

Fig. 3 Pure strategy of decreasing delay by compressing project time variance only

Given the desired reduction ratio γ of reducing the expected delay period. Required to evaluate the corresponding reduction ratio υ of reducing the standard deviation of project completion time. To find υ, we proceed as follows:

$$E(d)_{New} = (1-\gamma).E(d)_{old}$$
$$\sigma_{Pnew}.SDF(Z_{Cnew}) = (1-\gamma).E(d)_{old} \quad (3)$$

Since σ_{Pnew} is unknown, it is necessary to solve the transcendental equation in (3) to find σ_{Pnew}. This equation may be solved by trial and error or by using one of the tools of the Excel "Goal Seek."

Illustrative example:

Consider the above solved example but by employing the strategy of reducing σ_P rather than T_E. The transcendental equation in (3) will take the form:

$$\sigma_{Pnew}.SDF(Z_{Cnew}) = 0.6x19.16 = 11.496$$

The solution by trial and error in a table form is found by giving values to σ_{Pnew} and evaluating the left hand side (LHS)of the equation and repeat until we approach the value of the right hand side.

σ_P	Z_{Cnew}	$SDF(Z_{Cnew})$ From table 1	LHS
35	1.428571	0.45	15.75
32	1.5625	0.43	13.76
30	1.666667	0.415	12.45
29	1.724138	0.408	11.832
28.5	1.754386	0.404	11.514

σ_{Pnew} = 28.5 days. The standard deviation reduction ratio υ will be

$$\upsilon = (40 - 28.5)/ 40 = 0.2875.$$

The standard deviation of project completion time must be reduced by about 29% in order to have 40% reduction in expected delay period. In absolute figures, the standard deviation of the project completion time should reduce by about 12 days in order to gain about 8 days reduction in expected delay. The same argument as regards to whether to go with the reduction in standard deviation or not, would be decided by tradeoff between the cost of reduction of variance of project completion time and the value of penalties of the 8 days delay.

2.2.3. Mixed strategy of decreasing both T_E and σ_P with different ratios

The objective of adopting a mixed strategy is to minimize the total cost of compressing both expected project completion time and its standard deviation. Next, we formulate this minimization problem.

Decision variables in this problem are X_T and X_σ percentages of compression of expected project completion time and of its standard deviation respectively.

Parameters : C_T and C_σ costs of 1 % compression of expected project completion time and its standard deviation respectively. TC total cost of compression. T_E , σ_P expected project completion time and its standard deviation respectively, T_C contract time, $E(d)_O$ initial expected delay period, evaluated as explained below

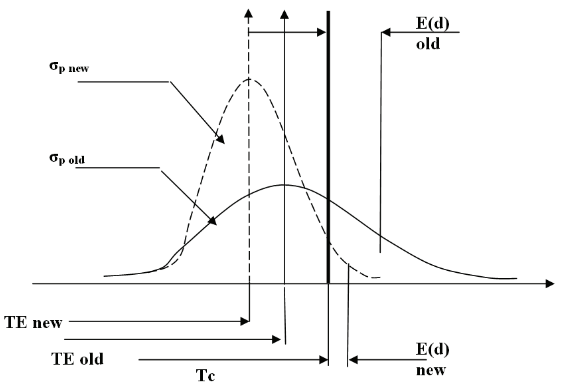

Fig. 4 Mixed strategy of decreasing delay by compressing both expected project time and its variance

Objective Function:

Minimize

$$TC = C_T.X_T + C_\sigma.X_\sigma$$

Subject to

$$\frac{\exp\left[-0.5.\left(\frac{T_C-(1-0.01X_T)T_E}{(1-0.01X_\sigma).\sigma_P}\right)^2\right]}{\sqrt{2\pi}.\left[1-\Phi\left(\frac{T_C-(1-0.01X_T)T_E}{(1-0.01X_\sigma).\sigma_P}\right)\right]} - \left[\frac{T_C-(1-0.01X_T)T_E}{(1-0.01X_\sigma).\sigma_P}\right].. \le (1-\gamma).E(d)_O$$

This nonlinear program has a linear objective function but the constraint is nonlinear. This program can be easily solved by SOLVER under EXCEL

Illustrative example

Given T_E = 100 days, σ_P = 20 days, T_C = 110 days, γ = 0.4, C_T = 4000 \$, C_σ = 3500 \$

Initially evaluate the expected delay period $E(d)_O$

ZC = (110 – 100) / 20 = 0.5

From table 1, we get SDF(0.5) = 0.641, then

$E(d)_O = \sigma_P$ *SDF(0.5) = 12.82 days*

Solving the nonlinear program by Solver/ Excel, we find the following compression percentages that necessary to be applied on both T_E and σ_P respectively to get the desired 40% reduction of the expected delay at a minimum cost.

XT = 14.162 %
Xσ = 15.1 %
TC = 109 467 $

3. Quality and Quantity of resources allocated to project activities and their effects on activities durations

Resources, considered in the present work, are mainly labor and equipment. By quality resources, we mean highly skilled and experienced labor and/or high quality equipment with minimum failure rates. The use of such quality resources helps to minimize the uncertainty in predicting productivity and availability of resources and eliminate or at least minimize the expected amount of rework. Hence, planners could assume small variations (variances) in activities durations. On the other hand, as the quality of resources rises the direct cost of activity would increase. This is the cost of reducing variance of activity duration. Quantitative increase of resources leads to compression of activities expected durations but without a noticeable reduction in their variances. Of course, quantitative and qualitative increase of resources allocated to different activities would result in decrease of their expected durations and variances as well. The problem of defining the best way to compress project completion time with minimum increase in direct cost is a well-known problem formulated and solved, in deterministic framework, in Operations Research. But, a similar problem of defining the best way to reduce variance (standard deviation) of project completion time, to writer's knowledge, is not existing and needs to be treated in future works.

The decrease in indirect cost of projects as completion times get shorter should be considered in evaluations of total cost increase due to compression of project completion times and their variances.

4. Conclusion and Future work

Estimation of expected delay in completing projects contributes significantly to the reliable assessment of risks of both time-over-run and cost-over-run. The method proposed in this work is simple and amenable to practical computations. A model is required to be built in future works to enable planners to select the optimum alternatives of decreasing project completion time variance alone and along with decrease of expected project completion time aiming at decreasing expected project delay.

References

[1] Hamdy A. Taha, Operations Research, 7th ed, Prentice Hall, 2003

[2] Ali Touran, "Calculation of Contingency in Construction Projects", IEEE, Transactions on Engineering Management, Vol 50, No 2, May 2003

[3] R. De Neufville, E.N. Hani and V. Lesage. " Building Models: Effects of bidder Risk aversion", Journal of Construction Div. ASCE, Vol. 103, No. 2, 1977

[4] M. Ranasinghe, "Contingency allocation and management for building projects", Construction Management Econ.., vol. 12, pp 233-243, 1994

المملكة الأردنية الهاشمية

الجامعة الهاشمية

المجلة الأردنية
للهندسة الميكانيكية والصناعية

JJMIE

مجلة علمية عالمية محكمة

http://jjmie.hu.edu.jo/

ISSN 1995-6665

المجلة الأردنية للهندسة الميكانيكية والصناعية

مجلة علمية عالمية محكمة

المجلة الأردنية للهندسة الميكانيكية والصناعية: مجلة علمية عالمية محكمة أسستها اللجنة العليا للبحث العلمي، وزارة التعليم العالي والبحث العلمي، الأردن، وتصدر عن عمادة البحث العلمي والدراسات العليا، الجامعة الهاشمية، الزرقاء، الأردن.

ترسل البحوث إلى العنوان التالي:

رئيس تحرير المجلة الأردنية للهندسة الميكانيكية والصناعية

عمادة البحث العلمي والدراسات العليا

الجامعة الهاشمية

الزرقاء - الأردن

هاتف : ٣٩٠٣٣٣٣ ٥ ٠٠٩٦٢ فرعي ٤١٤٧

Email: jjmie@hu.edu.jo

Website: www.jjmie.hu.edu.jo